Identification of the Mechanisms of mRNA Regulation by PUF Proteins

by

Nathan Hans Blewett

A dissertation submitted in partial fulfillment
of the requirements for the degree of
Doctor of Philosophy
(Cellular and Molecular Biology)
University of Michigan
2013

Doctoral Committee:

Associate Professor Aaron C. Goldstrohm, Chair
Professor David R. Engelke
Professor Ray C. Trievel
Professor Michael D. Uhler
Professor Nils G. Walter

This work is dedicated to my Mother, Father, Brother, Amanda, Chessie, and Snoopy

Acknowledgements

I would like to first thank my mentor, Aaron Goldstrohm. It's clear that he is dedicated to providing the most effective, thorough, and thoughtful leadership possible. I have been challenged to perform at a very high-standard, to construct defined testable hypothesis and argue my position strongly. Aaron also promotes a positive atmosphere for professional development, and the discussions that we have had were valuable. He is always willing to argue about a hypothesis, or experimental interpretation; provided a strong logical foundation. It has been an honor to be the first graduate student in his lab, I have learned much about what I'm capable of from his perseverance, and commitment to good science.

I would also like to acknowledge the members of the Goldstrohm Lab, there are an innumerable number of valuable discussions we've had, both scientifically, and regarding life. There is a lot of pressure to perform in the present funding climate, and I was blessed to work with a group of people who are supportive of each other. I have learned many things from each member of the Goldstrohm lab, and count myself lucky to work with such a crew.

Finally, I would like to thank the CMB program, especially: Jessica Schwartz, Bob Fuller, and Cathy Mitchell. Their efforts to help graduate students succeed are remarkable, and I am very grateful for their involvement in my studies.

Table of Contents

List of Figures

Chapter One

Introduction

Temporal, spatial, and cell-type specific expression of subsets of genes is crucial for many biological processes including: body-axis patterning, synaptic plasticity, and stem cell maintenance. Control of gene expression is exerted at multiple levels, beginning with the transcription of a nascent protein-encoding mRNA from DNA, by RNA polymerase II. Transcription of mRNAs is a highly regulated process that functions in concert with downstream post-transcriptional mRNA regulatory processes; this results in nuanced and layered control over the timing and level of protein expression from a particular mRNA (Lackner, Beilharz et al. 2007). This work will focus on post-transcriptional mechanisms of mRNA control.

Early mRNA processing events:

All eukaryotic mRNAs are capped at the 5′ end by a methylated guanosine residue, and most mRNAs, aside from histone mRNAs, are appended at the 3' end with a poly-adenosine, or, poly(A) tail that can range from approximately 80 adenosines in *S. cerevisiae*, to 200 + adenosines in mammalian mRNAs (Shatkin and Manley 2000). These features function synergistically to promote the stability, as well as translation of an mRNA (Preiss and Hentze 1998). The 5′ cap and 3′ poly(A) tail are added co-transcriptionally (Coppola, Field et al. 1983) in the nucleus, and any introns are spliced out to produce a functional mRNA capable of being translated into a protein. Only after a pre-mRNA has successfully undergone these events will

mRNA be exported to the cytoplasm for translation and further regulation (Saguez, Olesen et al. 2005).

Translation:

The processed mature mRNA is transported from the nucleus into the cytoplasm (Palayoor, Schumm et al. 1981; Schroder, Bachmann et al. 1987; Eckner, Ellmeier et al. 1991), where mRNA decay and translational machinery both are able to engage the mRNA and exert positive or negative regulation. After nuclear export the 5′ mRNA cap is bound by the cap-binding protein eIF-4E, which is conserved in all eukaryotes (Sonenberg, Morgan et al. 1978; Sonenberg, Rupprecht et al. 1979; Altmann, Edery et al. 1985; Altmann, Muller et al. 1989). It is thought that cap-bound eIF-4E interacts with eIF-4A, which is bound to the scaffold protein eIF-4G; this complex is termed eIF-4F (Edery, Humbelin et al. 1983; Grifo, Tahara et al. 1983; Pestova, Shatsky et al. 1996). Poly(A) Binding Protein (Pabp) associates with the poly(A) tail and contacts eIF-4G (Tarun and Sachs 1996; Tarun, Wells et al. 1997; Kessler and Sachs 1998) to cause circularization of a translationally competent mRNA (Ladhoff, Uerlings et al. 1981; Grifo, Tahara et al. 1983; Wells, Hillner et al. 1998).

The 40s ribosomal subunit is recruited to cap-bound eIF-4F complex, along with eIF2/GTP/Met-tRNAi (Hoerz and McCarty 1969; Both, Furuichi et al. 1975; Muthukrishnan, Both et al. 1975; Nasrin, Ahmad et al. 1986; Jivotovskaya, Valasek et al. 2006); the ternary complex composed of 40s subunit eIF2/GTP/Met-tRNAi forms the 43s pre-initiation complex (Anderson and Shafritz 1971; Levin, Kyner et al. 1973). The 43s ribosome then scans along the mRNA until reaching a start codon (Kozak and Shatkin 1978; Kozak 1980; Kozak 1980), when

the anti-codon of Met-tRNAi docks with the start codon in the ribosomal P-site (Clark, Dube et al. 1968; Marcus, Weeks et al. 1970; Sprinzl, Wagner et al. 1976; Lake 1977; Wurmbach and Nierhaus 1979). The 60s subunit joins the 40s subunit bound to a start codon, forming an 80s monosome (Kappen, Suzuki et al. 1973; Siekierka, Manne et al. 1983). Translation initiation then involves GTP hydrolysis by eIF-2, which results in the ejection of several initiation factors, (Lockwood, Sarkar et al. 1972; Merrick 1979; Peterson, Merrick et al. 1979; Peterson, Safer et al. 1979) and the ORF is translated into a protein.

Figure 1.1 Well-translated mRNAs are bound by the eIF-4F complex and undergo multiple rounds of translation initiation.

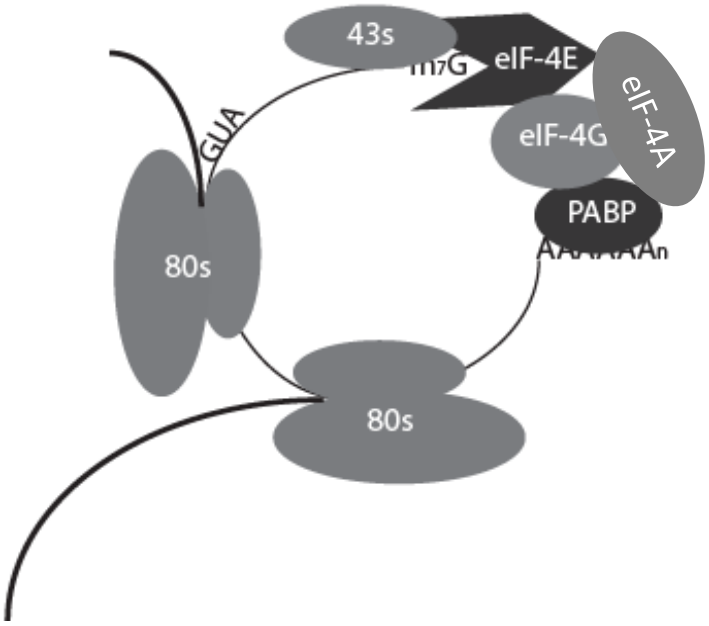

The eIF-4F complex is composed of 5′ cap-bound eIF-4E which directly interacts with eIF-4G bound to the RNA helicase eIF-4A. Formation of eIF-4F strengthens the interaction between eIF-4E and the cap, and recruits the small ribosomal subunit to direct translation initiation. Poly(A) Binding Protein (Pabp) binds to the poly(A) tail and interacts with eIF-4G, causing circularization of the mRNA, and protecting the 5′ and 3′ ends of the mRNA from mRNA degradation.

Physical association of eIF-4E with eIF-4A, eIF-4G and PABP is thought to increase the affinity of eIF-4E for the 5′ cap and lead to more efficient recruitment of ribosomes to the bound mRNA (Haghighat and Sonenberg 1997; Ptushkina, von der Haar et al. 1998; Kahvejian, Svitkin et al. 2005). Small ribosomal subunit recruitment, followed by scanning, and translation initiation occurs multiple times in succession for a single well-translated mRNA (Goodman and Rich 1963; Penman, Scherrer et al. 1963; Gross, Moerke et al. 2003). Initiation is the rate-limiting step for translation (Gualerzi, Risuleo et al. 1977; Bergmann and Lodish 1979), for poorly translated mRNAs initiation is often impaired, leading to a decrease in ribosome occupancy, and a reduction in protein output. During cellular differentiation, response to environmental stimuli, and progression through the cell-cycle, the production of certain proteins must be turned off to enable transition from one growth state to another. To accomplish this certain mRNAs must be transitioned from a circularized, stable and highly translated condition to an untranslatable state.

mRNA Decay:

All mRNAs will be targeted for destruction eventually, but individual mRNA half-lives range over several orders of magnitude (Herrick, Parker et al. 1990; Raghavan, Ogilvie et al. 2002; Sharova, Sharov et al. 2009). Degradation of mRNAs is a tightly regulated process that involves the coordinated action of mRNA decay enzymes, as well as proteins involved in their recruitment and catalytic activation. Decay of mRNAs typically initiates with removal of the poly(A) tail (Brewer and Ross 1988; Shyu, Belasco et al. 1991; Decker and Parker 1993) by deadenylase enzymes, which are a family of exo-ribonucleases that attack mRNAs from the 3′-5′

direction (Tucker, Valencia-Sanchez et al. 2001; Tucker, Staples et al. 2002; Uchida, Hoshino et al. 2004).

Shortening of the poly(A) tail acts as a signal that results in nucleation of a complex containing the mRNA decapping enzyme, as well as associated activators of decapping, leading to the subsequent removal of the 5′ cap (Muhlrad, Decker et al. 1994; Chowdhury, Mukhopadhyay et al. 2007; Chowdhury and Tharun 2009). The 5′ cap protects mRNAs from the activity of XRN1, the 5′-3′ exo-ribonuclease (Green, Maniatis et al. 1983; Stevens, Hsu et al. 1991; Larimer, Hsu et al. 1992; Schwer, Mao et al. 1998), by blocking access of the enzyme to its substrate, which is a 5′ monophosphate. XRN1 is highly processive; once an mRNA has been decapped, XRN1 rapidly destroys the body of the mRNA (Jinek, Coyle et al. 2011).

Deadenylation activated decapping, and subsequent 5′-3′ degradation represents the major pathway for mRNA turnover in the cytoplasm (Beelman, Stevens et al. 1996). Alternatively, mRNAs can be degraded by a complex termed the exosome which degrades RNA in a 3′-5′ manner (Anderson and Parker 1998; Lykke-Andersen, Brodersen et al. 2009; Lykke-Andersen, Tomecki et al. 2011).

Interplay Between Translation and mRNA Decay:

Decay enzymes generally do not have ready access to naked mRNAs; instead they must compete with proteins that promote mRNA translation and stability. The eIF-4F complex results in a circularized mRNA by virtue of eIF-4E bound to the 5’ cap, Pabp bound to the poly(A) tail, and eIF-4G bridging the two proteins. One consequence of mRNA circularization is that the

decapping and deadenylase machinery are not able to engage their respective substrates: the 5′ cap and 3′ poly(A) tail. *In vitro*, eIF-4E is able to outcompete the decapping enzyme for binding to the 5′ cap, and this strongly inhibits removal of the cap simply by eIF-4E binding tightly to it, and refusing the decapping enzyme access (Schwartz and Parker 2000; Tharun and Parker 2001). The activities of mRNA decay and translation are fundamentally opposed, and also tightly interwoven. For mRNA decay machinery to gain access to an mRNA, a transition must occur wherein the translation and stability promoting proteins are removed from the mRNA, and in a coordinated fashion, the mRNA decay machinery is deposited on the mRNA, committing it to destruction.

Figure 1.2 Post-transcriptional repression involves inhibition of translation and/or activation of mRNA decay.

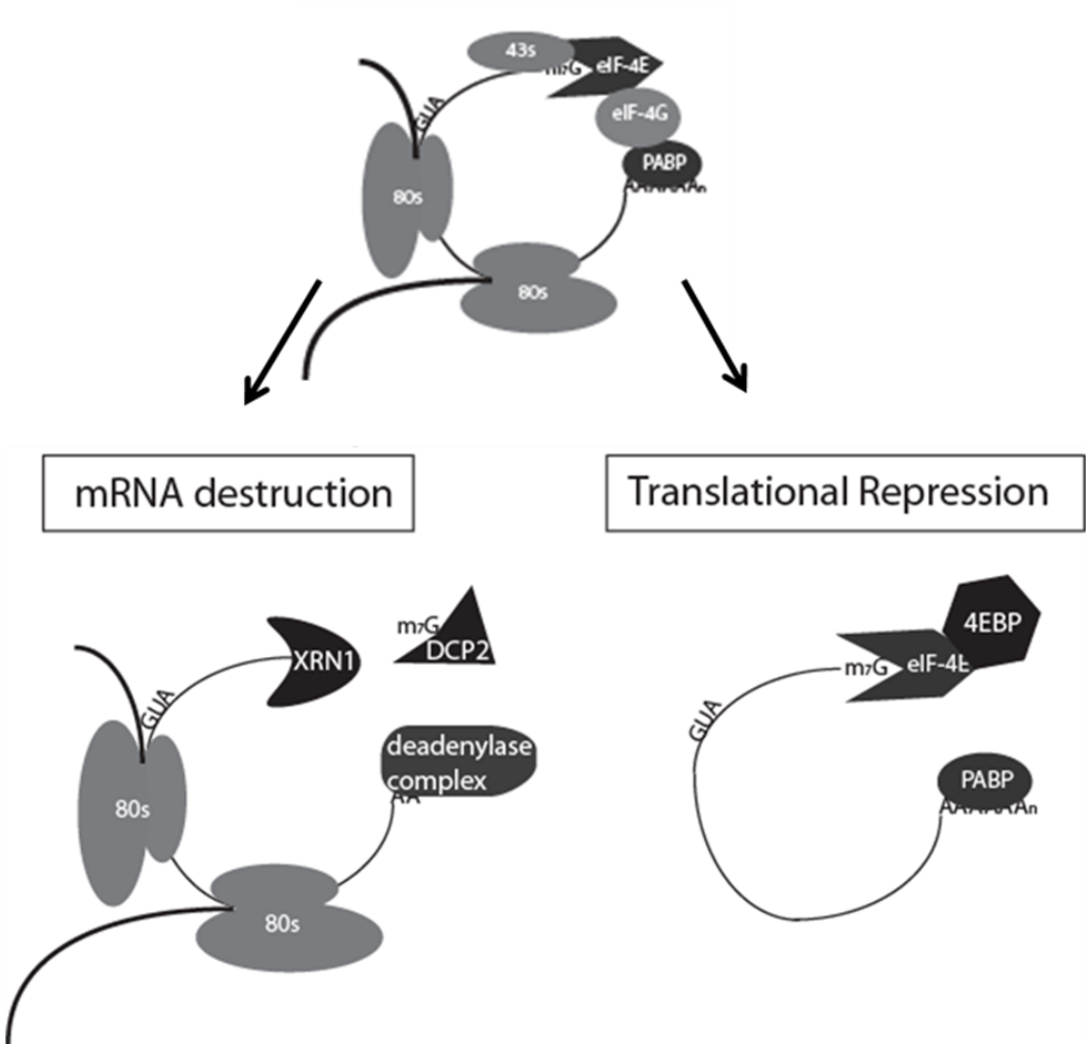

Post-transcriptional silencing of mRNA expression can occur through inhibition of translation initiation, or activation of mRNA decapping and destruction. Both pathways require eviction of the eIF-4F complex, and mRNA de-circularization. eIF-4E-Binding Proteins (4EBPs) block the interaction between eIF-4E and eIF-4G, resulting in a blockage of ribosome recruitment. Alternatively, an mRNA targeted for destruction is initially deadenylated, causing dissociation of Pabp, this is followed by recruitment of the mRNA decapping (DCP2), and decay machinery (XRN1). These two pathways are linked in some cases, where translational silencing can precede, and elicit mRNA destruction.

Cis-Elements Affecting mRNA Expression:

AU-Rich Elements

The stability of a particular mRNA is dictated in many cases by sequence elements found both in the Open Reading Frame (ORF), as well as in the 5′ and 3′ Untranslated Regions (UTRs) of an mRNA. Regulatory information is encoded in an mRNA is several ways that can have both stabilizing and destabilizing effects (Rabbitts, Forster et al. 1985; Jones and Cole 1987; Harland and Misher 1988; Wright, Rosenzweig et al. 1989; Oliveira and McCarthy 1995; Peng, Chen et al. 1998). mRNAs that produce proteins involved in functions related to cell cycle progression, apoptosis, or anti-proliferative activity often exhibit significantly shorter half-lives than average mRNAs (Capasso, Bleecker et al. 1987; Raghavan, Ogilvie et al. 2002).

One of the first sequence elements to be identified which confer instability to an mRNA was AU-Rich sequence Elements (AREs). ARE sequences were identified as a conserved, often overlapping AUUUA sequence found in proximity to uridine rich sequences, generally found within the 3′ UTR of an mRNA, but not exclusively (Shaw and Kamen 1986). The ARE sequence serves as a recognition element for a group of RNA-Binding Proteins referred to as AU-Rich Element Binding Proteins, (ARE-BPs). There are several well-known ARE-BPs, and the regulatory consequences of binding depend on the identity of the particular ARE-BP (Barreau, Paillard et al. 2005).

Tristetraproline (TTP) is one example of an ARE-BP that confers negative regulation to a targeted ARE-containing mRNA. Through a combination of electrophoretic mobility-shift assays (EMSAs), analysis of reporter constructs bearing the identified TTP-binding ARE

sequence, and TTP knock-out analysis on endogenous ARE-containing messages it was concluded that TTP binds to an ARE and this results in destabilization of the TTP-bound mRNA (Ogilvie, Abelson et al. 2005). TTP elicits mRNA destabilization by associating with the decapping enzyme, the 5′ – 3′ exonuclease, the 3′ – 5′ exosome, as well as deadenylase enzymes, which leads to strict regulation of the targeted mRNA presumably due to an increased local concentration of decay enzymes (Chen, Gherzi et al. 2001; Lykke-Andersen and Wagner 2005).

In contrast to the activity of TTP, the ARE-BP HuR is a well-studied example of an ARE-BP which increases the stability of bound mRNAs. During times of low oxygen partial pressure, the Vascular Endothelial Growth Factor (VEGF) mRNA is stabilized (Shima, Deutsch et al. 1995; White, Carroll et al. 1995). Further work on the mechanism of stabilization revealed that the HuR binds to an ARE sequence in the 3′UTR of VEGF. Reduction of HuR levels with an anti-sense HuR construct resulted in a decrease in VEGF stability, and conversely, overexpression caused an increase in stability (Levy, Chung et al. 1998).

Very little is known about the mechanism underlying HuRs ability to stabilize bound mRNAs. One approach utilized three complementary methods to identify HuR-bound, and functionally regulated mRNAs. The approach used Photoactivatable-Ribonucleoside-Enhanced Crosslinking and Immunoprecipitation (PAR-CLIP), followed by Illumina Sequencing of the isolated HuR bound mRNAs, the authors also performed RNA-Immunoprecipitation on HuR, and identified bound mRNAs via microarray. Finally, HuR was knocked-down via siRNA, and global transcript analysis was compared to non-targeting control knockdown. Interestingly, statistical analysis of bound mRNAs, and mRNAs affected by HuR knock-down revealed a

potential mechanism for transcript stabilization. An increase in the number of HuR binding sites correlated with increased HuR stabilizing effects, and these effects were stronger when the sites were found both within an intron and in the 3′UTR of a given mRNA. The authors suggested that HuR may regulate exon inclusion and exclusion, another intriguing finding was that mRNAs with demonstrated miRNA binding sites were strongly enriched also for HuR binding sites in relatively close proximity. Therefore, one potential model for HuR mediated stability may involve a physical competition with the repressive micro-RNA (miRNA) RNA-Induced Silencing Complex (RISC) (Mukherjee, Corcoran et al. 2011); however this data is of a correlative nature and must be interpreted cautiously.

Pumilio Binding Elements:

Another classic example of a cis-element conferring regulation to an mRNA comes from study of the *hunchback (hb)* mRNA in *D. melanogaster*, which encodes a major determinant of the posterior-anterior body-axis in flies (Bender, Horikami et al. 1988). During oogenesis, the *hb* mRNA is maternally deposited and is found throughout the oocyte (Tautz, et al., 1997) (Bender, et al., 1998). The *hb* gene encodes a transcription factor responsible for inhibiting production of genes involved in abdomen development (Struhl, et al., 1992). Once an oocyte is fertilized, *hb* mRNA is repressed in the anterior, and this requires sequence elements found in the 3′ UTR of the *hb* mRNA; repression of *Hb* is achieved through the action of two proteins, Nanos and Pumilio (PUM) (Hulskamp, Schroder et al. 1989; Murata and Wharton 1995).

Repression of maternal *hb* mRNA in the posterior leads to a gradient of Hunchback activity emanating from the anterior pole (Wharton and Struhl 1991). The 3′ UTR sequence

element required for graded Hunchback activity was termed a Nanos Response Element (NRE), however, subsequent analysis of proteins bound to *hb* mRNA showed that the protein bound to the NRE was PUM. *In vitro* binding analysis through electrophoretic mobility shift assays (EMSAs) revealed that PUM binds the NRE with high-affinity (20nM), via a conserved RNA-Binding Domain (RBD) (Wharton and Struhl 1991; Zamore, Williamson et al. 1997; Zamore, Bartel et al. 1999). For the sake of accuracy and simplicity, the NRE will be referred to hereafter as the Pumilio Binding Element (PBE). Further analysis of mRNAs bound by Pumilio in *D. melanogaster*, through RNA-immunoprecipitation and DNA micro-array, showed that PUM associates with nearly 1000 distinct mRNAs, and interestingly, the subset of mRNAs bound changes significantly depending on the developmental stage of the fly (Gerber, Luschnig et al. 2006).

Trans-acting factors: eIF-4E Binding Proteins:

Study of the family of eIF-4E binding proteins (4EBPs) has been a useful tool to illustrate the nuanced nature of mRNA regulation. 4EBPs are prototypical post-transcriptional mRNA regulators; the family is defined by the amino acid motif: tyrosine, three non-specific amino acids, followed by a leucine and a hydrophobic residue, (YXXXLφ) which binds to a conserved surface on the eIF-4E protein. The founding member of this family, rat Phas-I, was identified through efforts to delineate the effects of insulin signaling on translation. Translation initiation is often subject to regulation as it is the rate limiting step in translation. Early work on the impact of insulin signaling on translation showed that insulin causes an increase in general translation initiation (Lyons, Nordeen, Young, 1980). Further work on the Phas-I protein revealed that it is phosphorylated in response to insulin by the Mitogen Activated Protein Kinase,

and this was shown to be responsible for the increase in translation initiation (Haystead , Lawrence, 1994) (Lin, Lawrence, 1994)(Graves, Lawrence, 1995).

In an effort to identify functional orthologs in human cells, a far western assay was employed to find proteins that interact with eIF-4E. The far western assay is a method to identify proteins that interact with a protein of interest (Mahlknecht U. et al., 2001) (Blanar and Rutter, 1992). The eIF-4E cDNA was expressed in *E. coli*, then purified over a cap-analog affinity column, and labeled with a radioactive phosphate at the N-terminus. Labeled eIF-4E was then screened for interaction with a phage library expressing human placental cDNAs. Clones that interacted with eIF-4E were sequenced, and 4E-BP1 and 4E-BP2 were subsequently identified. The authors tested the ability of 4E-BP1 and 4E-BP2 to inhibit translation with an *in vitro* bi-cistronic reporter assay composed of a cap-dependent Chloramphenicol Acetyl Transferase gene (CAT), and a luciferase gene that is translated via an Internal Ribosome Entry Site (IRES). This experiment demonstrated that cap-dependent translation of the CAT reporter was inhibited by both 4EBPs, but the IRES driven luciferase gene was unaffected. Also, addition of excess eIF-4E relieved the inhibition (Pause Sonenberg, 1994); this suggests that 4E-BPs probably inhibit translation through competition with a translation promoting factor. A minimal fragment of eIF-4G that still retained eIF-4E binding activity in both yeast and humans was identified, further sequence analysis showed that eIF-4G proteins from several different eukaryotes all contain the conserved motif YXXXLφ which forms the eIF-4E interaction surface on eIF-4G. These findings were extended by deletion of the eIF-4E binding motif in 4E-BP1 and 4E-BP2, which abolished the interaction between the 4EBPs and eIF-4E (Mader Sonenberg, 1995).

Given that eIF-4G and 4E-BPs occupy the same surface on eIF-4E, it was proposed that 4EBPs compete with eIF-4G to inhibit translation initiation. This hypothesis was borne out through competition binding experiments which showed that the eIF-4F complex never contains a 4EBP, and conversely, eIF-4E bound to a 4EBP precluded the association of eIF-4G, as well as eIF-4A. When the eIF-4E binding motif was mutated in either 4E-BP1 or 4E-BP2, they were no longer able to displace eIF-4G from eIF-4E, and were not capable of repressing translation, showing a requirement for 4EBP binding to eIF-4E to occlude eIF-4G, and inhibit translation (Haghighat Sonenberg, 1995).

.

While all mRNAs have a 5′ cap and the vast majority utilize eIF-4E to direct translation, some mRNAs are more susceptible to 4EBP regulation than others (Dowling, Topisirovic et al. 2010; Thoreen, Chantranupong et al. 2012). Regulation and dysregulation of eIF-4E is a linchpin in the maintenance of cellular homeostasis. Overexpression of eIF-4E drives transformation in cell culture, but the transformation is reversed by expression of 4E-BP1 and 4EBP2 (Rousseau, Gingras et al. 1996). Also, overexpression of eIF-4E is found in a wide variety of human cancers, and in some cases is a prognostic indicator (De Benedetti and Graff 2004). Another important process that is impacted by eIF-4E regulation is synaptic plasticity (Gkogkas, Sonenberg et al. 2010), where 4E-BP2 knock-out mice show autism-like behaviors. Therefore, understanding the mechanisms used by the various 4EBPs will be important for the development of rational and targeted interventions for human diseases involving eIF-4E dysregulation.

Conservation and Divergence of 4EBPs

While the 4E-binding motif is conserved in most eukaryotes, 4EBP orthologs diverge significantly outside of this motif. eIF-4E is an important central target for control of eukaryotic gene expression, however all 4EBPs may not function in the same manner. Several 4EBP orthologs contain C terminal extensions (Table 1.1) which may modulate the activity of the particular 4EBP through association with alternative binding partners, such as RNA binding proteins, or mRNA decay enzymes. Extensive work has been done to elucidate how mammalian 4E-BP1 and 4E-BP2 repress mRNA translation with very little impact on mRNA stability.

Table 1.1. 4EBP orthologues

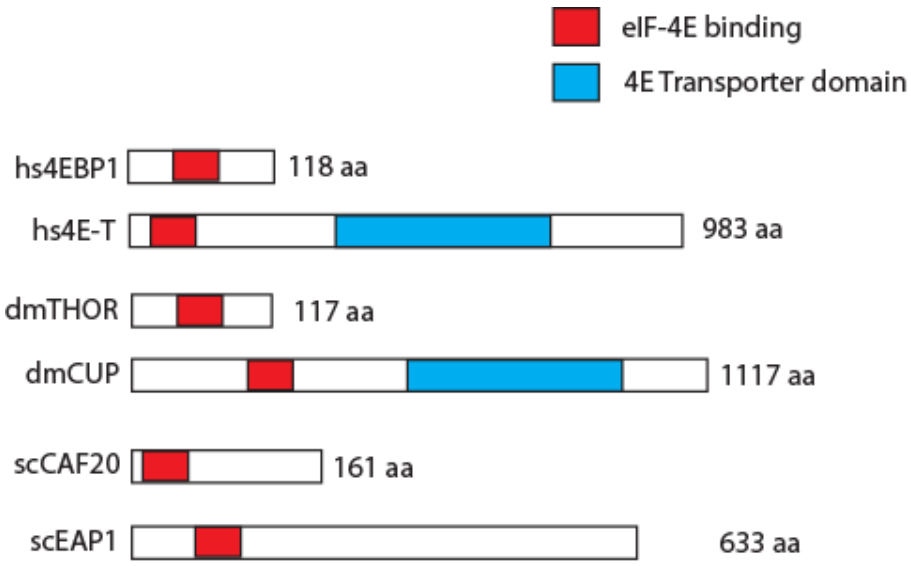

Schematic of 4EBP orthologues from *H. sapiens* (hs), *D. melanogaster* (dm), and *S. cerevisiae* (sc).

However, previous as well as recent work has highlighted the diversity of mechanisms utilized by other 4EBPs, invoking regulation of mRNA stability, translation, as well as localization of the mRNA, and eIF-4E respectively.

eIF-4E Transporter family of 4EBPs

H. sapiens 4E-T was identified by virtue of its ability to bind eIF-4E via far-western assay as described above. Subsequent cloning and characterization of the gene product revealed that 4E-T contains a functional bipartite nuclear import sequence, as well two nuclear export sequences which allow the protein to mediate the transport of eIF-4E between the nucleus and cytoplasm (Dostie, Ferraiuolo et al. 2000). Additional work showed that 4E-T co-localizes with mRNA decay factors and P-bodies that are thought to be sites of active mRNA degradation and/or translational repression through increased local concentration of decay enzymes and repressive co-factors. siRNA knock-down of 4E-T resulted in increased stability of an ARE reporter mRNA. The characterization of 4E-Transporter provided the first demonstration of a 4EBP impacting mRNA stability (Ferraiuolo, Basak et al. 2005).

More recent work on the *D. melanogaster* member of the 4E-T family, Cup, has exposed even more diverse mechanisms of repression used by this family of 4E-BPs. Cup contains several functionally identified regions which direct distinct activities: the N-terminus binds eIF-4E and stabilizes the mRNA, in contrast, a mid-domain, as well as a Q-rich domain both activate deadenylation and decay independently of each other (Igreja and Izaurralde 2011). Full-length Cup activates removal of the poly(A) tail, which results in translational repression, yet Cup is also able to stabilize the mRNA through a non-canonical eIF-4E binding motif. Interestingly when this motif is removed, Cup activates deadenylation, and as well as mRNA decapping and decay. These data indicate that the extended regions of 4EBPs do in fact modulate independent activities that do not necessarily involve inhibition of translation initiation.

CAF20 and EAP1:

As indicated in Table 1.1, *S. cerevisiae* encodes two 4E-BP proteins: Caf20p, and Eap1p. *CAF20* was originally identified as p20, a 20kDa protein that was routinely found associated with cap-bound eIF-4E (Altmann, Krieger et al. 1989). A sequence motif was identified in Caf20p that closely resembles the region of eIF-4G that binds to eIF-4E. *In vivo* and *in vitro* competition binding assays demonstrated that Caf20p outcompetes eIF-4G for eIF-4E binding; when Caf20p is bound to eIF-4E, eIF-4G was displaced. *In vitro* translation assays using yeast extract suggested that *CAF20* inhibited cap-dependent translation in the same manner as the mammalian 4E-BP1 and 4E-BP2 (Altmann, Schmitz et al. 1997).

EAP1 was identified as a 4EBP functional ortholog, through the use of a far-western assay to probe for 4E-interacting yeast proteins (Cosentino, Schmelzle et al. 2000). As shown in the Table 1.1 schematic, Eap1p contains a large C-terminal extension with no identifiable conservation of sequence motifs aside from the eIF-4E binding motif. Using an m^7G cap affinity column, association of eIF-4E with eIF-4G was monitored in the presence or absence of *EAP1*; the presence of *EAP1* effectively displaced eIF-4G from cap-bound eIF-4E. These findings were extended with the use of an *in vitro* yeast extract that can be programmed with a Chloramphenicol Acetyl Transferase (CAT) reporter mRNAs that rely on either cap-dependent, cap-independent translation intiation. Increasing amounts of Eap1p were added to translation extracts programmed with either cap-driven or Internal Ribosome Entry Site (IRES) driven reporter, CAT activity was then measured via autoradiogram. Eap1p repressed expression of the cap-dependent reporter, but not the IRES driven reporter, leading to the conclusion the Eap1p inhibits cap-dependent translation. On the surface it appeared that Eap1p and Caf20p repress

mRNA translation via the same mechanism as 4E-BP1 and 4E-BP2; however it must be noted that mRNA levels were not monitored in this study, and that mRNA decay was not shown to be active in the *in vitro* extract.

micro-RNA Pathway

Another way that eukaryotes modulate gene-expression in trans is through the micro-RNA (miRNA) pathway. miRNAs are 22-23 nucleotide non-coding RNA molecules that are evolutionarily conserved and generally carry-out negative regulation on specific mRNAs (Lau, Lim et al. 2001; Lee and Ambros 2001). Repression by miRNAs involves base-pairing of the miRNA to a sequence in an mRNA allowing each miRNA to target a subset of mRNAs containing partially complementary sequences (Lai 2002). The miRNA is bound by a RiboNucleoProtein (RNP) complex; the conserved central component of this complex is the Argonaute (Ago) protein family (Mourelatos, Dostie et al. 2002).

Once complexed with a miRNA, the RNA-Induced Silencing Complex (RISC) engages a target sequence and recruits inhibitory effector proteins to elicit repression (Wu, Fan et al. 2006; Wakiyama, Takimoto et al. 2007; Chen, Zheng et al. 2009; Zdanowicz, Thermann et al. 2009). Ago engages a miRNA and mRNA target, then recruits GW182 which associates with deadenylase and decapping enzymes, causing destruction of the targeted mRNA (Eystathioy, Chan et al. 2002; Behm-Ansmant, Rehwinkel et al. 2006). However, GW182 is also able to eject poly(A) binding protein and eIF-4E from a targeted mRNA, and elicit translational repression through mRNA de-circularization (Zekri, Kuzuoglu-Ozturk et al. 2013). Post-transcriptional

control of gene expression via the miRNA pathway affords nuanced utilization of general factors to target specific mRNAs for inhibition.

Activators of mRNA Decay:

Enzymes that carry out destruction of mRNAs frequently do so with the assistance of co-factors that either catalytically activate enzymatic activity, or facilitate access of the enzymes to an mRNA substrate. Purification of decapping activity from *S. cerevisaie* highlights the utility of enzymatic co-activators. Initial work to identify the protein responsible for yeast decapping activity suggested that the Dcp1p protein was enzymatically responsible for 5′ mRNA cap removal. Genetic inactivation of *DCP1* nearly completely blocked decapping, and purified Dcp1p retained the decapping activity (Beelman, Stevens et al. 1996; LaGrandeur and Parker 1998). Several years later, a mutant yeast protein named Dcp2p was identified to be necessary for decapping *in vivo* (Dunckley and Parker 1999), and it was hypothesized that Dcp2p was a co-factor for Dcp1p decapping activity. Further work utilizing recombinant, purified Dcp1p and Dcp2p showed conclusively that Dcp2p was able to catalyze 5′ cap removal on its own but with reduced activity compared with the purified yeast complex. However, co-purification of Dcp1p and Dcp2p dramatically stimulated the decapping activity, redefining Dcp2p as the decapping enzyme, and Dcp1p as an important co-activator of decapping (Steiger, Carr-Schmid et al. 2003).

Nuclear Magnetic Resonance (NMR) structures of Dcp2p and a non-hydrolyzable capped RNA substrate show that Dcp2p specifically binds the 5′ cap structure, as well as electrostatically to the RNA phosphate backbone adjacent to the cap. However, binding alone does not support efficient catalysis. Analysis of *in vitro* decapping by Dcp2p alone, and with the

holoenzyme including Dcp1p, under conditions of excess enzyme to substrate to study single-turnover conditions showed that Dcp1p activates the catalytic activity of Dcp2p 1000-fold (Deshmukh, Jones et al. 2008). Dcp2p appears as a lobed structure, and has been observed in a both "open" and "closed" conformation, with the "closed" conformation being more catalytically active. The mechanism of catalytic activation of Dcp2p by Dcp1p appears to stem from Dcp1p stabilizing the "closed" conformation (She, Decker et al. 2008). In metazoans another co-factor, Hedls, is also required for similar reasons (Fenger-Gron, Fillman et al. 2005).

Decapping is only one step in mRNA destruction, if decapping and 5′ - 3′ decay were not coordinated the cell would have to rely on diffusion to ensure that decapped mRNAs are in fact destroyed. However, the processes of mRNA decapping and 5′ - 3′ decay have been demonstrated to be functionally and physically linked, in *Drosphila;* this is due to physical association of Dcp1 with the 5′- 3′ exonuclease Xrn1/Pacman (Braun, Truffault et al. 2012).

Because translation of mRNAs involves the circularization of the mRNA, both the 5′ cap, and 3′ poly(A) tail are protected. For the decapping enzyme to gain access to the 5′ cap, the circularized mRNA must be remodeled to transition an mRNA from an eIF-4E/eIF-4G/eIF-4A-bound complex to an mRNA bound by the decapping machinery and committed to destruction. One way that this is achieved is through the action of the activators of mRNA decapping: Dhh1p and Pat1p. Deletion of Dhh1p and Pat1p cause accumulation of deadenylated capped mRNAs, indicating that these proteins are involved in a step of mRNA decay post-deadenylation and preceding decapping (Fischer and Weis 2002). Pat1p plays a dual role in this process, wherein it

is able to inhibit small and large ribosomal subunit joining, as well as catalytically activate the decapping enzyme.

Dhh1p also inhibits ribosomal subunit joining but does not affect the catalytic activity of Dcp2p (Nissan, Rajyaguru et al. 2010). Dhh1p is part of the DEAD box helicase family, a plausible mechanism that explains the function of Dhh1p in inhibition of translation initiation may involve Dhh1p facilitation of the removal of the eIF-4F complex through its helicase activity. Intriguingly, Dhh1p was initially found as a high-copy suppressor of both *POP2* and *CCR4* deletions. During this time, *POP2* and *CCR4* were thought to be transcription factors, in time, analysis of the enzymatic activity of Pop2p, and Ccr4p revealed that these proteins function specifically to remove the poly(A) tail. Nonetheless, while the activities of the deadenylase complex had yet to be identified, the authors noted an association between Dhh1p, and the Ccr4p complex (Hata, Sakai, 1998). Much like the link between decapping and 5′- 3′ decay, it is also clear that deadenylation is intimately linked to decapping via physical associations of a functional mRNA destruction complex.

mRNA-Binding Proteins:

RNA-binding proteins are often involved in recruiting specific regulators to an mRNA based on sequence specific recognition of RNA cis-elements. PUF (Pumilio and Fem-binding Factor) proteins serve as an excellent model to study regulation of gene expression via RNA-binding proteins (Murata and Wharton 1995; Zamore, Williamson et al. 1997; Zhang, Gallegos et al. 1997; Wharton, Sonoda et al. 1998).

The PUF domain is defined by eight repeats, each of which confers specificity for a single RNA nucleotide base. A large amount work has been done to identify the sequences that the PUF domain recognizes. Several techniques were used to determine the high-affinity consensus sequence which PUFs bind, among them were: initial identification of the 3′ UTR sequence element that is important for PUF regulation of the *hb* mRNA, RNA immuno-precipitation and microarray detection of mRNAs which associate with PUFs, as well as Systematic Evolution of Ligands by Exponential Enrichment (SELEX). Each of the above referenced experiments revealed a striking detail about PUF RNA-binding, across eukaryotes the high affinity PUF site begins almost invariably with the bases UGUA, highlighting the evolutionary advantage to retaining both the PUF RNA-Binding Domain (RBD) as well PUF Binding Elements (PBEs) in certain mRNAs. The sequence recognized diverges somewhat in the final four nucleotides for each PUF ortholog depending on changes to repeats 5-8, dictating the specific subset of mRNAs each PUF associates with (Gavis 2001).

PUF proteins are found in all eukaryotes, once bound to a target mRNA, PUF proteins repress mRNA expression through mechanisms which are still incompletely understood. Several mechanisms of repression have been proposed to account for the ability of PUF proteins to repress mRNA expression and the common theme involves PUF binding to its target sequence and recruitment of proteins which carry out negative regulation (Wreden, Verrotti et al. 1997; Goldstrohm, Seay et al. 2007; Van Etten, Schagat et al. 2012).

PUF Activation of Deadenylation and mRNA Decay

Deadenylation is functionally linked to mRNA decay through physical interactions between deadenylase and mRNA decay enzymes. These processes work on all mRNAs, however, some mRNAs experience greatly increased rates of deadenylation and decay. PUF proteins in both yeast and humans provide a well documented example of activation of deadenylation and mRNA decay for target mRNAs. In yeast, both Puf4p, and Puf5p bind distinct sites in the 3′ UTR of the *HO* endonuclease. *In vitro* experiments using recombinant Puf4p and Puf5p as well as the deadenylase complex, Ccr4p/Pop2p, demonstrated that both PUFs are able to significantly accelerate the rate of deadenylation *in vitro.* *In vivo* reporter repression assays, as well as analysis of *HO* mRNA deadenylation *in vivo* showed that Puf4p and Puf5p were required for both repression and deadenylation. Interestingly, genetic inactivation of deadenylation completely abolished the ability of Puf4p to repress the reporter, but Puf5p retained its full repressive activity. Deletion of either *PUF4* or *PUF5* dramatically increased the half-life of the *HO* mRNA, and deletion of both PUFs had an additive effect on *HO* half-life; this suggests that the two proteins exert their destabilizing effects through distinct pathways that require deadenylation for Puf4p, and an unknown mRNA decay pathway for Puf5p (Hook Wickens, 2007).

Analysis of the activity of human PUM1 and PUM2 in a HEK293 cell culture model has shown that expression of either PUM strongly reduces PUM-targeted reporter mRNA levels by 78%, and reporter protein by 71%, suggesting that mRNA decay activation by both PUM1 and PUM2 is responsible for the repression of reporter protein output. As interactions between the deadenylase complex and PUFs has been established in yeast, the authors asked whether human

PUMs may also retain a conserved association with the deadenylase complex. Indeed, co-immunoprecipitation of both PUM1 and PUM2 in RNase treated extracts showed that the human deadenylase complex orthologues: CNOT6, CNOT6L, CNOT7, and CNOT8, all associate with human PUMs in the absence of RNA indicating that the interaction is not simply bridged by a co-bound mRNA, or alternatively the associations may reflect an extremely close proximity which protects a small fragment of bridging RNA (Van Etten, Schagat et al. 2012).

CNOT7 and CNOT8 are mammalian orthologs of yeast *POP2* (Shimizu-Yoshida, Sasamoto et al. 1999). In yeast, Puf4p and Puf5p both directly bind Pop2p (Goldstrohm, Hook et al. 2006), and in humans both CNOT7 and CNOT8 directly interact with PUM1 and PUM2 in the absence of any other factors (Van Etten, Schagat et al. 2012). Thus PUF proteins from yeast to humans retain a conserved binding interface that enables a specific interaction with the CCR4/NOT deadenylase complex; the specific residues required for this interaction have yet to be identified. Having established PUM-directed mRNA decay, and interactions with the deadenylase complex *in vivo*, and *in vitro*, the importance of deadenylase activity for PUM repression was tested with the use of dominant negative deadenylase mutants that have a mutated catalytic core; expression of dominant negative CNOT8 inhibited PUM repression in a dose-dependent manner.

The authors also tested the ability of human PUMs to repress an mRNA that does not contain a poly(A) tail. Both *Drosophila*, and human PUFs, are able to repress a non-adenylated mRNA robustly (Chagnovich and Lehmann 2001; Van Etten, Schagat et al. 2012). Interestingly, repression of the non-adenylated reporter by human PUM was no longer associated with a

decrease in mRNA levels; these results indicate that PUF proteins are capable of carrying out repression via multiple mechanisms that appear to be utilizing distinct and separate repressive pathways.

Translational Repression by PUM

As mentioned above, PUM is also capable of repressing a target mRNA through a putative translational mechanism that does not require the presence of a poly(A) tail and does not impact mRNA levels, however, in the case of *Drosphila* PUM, the 5′ cap was found to be necessary for PUM repression; this was interpreted to mean that cap-dependent translation initiation is a target for PUM repression (Chagnovich and Lehmann 2001). Work to identify the effectors of PUM-mediated translational repression of *hb* mRNA identified Brat. Little was known about the mechanism of regulation via Brat at this time, but Brat mutant flies exhibited dysregulation of the spatial pattern of expression for the Hunchback transcription factor in developing embryos.

Because PUM and Nanos are necessary for *hb* regulation the authors tested whether PUM, Nanos, and Brat form a repressive complex. A yeast-four hybrid assay was employed using a GAL4-activation domain fusion library, the PUM RBD, Nanos, and a PBE containing mRNA. This showed that Nanos, the PUM RBD, and Brat form a ternary complex on the PBE RNA. Physical interaction between Nanos, PUM RBD, and Brat was then demonstrated with an *in vitro* binding assay. Finally, a glycine to aspartic acid mutation in Brat (G1330D) was shown to be defective for PUM RBD binding, but still associated with Nanos. As little, if any, effects

on the level of mRNA stability have been noted for pre-zygotic *hb* mRNA, Brat binding to Nanos and PUM was proposed to inhibit translation of *hb* (Sonoda and Wharton 2001).

Previous work had implicated PUM activated deadenylation of *hb* mRNA as the mechanism of translational silencing (Wreden, Verrotti et al. 1997). In an attempt to determine if translation initiation is inhibited by a PUM recruited complex, an inhibitory homologue of eIF-4E, 4E Homologous Protein (4EHP), was tested for involvement in *hb* repression. 4EHP binds to the 5′ cap much like eIF-4E, but 4EHP is unable to bind eIF-4G, this results in the formation of a complex that inhibits translation initiation. Mutant 4EHP alleles caused a shift in the Hunchback gradient in fly embryos, suggesting that it may be involved in *hb* regulation. A direct interaction with Brat was subsequently shown through *in vitro* binding assays. To further delineate 4EHPs role in *hb* regulation the authors formed a ternary Brat/PUM/PBE RNA complex *in vitro*, and asked if 4EHP was capable of binding to this complex, and in fact this was the case. These results were taken to suggest that PUM, Brat, and 4EHP form a repressive complex on *hb* mRNA, and this results in translational repression.

More recently, an intriguing mechanism has been proposed which suggests that the PUM RBD represses translation elongation at a step immediately post-initiation (Friend, Campbell et al. 2012). The authors suggest that the conserved PUF RBD associates with Ago proteins, which are involved in small RNA silencing pathways. Ago proteins are thought to complex with a number of effector proteins, as well as a 22-23nt miRNA which directs the repressive complex to specific mRNAs through base-pairing interactions However, Ago's involvement in PUF repression was reported to not require a miRNA. Also, a component of the translation

elongation machinery, eEF1A, was proposed to be the target of PUF/Ago repression. During translation elongation eEF1A hydrolyzes GTP to GDP which facilitates ribosome translocation to the next codon. *In vitro* GTP hydrolysis assays were used to argue that PUFs inhibit GTP hydrolysis by eEF1A and in this way stall ribosomes immediately after initiation at the start codon (Friend, Campbell et al. 2012). This model proposes a very striking, and completely unexpected mechanism for PUF repression via the conserved RBD. However, this model is generated from a variety of *in vitro* experiments and it will be beneficial to test the validity of it with a system amenable to *in vivo* mechanistic analysis of PUM repression.

The Pumilio N-terminus

Another important detail to consider is that the work implicating Ago and eEF1A was performed using the Pumilio RBD. Initial work on PUM in the developing *Drosophila* embryo utilized only the RBD to rescue a segmentation defect that Pumilio mutants exhibit during *Drosophila* development; however RBD rescue constructs expressed in *Pumilio* mutants were not viable and only marginally rescued the segmentation defect. This indicates that the N-terminus of PUM has activity that is important for mRNA regulation *in vivo* (Wharton, Sonoda et al. 1998). In fact, recent work on *Drosophila* Schneider 2 (S2) cells in culture demonstrated that full-length Pumilio represses its target mRNA 6-fold more strongly than the RBD alone; the repressive activity of the PUM RBD is weak in comparison to the N-terminus of PUM (Weidmann and Goldstrohm 2012).

Three autonomous repressor domains were identified in the Pumilio N-terminus which are each capable of individually exerting strong repression on target mRNAs in a modular fashion (Weidmann and Goldstrohm 2012). Removal of the poly(A) tail generally initiates mRNA decay, and there are several reports of PUF proteins associating with the deadenylase machinery and functionally promoting deadenylation. (Goldstrohm, Hook et al. 2006; Goldstrohm, Seay et al. 2007; Goldstrohm and Wickens 2008; Suh, Crittenden et al. 2009; Van Etten, Schagat et al. 2012) It seems likely that Pumilio may be activating deadenylation, and subsequent decapping, and also translational repression.

When bound to an mRNA, the PUM RBD provides a surface for interaction with negative regulators, lending specificity to general mRNA repression pathways. It is remarkable that this relatively small domain (335 amino acids) is able to exert multiple modes of repression. Activation of deadenylation and mRNA decay, inhibition of translation initiation, as well as blocking translation elongation all has been described. How can these mechanisms be reconciled? There is no doubt that Brat and 4EHP influence *Hb* gradient formation in the developing *Drosophila* embryo, and are capable of forming a ternary complex on the PBE. However, neither Brat, nor 4EHP are required for repression in S2 cells, it may be that in the developing embryo Brat and 4EHP activities augment PUM-activated deadenylation of *Hb* mRNA in a combinatorial manner. Only recently, a report suggested a radical model for repression via the PUM RBD which invoked inhibition of ribosome translocation immediately after initiation (Friend, Campbell et al. 2012). While compelling, it is unclear what contribution the proposed PUM-Ago interaction plays with regard to PUM repression *in vivo*. The specific mechanisms of repression utilized by the PUM RBD remain incompletely understood.

Another unresolved question is: how is yeast Puf5p able to inhibit *HO* mRNA in the absence of deadenylation? Puf5p accelerates the decay of *HO* mRNA, yet decay usually initiates with deadenylation. As with *Drosophila* Pumilio, Puf5p appears capable of exerting multiple mechanisms of repression. One way RNA binding proteins are known to exert regulation is through association with 4EBPs, as is the case with the Cytoplasmic Polyadenylation Element Binding protein (CPEB) (Stebbins-Boaz, Cao et al. 1999). It is possible that Puf5p may cause translational repression through an unknown co-factor, in addition to activation of deadenylation. It is clear that PUFs retain the conserved ability to activate deadenylation and mRNA decay in yeast, flies, and humans. Yet we know much less about the contribution of other repressive pathways. Our understanding of the fundamental processes of development, germ-line maintenance, and synaptic plasticity will be served well through detailed mechanistic definition of PUF repression across eukaryotes.

Chapter Two:

A quantitative assay for measuring mRNA decapping by splinted ligation reverse transcription polymerase chain reaction: qSL-RT-PCR

2.1 Introduction

Eukaryotic mRNAs are capped by a 7-methyl guanosine linked to the mRNA by a 5' to 5' triphosphate – the 5' cap. This structure promotes translation and protects mRNAs from degradation by exoribonucleases (Furuichi, LaFiandra et al. 1977; Green, Maniatis et al. 1983; Schwer, Mao et al. 1998). Enzymatic removal of the cap, referred to as decapping, results in reduced translation and rapid degradation of the mRNA (Coller and Parker 2004).

mRNAs are normally degraded by two competing pathways (Parker and Song 2004; Garneau, Wilusz et al. 2007). In the 5' pathway, decapping follows deadenylation and is catalyzed by the Dcp2 enzyme to produce a 7-methyl-GDP product (Figure 1.1)(Dunckley and Parker 1999; Wang, Jiao et al. 2002; Steiger, Carr-Schmid et al. 2003). The remaining mRNA, with a 5' monophosphate, is rapidly destroyed in a 5' to 3' direction by the exoribonuclease Xrn1 (Figure 1.1)(Hsu and Stevens 1993; Muhlrad, Decker et al. 1994; Muhlrad, Decker et al. 1995). In the 3' decay pathway, deadenylation is followed by exonucleolytic degradation from the 3' end (Muhlrad, Decker et al. 1995; Anderson and Parker 1998; Brown, Bai et al. 2000; Araki, Takahashi et al. 2001; Wang and Kiledjian 2001; Mukherjee, Gao et al. 2002). The DcpS "scavenger" decapping enzyme degrades the remaining capped species, yielding 7-methyl-GMP product (Liu, Rodgers et al. 2002; Liu, Jiao et al. 2004).

Figure 2.1

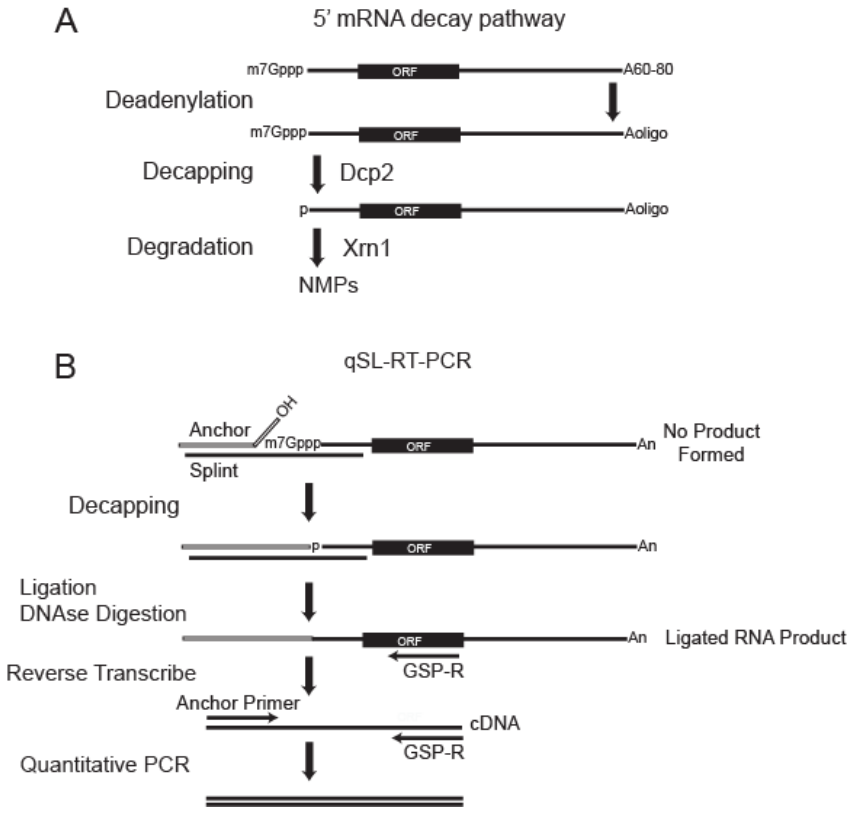

The 5′ mRNA decay pathway. (*A*) mRNAs possess a 5′ 7-methyl guanosine cap (7mGppp), open reading frame (ORF) and a 3′ poly-adenosine tail, averaging 60–80 nt in yeast. mRNA decay via the 5′ pathway initiates with deadenylation of the poly-Adenosine tail to a short oligo-adenylated form (Aoligo). Dcp2 decapping enzyme subsequently removes the cap. The decapped mRNA, with a 5′ monophosphate, is destroyed by Xrn1, producing monophosphorylated nucleotides (NMP). (*B*) Schematic of the quantitative splinted-ligation reverse transcriptase polymerase chain reaction assay (qSL-RT-PCR). First, Anchor RNA and complementary DNA Splint oligonucleotides are annealed to the 5′ end of the target mRNA. mRNAs containing a 5′ cap cannot be ligated, as the cap prevents ligation. Decapped RNAs have a 5′ monophosphate that is ligated to the Anchor RNA 3′ hydroxyl by T4 DNA ligase. After ligation, the splint is destroyed by DNase I. The ligated RNA is converted to cDNA by reverse transcription with a reverse gene-specific primer (GSP-R). The resulting cDNA is then detected by quantitative PCR using GSP-R and a forward primer that anneals to the anchor (Anchor Primer). An internal control qPCR is performed on the same cDNA samples using gene-specific primers that amplify within the coding sequence of the mRNA.

Decapping is highly regulated (Franks and Lykke-Andersen 2008). Trans-acting proteins modulate decapping activity. Decapping of specific mRNAs is influenced by cis-acting sequences and the sequence-specific RNA-binding factors that recognize them. Small RNAs also affect decapping (Rehwinkel, Behm-Ansmant et al. 2005; Behm-Ansmant, Rehwinkel et al. 2006). Assays that measure the decapped products are essential to study regulation of decapping. The ideal assay should be sensitive, rapid, reproducible, and have a broad linear range. The reagents should be readily available, and the assay should be feasible for any mRNA. In this report, we describe a new quantitative assay for detecting decapped mRNAs. First, discussion of previous assays is informative.

Detection of decapped mRNA produced *in vivo* has been a longstanding challenge. Several methods have been utilized including: selective binding to anti-cap antibody (Muhlrad, Decker et al. 1994; Muhlrad, Decker et al. 1995; Beelman, Stevens et al. 1996; Dunckley and Parker 1999; He and Jacobson 2001), selective degradation by Xrn1 (Hsu and Stevens 1993; Fischer and Weis 2002), and by trapping mRNA decay intermediates with a strong secondary structure (Decker and Parker 1993; Poole and Stevens 1997). Primer extension has been used to detect capped and uncapped RNA (Hsu and Stevens 1993; Muhlrad, Decker et al. 1995; Schwer, Mao et al. 1998; Coller, Tucker et al. 2001; Hu, Sweet et al. 2009; Hu, Petzold et al. 2010). Ligation mediated RT-PCR was also employed (Fromont-Racine, Bertrand et al. 1993; Couttet, Fromont-Racine et al. 1997; Couttet and Grange 2004). Recently, a modified ligation method was developed to detect decapped mRNAs by RT-PCR (Hu, Sweet et al. 2009; Hu, Petzold et al. 2010). A bridging DNA oligonucleotide – a "splint" – mediates specific and efficient ligation of a 5' anchor RNA oligonucleotide to the mRNA of interest. This splinted ligation method has

been used to create hybrid RNAs *in vitro* (Moore and Query 2000) and for detection of small RNAs (Maroney, Chamnongpol et al. 2007; Maroney, Chamnongpol et al. 2008) and 5' ends of bacterial mRNAs (Celesnik, Deana et al. 2007; Celesnik, Deana et al. 2008).

In this report, we advance the splinted ligation method to create a quantitative decapping assay with broad linear response and sensitivity, hereon referred to as quantitative splinted ligation reverse transcription PCR assay, or qSL-RT-PCR. This method measures decapped mRNA levels with at least four orders of magnitude in detection range from as little as 1.5 nanograms of total cellular RNA. We then apply qSL-RT-PCR to measure the *in vivo* decapping rate of the *RPL41A* mRNA.

2.2 Results

The qSL-RT-PCR assay specifically detects and quantitates decapped mRNA. With the goal of measuring decapped mRNA, we coupled splinted ligation with reverse transcription and quantitative polymerase chain reaction. The *RPL41A* mRNA from *Saccharomyces cerevisiae* (encoded by YDL184C) was used because the 5' end is mapped and the mRNA is abundant (50 copies per cell)(Yu and Warner 2001). *RPL41A* coding sequence is closely related to *RPL41B,* yet these mRNAs differ substantially in their UTR sequences, making it possible to develop a detection strategy specific for *RPL41A* (Yu and Warner 2001). An overview of the qSL-RT-PCR assay is shown in Figure 2.1B. First, an RNA Anchor oligonucleotide is ligated to the 5' end of the mRNA of interest. The 5' half of the DNA splint specifically anneals to the 5' end of the mRNA of interest while the 3' half anneals to an Anchor RNA oligonucleotide. DNA ligase joins the 3' hydroxyl of the RNA anchor to the 5' monophosphate of the decapped mRNA. Following ligation, the DNA splint is destroyed by DNAse 1. Next, the ligated RNA is purified and analyzed by quantitative RT-PCR.

To begin the qSL-RT-PCR assay, total RNA was purified from yeast cells lacking the *XRN1* gene (Figure 2.1A). This genetic background stabilizes the decapped mRNA to permit efficient detection (Muhlrad, Decker et al. 1995). qSL-RT-PCR was performed to measure the cycle threshold (Ct) and melting temperature of the amplified product. Reactions were separated by agarose gel electrophoresis to detect the expected product of 224 basepairs (Figure 2.2A, lane 1). As an internal control, the *RPL41A* was detected using standard qRT-PCR with specific

primers to amply an internal 158 basepair product (Figure 2.2A, lane 2).

Control reactions are necessary to demonstrate specificity of the assay (Figure 2.2B). First, RNA was treated with the exoribonuclease, Terminator, which selectively degrades uncapped mRNA, but not capped mRNA. Terminator abolished detection of decapped mRNA (Figure 2.2A, lane 3). As a positive control, mRNA was decapped with Tobacco Acid Pyrophosphatase (TAP), which increased the amount of decapped *RPL41A* mRNA detected (Figure 2.2A, lanes 5). Total *RPL41A* was detected by qRT-PCR in these samples (Figure 2.2A, lanes 4 and 6). We note that TAP treatment did not decrease the Ct of qSL-RT-PCR to equivalent value of qRT-PCR. Several considerations account for this: First, the amplicons and forward primer differ, and therefore parameters of reverse transcription and quantitative PCR differ. Second, the qSL-RT-PCR signal depends on the efficiency of Anchor ligation and TAP. Importantly, the TAP control demonstrates that qSL-RT-PCR detects an increase in decapped *RPL41A* mRNA in Δxrn1 cells (Figure 2.2A, compare lanes 1 and 5) and Δdcp2 cells (Figure 2.2A, compare lanes 11 and 13). Ligation of the anchor RNA to the decapped mRNA is requisite for detection by qSL-RT-PCR (Figure 2.2B). Therefore, omission of DNA ligase is an important negative control that resulted in loss of signal from the qSL-RT-PCR assay (Figure 2.2A, lane 7), but does not affect the internal qRT-PCR (Figure 2.2A, lane 8). This control is crucial to exclude artifactual amplification by residual DNA splint. To control for DNA contamination, mock reverse transcription reactions were performed wherein reverse transcriptase is omitted (Figure 2.2B). As expected, no product was detected by either assay (Figure 2.2A, lanes 9 and 10).

Figure 2.2

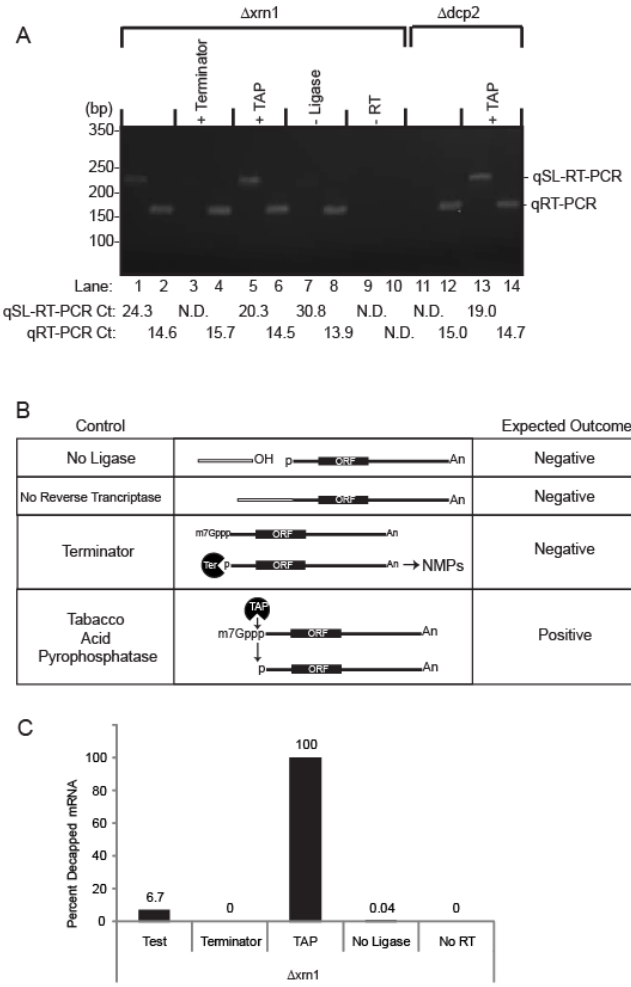

The qSL-RT-PCR assay specifically detects decapped mRNA. (*A*) qSL-RT-PCR was used to detect endogenous decapped *RPL41A* mRNA present in 10 µg of total RNA isolated from yeast strains lacking either the *XRN1* (Δxrn1) or the *DCP2* (Δdcp2) genes (odd-numbered lanes). Standard qRT-PCR was used to detect total *RPL41A* RNA (even-numbered lanes). In control reactions, total RNA was treated as indicated at the *top* of the gel, including Terminator (lanes *3*,*4*) or Tobacco Acid Pyrophosphatase (+TAP) treatment (lanes *5*,*6*,*13*,*14*). In lanes *7* and *8*, DNA ligase was omitted (−Ligase). Reverse transcriptase was omitted from reactions in lanes *9* and *10* (–RT). Cycle thresholds measured for each sample are indicated at the *bottom* of the figure. Reactions that did not yield a detectable cycle threshold are labeled "N.D." (Not Detected). (*B*) Critical controls for the qSL-RT-PCR assay demonstrate specificity for decapped mRNA. Control reactions are indicated on the *left*. In the *middle*, a diagram of each control is depicted. On the *right*, the expected outcome of qSL-RT-PCR is indicated for each control reaction. (Terminator) The Terminator enzyme specifically destroys uncapped mRNA with a 5′ monophosphate but does not degrade capped mRNA, thereby demonstrating specificity of the assay for decapped RNA. Tobacco Acid Phosphatase removes 5′ cap, leaving a 5′ monophosphate that is detected by the qSL-RT-PCR assay, thereby serving as a positive control. (No ligase) Omission of DNA ligase prevents ligation of anchor to mRNA, thereby preventing amplification of product. (No Reverse Transcriptase) In the absence of reverse transcriptase, no product should be generated, thereby demonstrating dependence on cDNA conversion of mRNA. (*C*) Relative amounts of decapped *RPL41A* mRNA in *A* were determined for the indicated reactions from the strain lacking Xrn1. Calculations are described in the Materials and Methods.

To further validate the detection of decapped mRNA, RNA was purified from cells lacking decapping enzyme, Dcp2 (Wang, Jiao et al. 2002; Parker and Song 2004). In this strain, no decapped *RPL41A* was detected by qSL-RT-PCR (Figure 2.1A, lane 11), yet *RPL41A* mRNA was present (Figure 2.2A, lane 12). This result demonstrates that the decapped *RPL41A* is generated by Dcp2. When this RNA sample was treated with TAP, decapped RNA was readily detected by qSL-RT-PCR (Figure 2.2A, lane 13). We conclude that the qSL-RT-PCR specifically detects decapped mRNA.

To compare the amounts of decapped mRNAs, we used the comparative Ct method (Livak and Schmittgen 2001; Schmittgen and Livak 2008). Ct values (Figure 2.2A) from the qSL-RT-PCR assay were normalized to the total amount of *RPL41A* using Ct values from qRT-PCR for that sample. The amount of decapped *RPL41A* was then calculated relative to the TAP treated sample (Figure 2.2A, lanes 5 and 6), which was set to 100% for detected decapped *RPL41A* mRNA (Figure 2.2C). In the test sample, 6.7% of the *RPL41A* mRNA was decapped and detectable by qSL-RT-PCR. Terminator treatment completely destroyed decapped mRNA. When DNA ligase was omitted, the relative amount of decapped mRNA was 0.04%, or 147 fold below the test sample, thus background signal was low. Taken together, we conclude that the qSL-RT-PCR assay is highly specific for decapped mRNA and can measure differences in the amount of decapped mRNA.

Figure 2.3

A

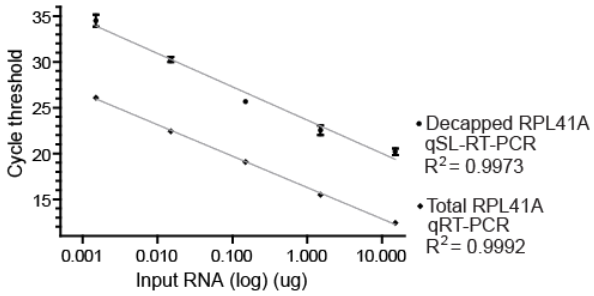

B

	Total RPL41A qRT-PCR			Decapped RPL41A qSL-RT-PCR		
Input RNA (ug)	Mean Ct	SD	n=3	Mean Ct	SD	n=3
15	12.43	0.05		20.20	0.35	
1.5	15.52	0.03		22.56	0.52	
0.15	19.09	0.07		25.68	0.19	
0.015	22.43	0.01		30.28	0.28	
0.0015	26.10	0.08		34.52	0.65	

C

	Total RPL41A qRT-PCR			Decapped RPL41A qSL-RT-PCR			Fold Above Background
	Mean Ct	SD	n=3	Mean Ct	SD	n=3	
WT	13.77	0.38		31.53	0.05		2.53
WT, No Ligase	13.86	0.13		32.87	0.16		
Δxrn1	13.12	0.20		24.31	0.03		171
Δxrn1, No Ligase	13.44	0.19		31.73	0.76		

D

	Total YLR084C qRT-PCR			Decapped YLR084C qSL-RT-PCR			Fold Change
	Mean Ct	SD	n=3	Mean Ct	SD	n=3	
Δxrn1	24.61	0.08		31.57	0.1		5.81 increase
Δxrn1, with TAP	24.86	0.11		29.03	0.15		
Δxrn1, with Terminator	25.49	0.17		37.08	0.34		45.6 decrease
Δxrn1, No Ligase	24.42	0.03		N.D.	N.D.		
Δxrn1, No RT	36.46	0.51		N.D.	N.D.		

The qSL-RT-PCR assay has a broad, linear dynamic range for sensitive detection of decapped *RPL41A* RNA. (*A*) Five 10-fold serial dilutions of total RNA from Δxrn1 cells were analyzed using qSL-RT-PCR and qRT-PCR assays to detect decapped and total *RPL41A* mRNA, respectively. Triplicate samples were analyzed and the mean cycle threshold (Ct) values are plotted against input RNA amount (15, 1.5, 0.15, 0.015, and 0.0015 µg) on a logarithmic scale. Standard deviation is indicated above and below each data point. (*B*) Mean Ct values and standard deviations (SD) from *A* are shown in the table. Nonlinear regression analysis was used to determine correlation coefficients (R^2) for each curve. (*C*) qRT-PCR and qSL-RT-PCR assays were performed on 10 µg of total RNA to measure *RPL41A* mRNA in wild-type BY4742 cells (WT) and Δ*xrn1*. Mean Ct values and standard deviations are indicated as determined from triplicate samples. Fold increase above background was calculated relative to control reactions lacking T4 DNA ligase for each strain, determined from ΔCt of qSL-RT-PCR. (*D*) qRT-PCR and qSL-RT-PCR assays were performed on 7.5 µg of total RNA to measure *YLR084C* mRNA in Δ*xrn1* cells. Control samples were treated with TAP or Terminator. T4 DNA ligase or Reverse Transcriptase were omitted from control reactions as indicated. Mean Ct values and standard deviations are indicated and were determined from triplicate samples. Fold change in decapped mRNA level was calculated from the ΔCt of qSL-RT-PCR values. Reactions that did not yield a detectable cycle threshold are labeled "N.D." (Not Detected).

The qSL-RT-PCR assay has a broad linear detection range and high sensitivity. To determine the detection range and sensitivity of the qSL-RT-PCR, the amount of input RNA was varied. Total RNA was purified from yeast cells (Δ*xrn1*) and a series of ten-fold dilutions were made. Three replicate dilutions series were made to assess variability. qSL-RT-PCR was performed on each sample and the resulting mean Ct values were plotted against the amount of input RNA (Figure 2.3A). Both decapped and total *RPL41A* mRNA were detected over the entire range of RNA concentrations. Signal of the decapped mRNA was proportional to the input RNA. Linearity of the response was excellent: non-linear regression analysis yielded correlation coefficients of $R^2 = 0.9793$ for qSL-RT-PCR and $R^2 = 0.9992$ for qRT-PCR (Figure 2.3A). Strikingly, decapped *RPL41A* was measured in as little as 1.5 nanograms of input RNA. These results were reproducible, as shown in Figure 2.3A, in which plots the mean Ct values for three replicates are graphed with standard deviations for each measurement. Because standard deviations are small, the values are also listed in Figure 2.3B. These results demonstrate that the qSL-RT-PCR assay provides a sensitive means to measure decapped mRNA with a broad, linear detection range and excellent reproducibility.

Based on the observed sensitivity, we tested the ability of qSL-RT-PCR to detect decapped *RPL41A* mRNA in wild-type cells. Equal mass of RNA (10 μg), purified from wild-type or Δ*xrn1* yeast cells, was analyzed by qRT-PCR and qSL-RT-PCR. The mean Ct values were determined for each assay from three replicates (Figure 2.3C). As a control for false-positive background signal, DNA ligase was ommitted from control reactions. The amount of *RPL41A* mRNA in each strain was measured by qRT-PCR (Figure 2.3C). In Δxrn1 cells, decapped mRNA was detected 171 fold above background (ΔCt=7.42, P=0.000074), whereas in

wild-type cells, decapped RNA was 2.53 fold above background (ΔCt=1.43, P=0.00018). Therefore, decapped *RPL41A* mRNA was detectable in wild-type cells, though the signal is close to background under these conditions. It is noteworthy that Hu and coworkers detected decapped mRNA in wild-type cells using splinted ligation and RT-PCR (Hu, Sweet et al. 2009; Hu, Petzold et al. 2010). As expected, decapped mRNA is stabilized by deletion of *XRN1* and, therefore, is readily detectable above background.

To further demonstrate the sensitivity of qSL-RT-PCR, we tested its ability to detect a low abundance, cell cycle regulated mRNA encoded by the *YLR084C* gene. *YLR084C* mRNA was measured by qRT-PCR from replicate RNA purifications from Δ*xrn1* strain and detected at a mean Ct of 24.61 (Figure 2.3D), which is approximately 1000 fold below that of *RPL41A* (Mean Ct ~ 14, Figure 2.2A and 2.3C). To detect decapped *YLR084C* mRNA, we first mapped the 5' end of this mRNA using 5' rapid amplification of cDNA ends. A specific splint DNA oligonucleotide was created and used in the qSL-RT-PCR assay to detect decapped *YLR084C* mRNA (Mean Ct = 31.57, Figure 2.3D). Treatment of the RNA with TAP increased the decapped *YLR084C* by 5.81 fold, whereas Terminator treatment decreased it by 45.6 fold (Figure 2.3D). Ommision of ligase completely abolished detection of decapped *YLR084C* mRNA but had no effect on detection by qRT-PCR (Figure 2.3D). Ommision of reverse transcriptase resulted in significant loss of detection of both total and decapped *YLR084C* mRNA (Figure 2.3D). Taken together, the results presented here demonstrate that qSL-RT-PCR detects abundant (*RPL41A*) and rare (*YLR084C*) decapped mRNAs.

Figure 2.4

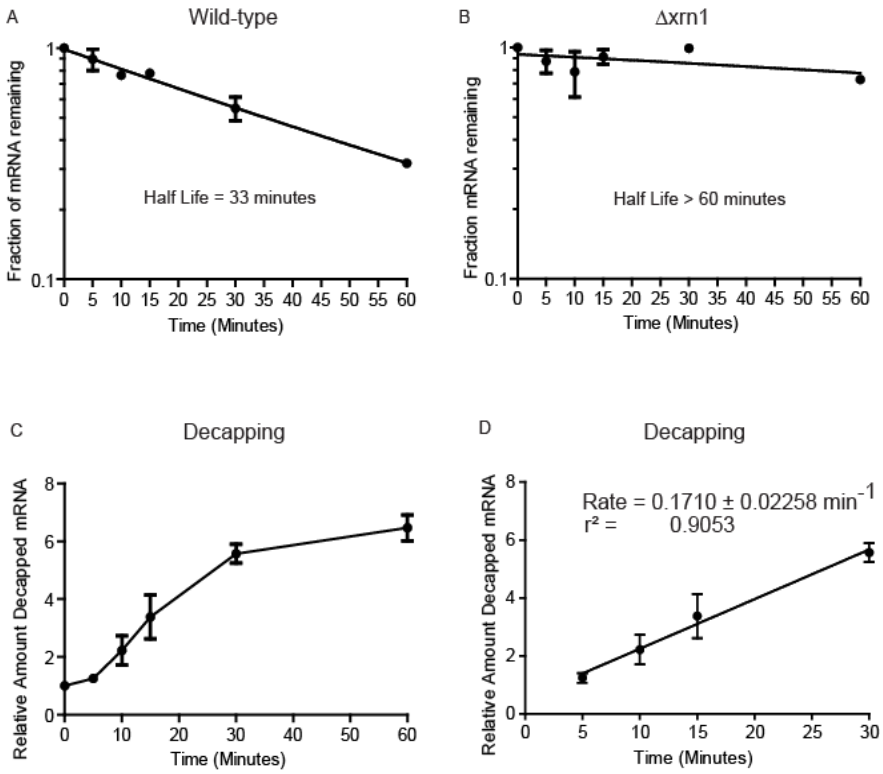

The in vivo decapping rate of *RPL41A* mRNA was determined using qSL-RT-PCR assay. The half-life of *RPL41A* was measured in wild-type yeast (*A*) and in a strain wherein the *XRN1* gene is deleted (Δ*xrn1*) (*B*). (*C*) Decapped *RPL41A* mRNA was measured using the qSL-RT-PCR assay in the Δ*xrn1* strain following transcription shutoff. Relative amount of decapped RNA was calculated after normalization to total *RPL41A* at each time-point, relative to time = 0. (*D*) The rate of decapping was determined by linear regression analysis of the data in the graph in *C* with linear reaction kinetics between 5 and 30 min. The slope of the line, the reaction rate, is shown along with error and correlation coefficient. In all graphs, the mean value of the replicates is plotted and standard error is indicated above and below the data points.

Measurement of in vivo decapping rate. To determine the rate of decapping of *RPL41A* mRNA *in vivo*, transcription was inhibited with Thiolutin, samples were collected at time points, and accumulation of decapped *RPL41A* was measured. The half-life of *RPL41A* is 33 minutes in wild-type yeast cells (Figure 2.4A). To measure the accumulation of decapped mRNA, degradation was blocked by deletion of *XRN1* gene, which greatly stabilized *RPL41A*, with over 70% of the mRNA remaining after 60 minutes (Figure 2.4B). Thus, *RPL41A* mRNA is predominantly degraded by the 5' pathway. qSL-RT-PCR was then performed on each time

point. The resulting Ct values were normalized to total *RPL41A* detected in that sample. Next, the amount of decapped *RPL41A* at each time point was determined using the comparative Ct method (Schmittgen and Livak 2008). As expected, decapped *RPL41A* increased over the time course (Figure 2.4C). Mean Ct values from biological replicates were plotted with standard error for each measurement (Figure 2.4). The resulting curve demonstrated a brief lag phase during the first 5 minutes, followed by a linear phase until 30 minutes (Figure 2.4C). The curve then plateaus between 30 and 60 minutes. The linear phase between 5 and 30 minutes was analyzed using linear regression analysis. The slope of the resulting line measures the rate constant of 0.171 +/- 0.0226 min^{-1}. Therefore, qSL-RT-PCR detected accumulation of decapped endogenous mRNA and measured the decapping rate constant.

2.3 Discussion

In this report, we develop a quantitative assay, qSL-RT-PCR, that measures decapped mRNA produced *in vivo* by natural mRNA decay. The assay is versatile; any endogenous mRNA may be analyzed using qSL-RT-PCR. The assay has broad dynamic range with a linear response over four orders of magnitude of input RNA (Figure 2.3). The sensitivity of qSL-RT-PCR far exceeds northern blotting. Indeed, decapped mRNA can be detected from as little as 1.5 nanogram of total cellular RNA (Figure 2.3). The measurements are highly reproducible (Figures 2.3 and 2.4). qSL-RT-PCR is fast and all of the reagents are readily available.

The specificity of qSL-RT-PCR is a major strength. By design, qSL-RT-PCR measures only one species - decapped mRNA. Specificity is imparted by splinted ligation; T4 DNA ligase has strong preference for perfect base pairing on each side of the nick to be ligated (Engler 1982; Wu and Wallace 1989). A 3' hydroxyl and 5' monophosphate are essential for ligation; therefore, RNAs that do not receive a 5' cap (with a 5' triphosphate) or degradation products from RNase A (with a 5' hydroxyl) are not detected. Specificity also imposes restrictions. First, the mRNA's 5' end must be mapped with single nucleotide resolution. Second, decapped products that are dephosphorylated or trimmed will not be detected. Third, competing decay pathways may diminish the magnitude of decapped RNA (He and Jacobson 2001).

When performing qSL-RT-PCR, we recommend optimization of several parameters. First, the critical controls described here should be performed. To optimize splinted ligation, the length of the DNA splint oligonucleotide is important – longer splints work better. The effect of splint length on ligation efficiency was systematically investigated: greater than 40 base pairs of complementarity worked best (Kurschat, Muller et al. 2005). Titration of the splint can improve the assay and reduce background. Efficient DNase I digestion of the splint after ligation is crucial. PCR conditions should be optimized, specifically primer design and amplification efficiencies.

Measurement of decapping rates *in vivo* has proven difficult, yet meeting this challenge is essential to study regulation of decapping. We have demonstrated the ability of qSL-RT-PCR to measure the decapping rate constant of a natural mRNA. To stabilize the decapped mRNA, 5' decay must be inhibited by inactivation of Xrn1. As no specific inhibitors of Xrn1 have been identified, Xrn1 was inactivated genetically. In other eukaryotes, genetic inactivation or RNAi-mediated depletion of Xrn1 may block decay of decapped mRNAs, thereby permitting determination of decapping rates.

Comparison of the *RPL41A* decapping rate with the previously estimated rates for *MFA2* and *PGK1* mRNAs is informative. *MFA2* and *PGK1* mRNAs, modified with a secondary structure, were monitored by Northern blot (Muhlrad and Parker 1992; Muhlrad, Decker et al. 1995; Cao and Parker 2001). The half-life of oligo-adenylated mRNA intermediate was measured for each mRNA and used to calculate respective decapping rate constants (Cao and Parker 2001). In Figure 2.5, we compare the decapping rates of all three mRNAs. For reference,

the first-order decay rates of each mRNA, calculated from their half-lives, are plotted on the same graph (Figure 2.5).

From this data, several observations emerge. First, the decapping rate constants measured by the two methods are similar in magnitude (*MFA2* = 0.462 min^{-1}, *PGK1* = 0.2772 min^{-1}, *RPL41A* = 0.171 min^{-1}). Second, the mRNAs with short half-lives are decapped faster than those with longer half-lives (Figure 1.5). Third, decapping rates are faster than the decay rate, indicating that decapping is not the rate-determining step. Indeed, deadenylation is often the rate-limiting step of mRNA decay (Shyu, Belasco et al. 1991; Muhlrad and Parker 1992; Decker and Parker 1993). Interestingly, the *in vivo* decapping rates are slower than those measured *in vitro* with purified enzyme and substrate (Jones, Quang-Dang et al. 2008). This discrepancy likely reflects competitive binding of other proteins to the cap *in vivo*, such as eIF4E, or perhaps limiting concentration of decapping enzyme. We anticipate that qSL-RT-PCR assay will prove useful for analysis of other RNAs and processes, for instance other processing events such as

Figure 2.5

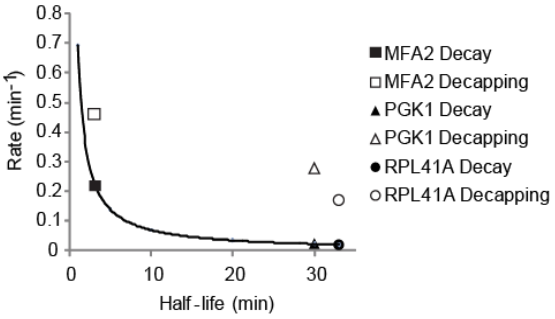

Comparison of mRNA half-life, decay, and decapping reaction rates. The reaction rates of decay (in black) and decapping (in white) are compared with mRNA half-lives of three mRNAs, *MFA2*, *PGK1*, and *RPL41A*. Decay rates were derived from each mRNA's half-life. The trend-line curve plots the decay rate for mRNAs with half-lives ranging from 1 to 33 min. Decapping rates and mRNA half-lives for *PGK1* and *MFA2* were measured previously by Northern blot analysis of the poly(*G*) tract containing RNA (Muhlrad and Parker 1992; Muhlrad et al. 1995; Cao and Parker 2001). *RPL41A* decapping rate and half-life were measured by qSL-RT-PCR and qRT-PCR, respectively, as shown in Figure 4.

endonucleolytic cleavage (Gatfield and Izaurralde 2004; Doma and Parker 2006; Eberle, Lykke-Andersen et al. 2009; Tomecki and Dziembowski 2010). Lastly, the ability to monitor decapping rates of natural mRNAs *in vivo* will greatly facilitate study of the features and factors that regulate decapping to control decay and translation.

2.4 Materials and Methods

Yeast Strains

AGY81: BY4742 MATalpha his3delta1 leu2delta0 lys2delta0 ura3delta0 Open Biosystems

AGY95: BY4742 MATalpha xrn1::KANr

AGY39: yRP1358 MATa his4-539 leu2-3112 lys2-201 trp1 ura3-52 ***dcp2::TRP1***

(Dunckley and Parker 1999)

Oligonucleotides: Synthetic oligonucleotides were purchased from Integrated DNA technologies.

NB33: Anchor RNA oligonucleotide

5’-GCUGAUGGCGAUGAAUGAACACUGCGUUUGCUGGCUUUGAUG-3’

NB34: *RPL41A* splint

5’GCTCTCATTTCGATTGAATCGATGTGGTCTCATCAAAGCCAGCAAACGCAGTGTTC ATTCATCGCCATCAGC-3’

NB35: Anchor forward PCR primer

5’-GCTGATGGCGATGAATGAACACTGC-3’

NB39: *RPL41A* reverse PCR primer

5’-CTAACATGTTAATTCATCAATGACATTACGATACTCTTG-3’

NB47: *RPL41A* forward PCR primer

5’-GAGAGCCAAGTGGAGAAAGAAGAGAACTAGA-3’

NB62: *YLR084C* splint

5’GGGATGATTAAAGCGCACACTTTCCTTCCATCAAAGCCAGCAAACGCAGTGTTCAT TCATCGCCATCAGC-3’

NB56: *YLR084C* reverse transcription primer

5’-GAGTGTCCAGAGACGATGAACAAAC-3’

NB58: *YLR084C* reverse PCR primer

5’- GTTTTCTCTTGCGTTTCTTCGTTTCCCG-3’

NB63: *YLR084C* forward PCR primer

5’-GCGCTTTAATCATCCCCATACTAGACTTTG-3’

RNA purification: Yeast cultures were grown in YPAD media at 30 °C to an $O.D._{600nm}$ of 0.8. Cells were harvested at 4000 x g for 10 minutes and washed once with H_2O, and suspended in 400 µL of TES (10 mM Tris-HCl pH 6.8, 10 mM EDTA, 0.2% w/v SDS). Next, the RNA was extracted using acid phenol (pH 4.3) at 65 °C, extracted twice with chloroform, and precipitated with ethanol and 0.3 M sodium acetate (pH 5.2) at -20 °C. RNA was pelleted by centrifugation and washed with 70% ethanol. Purified RNA was resuspended in RNAse-free H_2O and analyzed using a Nanodrop spectrophotometer (Thermo Scientific) and by formaldehyde gel electrophoresis.

Transcription shut-off: To measure mRNA decay rates, thiolutin, provided by Pfizer, was used to inhibit transcription (Jimenez, Tipper et al. 1973; Passos and Parker 2008). Cultures of yeast (35 mL) were grown in YPAD to an $O.D._{600nm}$ of 0.8. Cells were treated with 5 µg/mL thiolutin and 5 mL samples were collected at the indicated times. Cells were pelleted at 13,000 x g for 1 minute and rapidly frozen in a dry ice-ethanol bath. Total RNA was then extracted from each sample.

Splinted-Ligation: Total RNA (10 µg, unless otherwise indicated) was mixed with 20

picomoles of *RPL41A* splint oligonucleotide NB34 and 30 picomoles of RNA anchor NB33. For *YLR084C,* 7.5 □g of total RNA was mixed with 20 picomoles of splint NB62 and 30 RNA anchor NB33. To anneal oligos, samples were sequentially incubated for 5 minutes from 70 ºC to 60 ºC to 42 ºC and finally to 25 ºC. Next, 20 units RNase Inhibitor Plus (Promega), 20 units High Concentration T4 DNA ligase (Promega) and T4 DNA ligase buffer were added to each sample and incubated overnight at 15 ºC. To degrade the splint and genomic DNA, each sample was treated with 10 units of RQ1 DNase (Promega) or Turbo DNase (Ambion) in the supplied 1 x DNase buffer for up to 3 hours at 37 ºC. RNA was then extracted using acid-phenol:chloroform and then chloroform. The RNA was precipitated with ethanol and 0.3 M sodium acetate (pH 5.2) and 20 µg glycoblue co-precipitant (Ambion). After washing with 70% ethanol, the RNA was suspended in 13.3 µL RNase-free H_2O.

Reverse transcription: Prior to reverse transcription, RNA samples were treated with DNase 1 to destroy any contaminating genomic DNA. For splinted ligation samples, this step is incorporated into the Splinted Ligation method, described above. One unit of RQ DNase 1 (Promega) was used per µg of total RNA. DNase treatment was performed in supplied DNase buffer for 1 hour at 37 ºC. Reactions were then heat-inactivated for 15 minutes at 65 ºC in 1 x DNase stop buffer. Two µg, unless otherwise noted, of DNase-treated RNA was added to reverse transcriptase assays. Reverse transcription reactions contained 20 picomoles of gene-specific reverse primer (NB39 for *RPL41A* or NB56 for *YLR084C),* 0.5 mM each dNTP, 1.2 mM $MgCl_2$, 1 x GoScript buffer, and 1 µL of GoScript (Promega) in a 20 µL reaction and incubated 1 hour at 42 ºC, then heat-inactivated 15 minutes at 65 ºC.

Quantitative PCR: Amplification of PCR products was measured using GoTaq qPCR master mix (Promega) with 200 nM of each primer in 50 µL reactions. For detection of splinted ligation

products, the anchor forward PCR primer NB35 and *RPL41A* reverse PCR primer NB39 were used with 2 µL of template cDNA from splinted ligation reactions. For detection of total *RPL41A* mRNA, primers NB47 and NB39 were used. Splinted ligation product of *YLR084C* was detected using NB35 and NB58. Total *YLR084C* mRNA was detected using NB58 and NB63. A Bio-Rad CFX 96 C1000 real-time PCR instrument was used for all assays. Cycling parameters were: Step 1) 95 ºC for 2 minutes, 2) 95 ºC for 30 seconds, 3) 57 ºC for 30 seconds, 4) 72 ºC for 40 seconds with steps 2-4 repeated 40 cycles. Reactions were analyzed by thermal melting curve and by gel electrophoresis. PCR amplification efficiencies of each primer set were determined (Pfaffl 2001). Primers NB35 and NB39 amplification efficiency was 102.7% and primers NB47 and NB39 were 102.9%.

Tobacco Acid Pyrophosphatase treatment: Ten µg total RNA was decapped by treatment with 20 units RNase Inhibitor Plus (Promega) and 5 units Tabacco Acid Pyrophosphatase (Epicentre Biosystems) in the supplied 1 x TAP buffer for 30 minutes at 37 ºC.

Terminator treatment. Ten µg of total RNA was incubated with 20 units RNase Inhibitor Plus and 10 units of Terminator (Epicentre Biosystems) in the supplied 1 x Terminator buffer for 30 minutes at 37 ºC.

Data analysis. Quantitative PCR assays were analyzed and cycle threshold (Ct) values determined using CFX Manager software (Bio-Rad). Calculations and graphs were created using Graphpad Prism version 5.0. Students t-test was used to measure significance. Relative changes were calculated using the comparative Ct method, ΔΔCt (Livak and Schmittgen 2001; Schmittgen and Livak 2008). First, the Ct value from qSL-RT-PCR assay for each timepoint sample ("target") was normalized to the Ct of total *RPL41A* detected by qRT-PCR in that same sample ("reference") by calculating $\Delta Ct_{test} = Ct_{target\ test} - Ct_{reference\ test}$. For time-course

experiments, the ΔCt of decapped *RPL41A* RNA at time = 0 minutes ("calibrator") was calculated using the equation $\Delta Ct_{calibrator} = Ct_{target\ calilbrator} - Ct_{reference\ calibrator}$. The ΔΔCt for each timepoint was then calculated from the equation $\Delta\Delta Ct = \Delta Ct_{test} - \Delta Ct_{calibrator}$. Relative expression for each timepoint was then calculated using the equation Ratio = $2^{-\Delta\Delta Ct}$ (Livak and Schmittgen 2001; Schmittgen and Livak 2008). The relative amount of decapped RNA detected, relative to time = 0 minutes, was then plotted against the time the sample was harvested following transcription shutoff. The decapping rate was then determined by linear regression curve fitting using GraphPad Prism. The measured rate was 0.1710 +/- 0.0228 min^{-1} with a correlation coefficient of 0.9053 between 5 and 30 minutes determined from two biological replicates (Figure 3).

To determine the percentage of decapped RNA (Figure 2), relative expression was determined using the ΔΔCt method (Livak and Schmittgen 2001; Schmittgen and Livak 2008). To do so, $\Delta\Delta Ct = \Delta Ct_{test}$ was calculated for each sample (including test, terminator treated, TAP treated, no DNA ligase, and no reverse transcriptase controls) and - $\Delta Ct_{calibrator}$ was calculated using the TAP treated sample as the "calibrator". Next, the ratio relative was calculated and the TAP treated sample (ratio = 1) was set to 100%.

RPL41A mRNA half-lives were determined from the qRT-PCR analysis of time-course samples following addition of Thiolutin transcription inhibitor (Figure 4A and B). The amounts of mRNA remaining at each timepoint relative to time = 0 minutes were determined from Ct values by calculating $2^{\Delta Ct}$ where ΔCt = [Ct (calibrator t=0) - Ct (test timepoint)]. Half-life of *RPL41A* in wild-type cells is based on six biological replicates and half-life in Δxrn1 cells is determined from two biological replicates. The resulting data was then plotted against time and non-linear regression analysis of three biological replicate samples were fitted using first order decay

kinetics (GraphPad Prism 5)(Figure 4A and B). mRNA decay rates for *RPL41A*, *PGK1*, and *MFA2* (Figure 5) were calculated from the measured mRNA half-lives (Muhlrad and Parker 1992; Muhlrad, Decker et al. 1995) using the equation Rate = $\ln(2)/(t_{1/2})$.

Acknowledgements

We thank members of the Goldstrohm lab and Dr. Trista Schagat for helpful discussions. We thank Pfizer for providing Thiolutin. In addition, we thank Dr. Wenqian Hu for his intellectual contributions. Nathan Blewett was supported by the Cellular and Molecular Biology Training Grant NIH NIGMS 5T32GM007315-34. Jeff Coller is supported by a grant from the National Institute of Health (GM080465).

Chapter 3

An eIF4E-binding protein promotes mRNA decapping and is required for PUF repression

3.1 INTRODUCTION

Precise regulatory mechanisms are crucial for the execution of gene expression programs and integration of signals. As intermediaries between genes and proteins, messenger RNAs (mRNAs) are an important nexus for regulation. Post-transcriptional control of mRNA stability and translation is achieved through the concerted action of RNA binding factors, RNA decay enzymes and the translation machinery (Parker and Song 2004; Sonenberg and Hinnebusch 2009). Specific mRNAs are targeted for regulation by RNA binding factors that recognize sequences often found in the 3' untranslated region (3'UTR). One class of regulator is PUF proteins (Pumilio and Fem-3 binding factor) (Wickens, Bernstein et al. 2002; Miller and Olivas 2011), defined by a conserved RNA binding domain that mediates high affinity binding to specific, 8-10 nucleotide, single-stranded RNA sequences (Murata and Wharton 1995; Zamore, Williamson et al. 1997; Zhang, Gallegos et al. 1997; Wang, McLachlan et al. 2002; Lu, Dolgner et al. 2009). PUFs control diverse biological processes including cell proliferation, development, fertility, and neurological functions (Lehmann and Nusslein-Volhard 1987; Lin and Spradling 1997; Wreden, Verrotti et al. 1997; Zhang, Gallegos et al. 1997; Forbes and Lehmann 1998; Asaoka-Taguchi, Yamada et al. 1999; Parisi and Lin 1999; Crittenden, Bernstein et al. 2002; Schweers, Walters et al. 2002; Dubnau, Chiang et al. 2003; Menon, Sanyal et al. 2004; Kedde,

van Kouwenhove et al. 2010; Chen, Zheng et al. 2012). At the root of these functions lies the ability of PUFs to repress protein production from target mRNAs (Miller and Olivas 2011). The preponderance of evidence indicates that the major mechanism of PUF mediated translational repression is by enhancing mRNA degradation (Olivas and Parker 2000; Goldstrohm, Hook et al. 2006; Miller and Olivas 2011; Weidmann and Goldstrohm 2012). In several cases, PUFs were shown to accelerate mRNA decay by removal of the 3' poly(adenosine) tail (Olivas and Parker 2000; Chagnovich and Lehmann 2001; Gamberi, Peterson et al. 2002; Goldstrohm, Hook et al. 2006; Goldstrohm, Seay et al. 2007; Hook, Goldstrohm et al. 2007). PUFs were also reported to inhibit translation (Wharton, Sonoda et al. 1998; Sonoda and Wharton 2001; Gu, Deng et al. 2004; Cho, Gamberi et al. 2006; Chritton and Wickens 2010). A remaining challenge is to discover the co-repressors and mechanisms of PUF mediated repression.

S. cerevisiae possess six PUFs, each of which bind a distinct set of mRNAs, dictated by their unique RNA binding specificities (Wickens, Bernstein et al. 2002; Gerber, Herschlag et al. 2004). Puf4p and Puf5p/Mpt5p bind multiple mRNAs (Gerber, Herschlag et al. 2004; Seay, Hook et al. 2006) and share at least one well-characterized target, the mRNA encoding *HO* endonuclease, which catalyzes switching of mating type (Tadauchi, Matsumoto et al. 2001; Goldstrohm, Hook et al. 2006; Hook, Goldstrohm et al. 2007). Puf4p and Puf5p were previously shown to bind specific sites in the *HO* mRNA 3'UTR and accelerate deadenylation and degradation of the message (Goldstrohm, Hook et al. 2006; Hook, Goldstrohm et al. 2007). Deadenylation is essential for repression by Puf4p (Hook, Goldstrohm et al. 2007); however, Puf5p can still repress *HO* mRNA when deadenylation was blocked by deletion of the *CCR4* gene (Goldstrohm, Hook et al. 2006), which encodes the major deadenylase (Tucker, Valencia-

Sanchez et al. 2001; Tucker, Staples et al. 2002; Goldstrohm, Seay et al. 2007). This finding indicated that Puf5p can repress by a second, deadenylation independent mechanism (Hook, Goldstrohm et al. 2007). Additional co-repressor(s) may be necessary for Puf5p activity.

We report here that an eIF4E binding protein (4E-BP), Eap1p, serves as an essential co-repressor for Puf5p. 4EBPs are found throughout eukaryotes and are thought to inhibit translation by binding to the 5' cap bound initiation factor eIF4E, thereby blocking interaction with initiation factor, eIF4G (Sonenberg and Hinnebusch 2009). 4E-BPs possess a conserved eIF4E binding motif, YxxxxL (φ indicates a hydrophobic amino acid, x indicates any residue) (Haghighat, Mader et al. 1995; Mader, Lee et al. 1995). 4E-BPs might globally reduce cap-dependent translation; however, specific examples demonstrate more specialized roles (Sonenberg and Hinnebusch 2009). Two 4E-BPs have been identified in *S. cerevisiae*, Caf20p and Eap1p (Altmann, Schmitz et al. 1997; Cosentino, Schmelzle et al. 2000). Both contain an eIF4E-binding motif, but are otherwise unrelated. Neither protein is essential for growth under standard conditions, but several mutant phenotypes have been described (Chial, Stemm-Wolf et al. 2000; Cosentino, Schmelzle et al. 2000; Mendelsohn, Li et al. 2003; Ibrahimo, Holmes et al. 2006; Meier, Deloche et al. 2006; Sezen, Seedorf et al. 2009). Eap1p was originally identified based on its ability to bind to eIF4E and was shown to compete with eIF4G (Cosentino, Schmelzle et al. 2000). Therefore, like other 4E-BPs, Eap1p was proposed to repress by inhibiting translation initiation.

In this work, we show that Eap1p is required for Puf5p mediated mRNA repression, but is not necessary for Puf4p function. In contrast, Caf20p is fully dispensable for regulation by

both Puf4p and Puf5p. Translational analysis demonstrates that Eap1p does not affect global translation nor does it inhibit poly-ribosome association of Puf5p targeted mRNAs. Instead, we identify a novel activity of Eap1p to promote degradation of specific mRNAs, including a Puf5p target mRNA. Intriguingly, this activity is facilitated by the interaction of Eap1p with eIF4E. We find that deletion of *EAP1* gene causes deadenylated, capped mRNA to substantially accumulate, indicating that Eap1p functions to promote removal of the mRNA's 5' 7-methyl guanosine cap. In accordance, co-immunoprecipitation experiments indicate that Eap1p associates with Puf5p and the decapping factor Dhh1p. Together, these results provide a new regulatory mechanism for a member of the diverse class of eIF4E binding proteins: enhancement of mRNA decapping.

3.2 RESULTS

The eIF4E binding protein, Eap1p, is essential for Puf5p mediated repression. To identify co-repressors necessary for PUF mediated repression, we undertook a genetic approach using a reporter gene that is repressed by Puf4p and Puf5p (Goldstrohm, Hook et al. 2006; Hook, Goldstrohm et al. 2007). The *HIS3-HO* 3'UTR reporter gene was created by replacing the open reading frame of *HO* with the auxotrophic marker gene *HIS3* (Fig. 3.1A)(Goldstrohm, Hook et al. 2006). In wild type cells, wherein Puf4p and Puf5p levels do not fully silence the reporter, introduction of the reporter confers histidine biosynthesis and thus growth on medium lacking histidine (Fig. 3.1B, WT strain). As previously demonstrated (Goldstrohm, Hook et al. 2006; Hook, Goldstrohm et al. 2007), increased expression of Puf4p or Puf5p repressed *HIS3-HO* expression, thereby abrogating growth in the absence of histidine (Fig. 3.1B, wild type strain with *PUF5* and *PUF4* expression plasmids). Importantly, repression depends on the PUF binding sites and the RNA binding activity of each PUF (Goldstrohm, Hook et al. 2006; Hook, Goldstrohm et al. 2007). If a co-repressor is required for PUF repression, deletion of its gene will result in loss of repression and thus growth on medium lacking histidine. We tested candidate genes with known roles in mRNA degradation and translational control. Deletion of one gene encoding a 4E-BP, *EAP1,* abrogated Puf5p repression, but had no effect on Puf4p repression (Fig. 3.1B, *eap1* strain with *PUF5* versus *PUF4*). Therefore, *EAP1* is necessary for Puf5p repression and dispensable for Puf4p function, indicating a unique mode of repression by

Puf5p. Because Eap1p binds to eIF4E (Cosentino, Schmelzle et al. 2000), our data suggests that Puf5p may repress translation using Eap1p as a co-repressor.

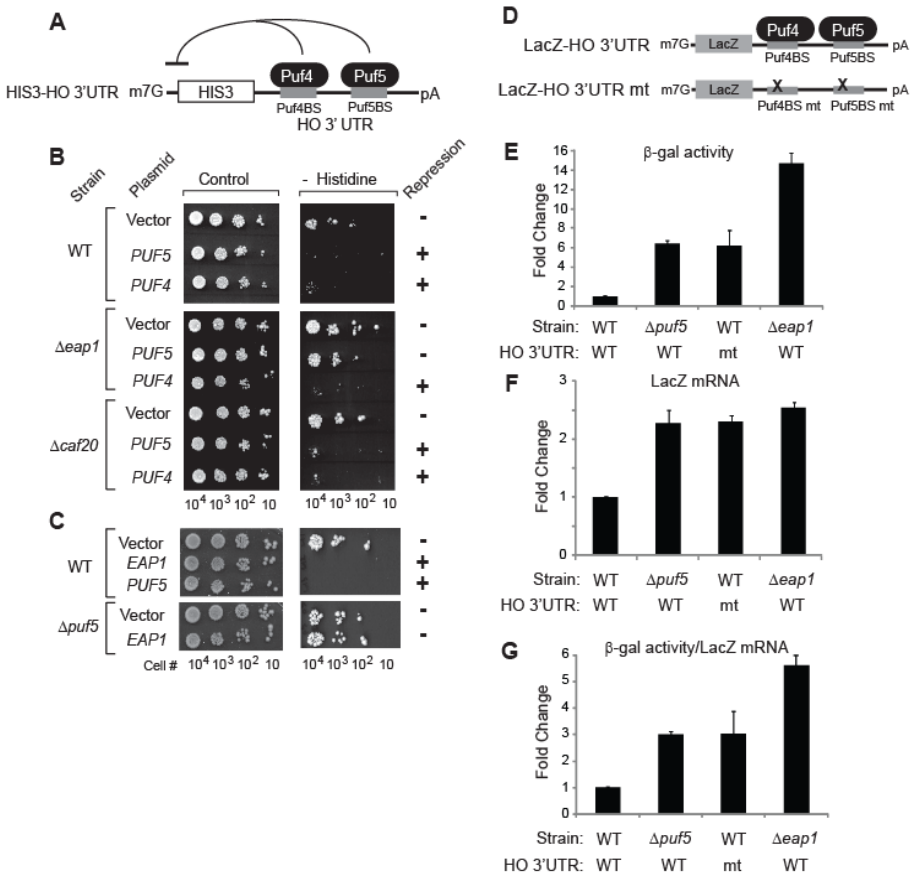

FIG. 3.1 *EAP1* is required for Puf5p mediated repression. A) The *HIS3-HO 3'UTR* reporter contains the *HIS3* open reading frame (ORF) with the *HO* 3' untranslated region (3'UTR) containing Puf4p (Puf4BS) and Puf5p (PUF5BS) binding sites. **B)** Growth assays measure repression of *HIS3-HO* reporter in wild type (WT), *eap1* (Δ*eap1*) or *caf20* (Δ*caf20*) deletion strains transformed with plasmids expressing *PUF4*, *PUF5*, or control plasmid. The indicated number of cells were spotted onto media with histidine (control) or without histidine (-histidine). Repression by each gene was scored by no growth on media lacking histidine, "+", or growth "-". **C)** Growth assay for repression by *PUF5* and *EAP1* in wild type and *puf5* deletion (□*puf5*) cells. **D)** Diagram of the *LacZ-HO* 3'UTR reporter mRNA. The *LacZ HO* 3'UTR mt reporter was created by mutating the Puf4p and Puf5p binding sites (Puf4BS mt and Puf5BS mt). **E)** Graph of □-galactosidase activity from wild type (WT) or mutant (mt) *LacZ* reporters measured from equal number of wild type (WT), □*puf5* or □*eap1* cells. Fold change in relative light unit values are plotted relative to wild type reporter in wild type cells. **F)** Graph of fold change in *LacZ HO* (WT or mt) mRNA levels, as measured by northern blot (Fig. S1) and calculated relative to wild type reporter in wild type cells. G) Graph of fold change in ratio of β-galactosidase activity in Panel E to LacZ mRNA level in panel F. In each graph, mean values are plotted with standard error from multiple biological replicates.

We also tested the second known yeast 4E-BP, *CAF20*. In contrast to Eap1p, Caf20p is not necessary for repression by either *PUF4* or *PUF5*, as revealed by the ability of each PUF to repress in cells lacking the *CAF20* gene (Fig. 3.1B, Δ*caf20*). This indicates that Puf4p represses through a separate mechanism that does not require a 4E-BP.

To further measure the contribution of Eap1p to Puf5p to repression, we created a reporter gene encoding β-galactosidase (β-gal) controlled by the *HO* 3'UTR (*LacZ-HO* 3'UTR, Fig. 3.1D). Protein expression from *LacZ-HO* was measured from identical number of cells using a luminescence-based β-gal activity assay in three genetic backgrounds: wild type, *eap1* deletion, and *puf5* deletion. If Eap1p and Puf5p function together to repress *HO*, then β-gal activity should increase when each is absent. Indeed, deletion of *PUF5* resulted in a 6.5-fold increase in β-gal activity relative to wild type (Fig. 3.1E) and deletion of *EAP1* caused a 14.8-fold fold increase (Fig. 3.1E). As a positive control for comparison, mutation of both PUF binding sites (Fig. 3.1D, *LacZ-HO* 3'UTR mt) resulted in a 6.2-fold increase (Fig. 3.1E)(Hook, Goldstrohm et al. 2007). These results indicate that Eap1p represses β-gal synthesis or promotes its decay.

To gain additional insight, the steady-state level of *LacZ* mRNA was measured by northern blot (Fig. 3.S1). Deletion of *EAP1* increased *LacZ-HO* mRNA by 2.5-fold (Fig. 3.1F), suggesting that Eap1p represses *LacZ* mRNA synthesis or promotes mRNA degradation. Consistent with their role in promoting decay of *HO* mRNA, PUF binding site mutations or deletion of *PUF5* caused a 2.3-fold increase the reporter mRNA (Fig. 3.1F). Deletion of *EAP1* increased the ratio of β-gal activity to *LacZ* mRNA by 5.6-fold relative to wild type cells (Fig.

3.1G), suggesting that the amount of protein synthesized per mRNA may increase. Together, our data demonstrate that both Puf5p and Eap1p repress a target mRNA and that Puf5p activity is dependent on Eap1p. The results show that Eap1p reduces both protein and mRNA expression and, given that 4E-BPs are generally thought to inhibit translation, we next investigated the affect of Eap1p on *HO* translation.

Eap1p does not inhibit poly-ribosome association of a Puf5p regulated mRNA. 4E-BPs are proposed to inhibit translation by blocking interaction of eIF4E and eIF4G during initiation (Sonenberg and Hinnebusch 2009). In this context, we hypothesized that Puf5p may utilize Eap1p to inhibit *HO* translation. To measure the effect of Eap1p on the translation state of *HO* mRNA, we performed sucrose gradient ultracentrifugation to separate ribosome bound and unbound mRNAs. If Eap1p inhibits initiation, Eap1p should decrease the percentage of *HO* mRNA bound to ribosomes (ribosome occupancy) and reduce the number of ribosomes bound to *HO* mRNA. Therefore, deletion of *EAP1* should increase the ribosome occupancy and density of *HO* mRNA.

To test these predictions, cell extracts from wild type and *eap1* deletion strains were separated on 7-47% sucrose gradients. Each gradient was fractionated while monitoring UV absorption to show separation of 80S ribosomes and poly-ribosomes (Fig. 3.2A and 3.2B), corroborated by ethidium bromide staining of ribosomal RNAs (Fig. 3.2C). The chromatograms of wild type and *eap1* deletion strains were highly similar, indicating that Eap1p does not substantially alter global translation (compare Fig. 3.2A, WT and Fig.3.2B, Δ*eap1*).

We next detected *HO* mRNA in the gradient fractions from three biological replicates to quantitate *HO* translation state. In wild type cells, 97% of total *HO* mRNA was in poly-ribosome bound fractions (Fig. 3.2D and 3.2E, WT, fractions 7-19). For comparison, the average ribosome occupancy for mRNAs in *S. cerevisiae* is 71% (Arava, Wang et al. 2003). *HO* mRNA was predominantly detected in fractions containing 3 or more ribosomes, steadily increasing into the fractions containing 7 or more ribosomes (Fig. 3.2D, WT fractions 9-19). Less than 1% of *HO* mRNA was found in ribosome free fractions (Fig. 3.2D, fraction 1-3) and only 2% was present in fractions containing mono-ribosomes (Fig. 3.2D, lanes 1-9). As a control, poly-ribosomes were dissociated with EDTA. This treatment caused *HO* mRNA to shift from the bottom to the top of the gradient (Fig. 3.S2), consistent with *HO* being poly-ribosome associated. These results indicate that *HO* mRNA efficiently engages with ribosomes in wild type cells, contradicting the prediction that Eap1p inhibits translation initiation of *HO* mRNA.

Next, the effect of Eap1p on *HO* translation state was investigated. Deletion of *EAP1* did not alter the ribosome occupancy of *HO* mRNA; 98% associated with poly-ribosomes, nearly identical to wild type (Fig. 3.2D and 2E, Δ*eap1* fractions 7-19). Like wild type, less than 1% of *HO* mRNA was present in the ribosome free fractions (Fig. 3.2D, Δ*eap1,* fractions 1-3). The ribosome density of *HO* mRNA actually *decreased* slightly in the *eap1* deletion strain, with the peak density shifting from poly-ribosome fraction 16 in wild type cells to less dense fraction 15 in *eap1* deletion cells (Fig. 3.2D and 2.2E, Δ*eap1*). These observations contradict the prediction that deletion of *EAP1* would increase ribosome occupancy and density of *HO* mRNA.

Figure 3.2.

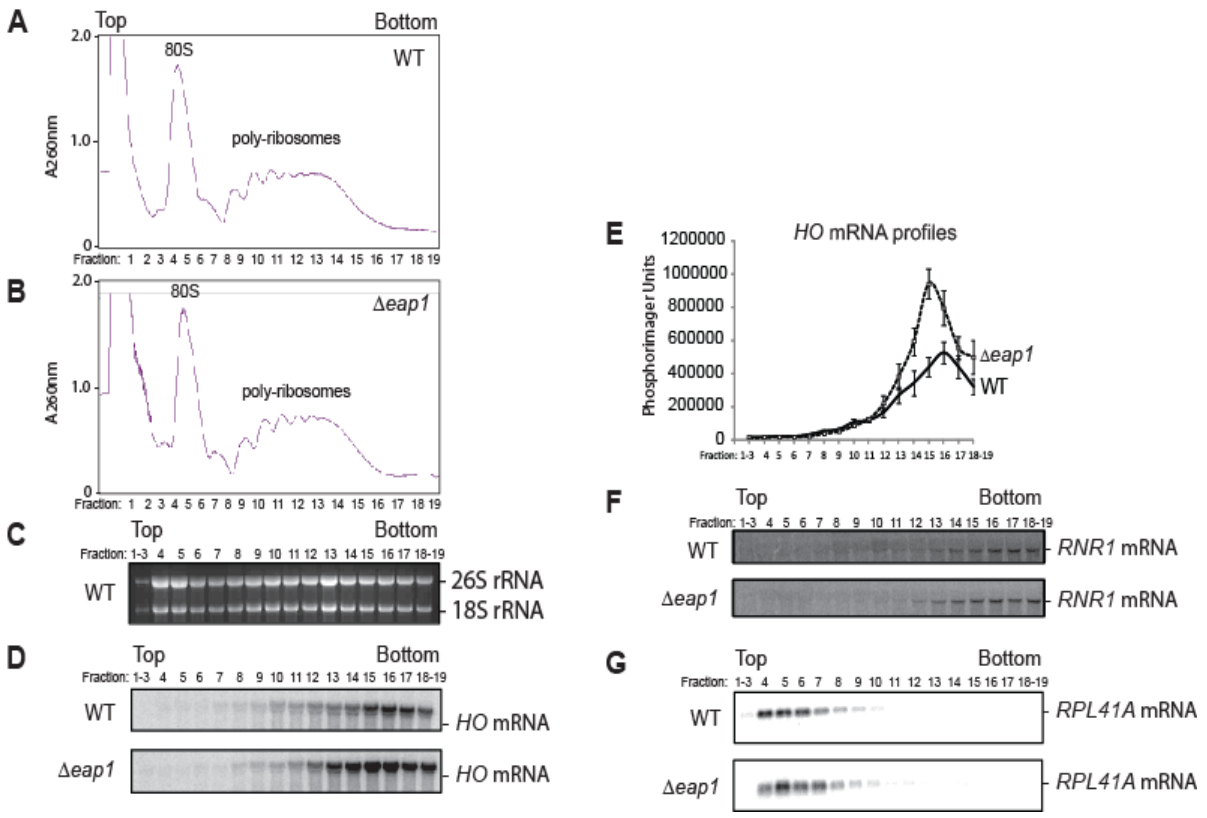

FIG. 3.2 Eap1p does not inhibit poly-ribosome association of a Puf5p regulated mRNA. Ribosome profiles of sucrose density gradients from wild type (WT) (**A)** and *eap1* deletion (Δ*eap1*) **(B)** cells. UV absorbance at 260 nm (A260 nm) was measured during collection of fractions to generate the chromatograms. "Top" and "Bottom" refer to the relative position in the gradient tube. Ribosome species are indicated within the chromatogram. **C)** The ethidium bromide stained gel shows the ribosomal RNA (26S and 18S rRNA) content of each fraction from WT cells. **D)** Northern blot of *HO* mRNA in gradient fractions from wild type (WT) and Δ*eap1* strains. **E)** Quantitation of *HO* mRNA profile across gradient fractions from three biological replicate samples of wild type and Δ*eap1* strains. Mean values are plotted with standard errors. Northern blot of *RNR1* **(F)** and *RPL41A* **(G)** mRNAs in gradient fractions from wild type (WT) and Δ*eap1* strains.

The major difference observed between wild type and *eap1* deletion strains is a change in the abundance of *HO* mRNA, which increased by 1.7 fold in the *eap*1 deletion (Fig. 3.2D and 3.2E, Δ*eap1*). We conclude that Eap1p does not inhibit translation initiation of *HO* mRNA but instead decreases the abundance of *HO* mRNA, suggesting an effect on *HO* mRNA synthesis or stability.

We also investigated the effect of Eap1p on the translation state of two mRNAs that are not PUF targets: the ribonucleotide reductase mRNA, *RNR1*, and the large ribosomal subunit protein L47 mRNA, *RPL41A* (Gerber, Herschlag et al. 2004; Goldstrohm, Hook et al. 2006; Seay, Hook et al. 2006). Like *HO, RNR1* is a low-abundance, cell-cycle regulated mRNA with a large ORF of 2667 nucleotides (compared to *HO* ORF 1761nt). The distribution of *RNR1* mRNA was not altered by Eap1p (Fig. 3.2F). All *RNR1* associated with poly-ribosomes in wild type and *eap1* deletion cells (Fig. 3F. compare fractions 12-19 from WT and *Δeap1*). *RPL41A* is an abundant mRNA with a 78 nucleotide ORF that engages, on average, one ribosome in wild type cells (Fig. 3.2G, WT, peak fractions 4-6)(Arava, Wang et al. 2003). The ribosome association of *RPL41A* mRNA was not altered by deletion of *EAP1* (Fig. 3.2G, *Δeap1*). Therefore, *EAP1* does not change the ribosome association of two mRNAs that are not targeted by PUFs.

Eap1p associates with poly-ribosomes. We next evaluated whether Eap1p associates with ribosomes. If Eap1p blocks translation initiation, then Eap1p would be expected to be found exclusively in translationally inactive, ribosome free fractions of the sucrose gradient. Eap1p with a FLAG tag was expressed in the *eap1* deletion strain and extracts were fractionated

by sucrose density gradients using conditions that separate ribosomal subunits, mono- and poly-ribosomes (Fig. 3.3A). Three peaks of Eap1p were observed in the gradient fractions. At the top of the gradient, a peak was present in the ribosome free fractions (Fig. 3.3A, fractions 1 and 2). A second peak cofractionated with 60S ribosomal subunit (Fig. 3.3A, fraction 5 and 6). A third major peak of Eap1p fractionated with poly-ribosomes (Fig. 3.3A, fractions 14-16). Interestingly, a slower migrating Eap1p species was observed in the first two gradient fractions, perhaps the result of post-translational modification(s).

Eap1p binds eIF4E and this interaction may mediate Eap1p association with poly-ribosomes. First, we assessed the distribution of eIF4E in the gradient fractions. Western blot of eIF4E revealed that the protein was distributed throughout the gradient, with a major peak at the top of the gradient (Fig. 2.3A, middle panel, fractions 1-4) and a secondary peak corresponding to the 80S mono-ribosome (Fig. 2.3A, fractions 6-8). Like Eap1p, eIF4E was also present in poly-ribosome fractions (Fig. 2.3A, fractions 9-16). To test if Eap1p binding to eIF4E is necessary for poly-ribosome association, the eIF4E binding motif, $Y_{109}XXXXL_{114}$, was mutated by introducing two alanine substitutions, Y109A and L114A, to create Eap1p mt (Cosentino, Schmelzle et al. 2000). This mutant was expressed in the *eap1* deletion strain and then extract from these cells was fractionated on a sucrose gradient. The Eap1p mutant was only detected in the first three fractions at the top of the gradient (Fig. 2.3A, Eap1 mt, fractions 1-3), indicating that association of Eap1p with poly-ribosomes is dependent on binding to eIF4E.

Figure 3.3.

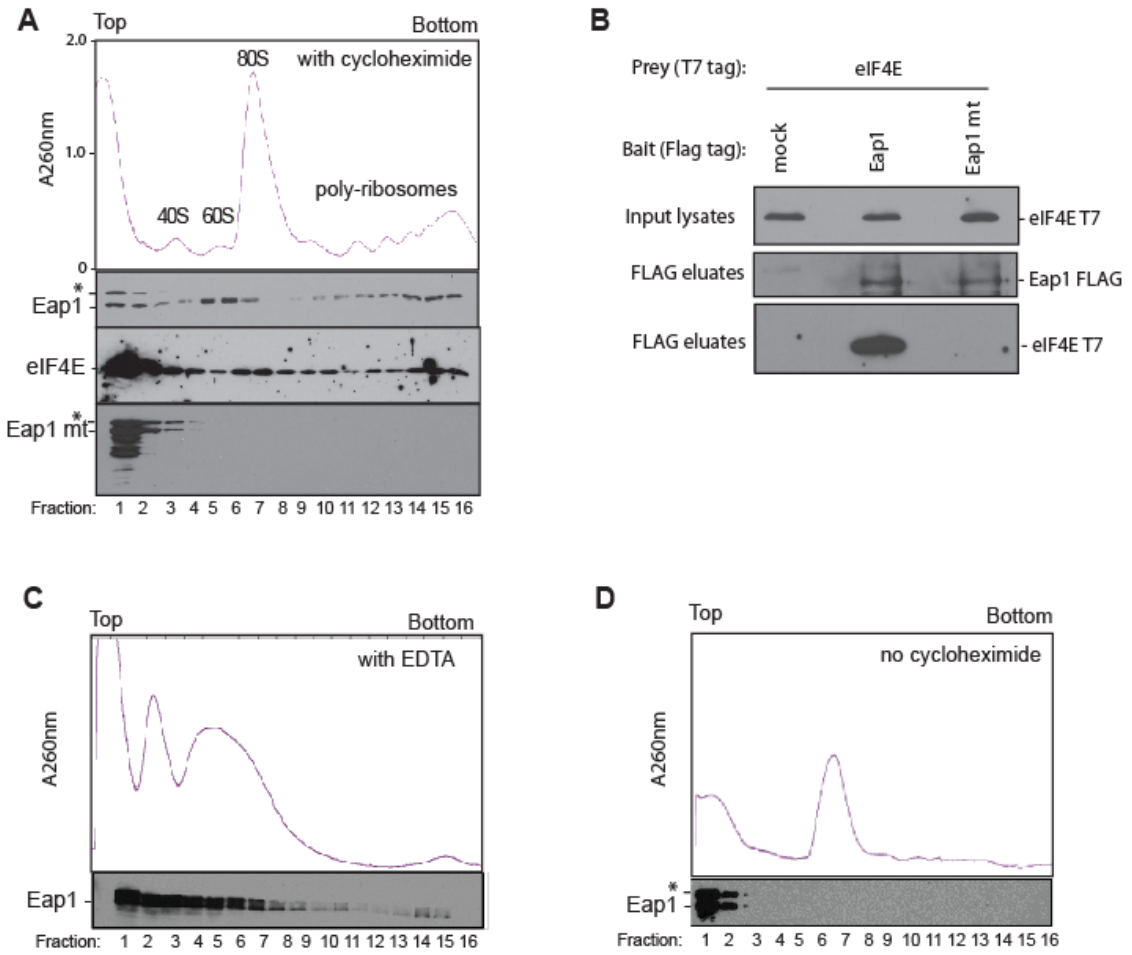

FIG. 3.3. Eap1p fractionates with poly-ribosomes. A) Top panel: Absorbance (A260 nm) chromatogram of sucrose density gradient of sample from *eap1* deletion strain expressing FLAG-tagged Eap1p with T7-tagged eIF4E. Western blots of wild type Eap1p (second panel), eIF4E (third panel) and Eap1p with mutations in the eIF4E binding motif, Y109A and L114A, (Eap1 mt, bottom panel) in gradient fractions. Cycloheximide was present in each sample. Western blot of Eap1 mt was over-exposed 10 fold relative to wild type Eap1. The "*" indicates Eap1p with slower electrophoretic mobility than the expected 70 kDa size. **B)** Western blots of RNase treated immunoprecipitations of FLAG-tagged, wild type or mutant Eap1p from cells co-expressing T7-tagged eIF4E. Mock FLAG immunoprecipitation was from cells expressing eIF4E-T7 but not Eap1p-FLAG. **C)** Chromatogram from cell extracts treated with EDTA to dissociate poly-ribosomes. FLAG-tagged Eap1p was detected by western blot. **D)** Chromatogram from extracts incubated in the absence of cycloheximide resulted in ribosome run-off and accumulation of 80S ribosomes. Eap1p was detected by western blot.

To confirm that Eap1p mt no longer bound to eIF4E, wild type Eap1p or Eap1p mt were immunoprecipated. eIF4E was detected only in the wild type Eap1p immunoprecipitate (Fig. 3.3B); therefore, the mutations disrupted interaction with eIF4E.

Two controls were performed to verify that Eap1p associated with poly-ribosomes. First, extracts were treated with EDTA, resulting in collapse of poly-ribosomes into 40S and 60S peaks (Fig. 3.3C) and causing Eap1p to fractionate predominantly at the top of the gradient (Fig. 3.3C, fractions 1-7). Importantly, the portion of Eap1p that fractionated with poly-ribosomes in wild type cells (Fig. 3.3A, fractions 9-16) was greatly diminished (Fig. 3.3C, fractions 9-16). Second, ribosomes were allowed to elongate and "run-off" by omitting cycloheximide (Lee, Udagawa et al. 2007), resulting in accumulation of 80S particles (Fig. 3.3D, fractions 6-7). If Eap1p is engaged with translating poly-ribosomes, then run-off should cause Eap1p to shift into lighter fractions. Indeed, Eap1p was only detected at the top of the gradient (Fig. 3.3D, fractions 1-2). Collectively, these data indicate that Eap1p associates with poly-ribosomes. This finding was unexpected and is not consistent with the model that Eap1p inhibits translation initiation. Instead, our findings indicate that Eap1p may promote a distinct mode of repression that remained to be discovered.

Eap1p accelerates mRNA decay. Puf5p promotes degradation of the mRNAs it targets (Goldstrohm, Hook et al. 2006; Seay, Hook et al. 2006; Goldstrohm, Seay et al. 2007; Hook, Goldstrohm et al. 2007). Because Eap1p serves as a co-repressor for Puf5p, and that *HO* (Fig. 3.2D) and *LacZ-HO* 3'UTR (Fig. 3.1F) mRNA levels increased in the *eap1* deletion, we reasoned that Eap1p may affect mRNA decay. To test this hypothesis, mRNA decay rates were measured in the presence or absence of Eap1p. Cells were treated with thiolutin to inhibit transcription and RNA samples were collected over time. Next, specific mRNAs were detected by northern blot (Fig. 3.4). In wild-type cells, *HO* mRNA half-life was 12 minutes (Fig. 3.4A), consistent with past measurements (Goldstrohm, Hook et al. 2006; Hook, Goldstrohm et al. 2007). Deletion of *EAP1* dramatically stabilized *HO*, increasing the half-life to 41 minutes (Fig. 3.4A). These results represent the first demonstration that *EAP1* affects the rate of mRNA decay.

We next tested whether the interaction of Eap1p with eIF4E was required for acceleration of mRNA decay. To do so, the *eap1* deletion strain was complemented with plasmid expressing either wild type Eap1p (*EAP1*) or eIF4E binding defective mutant (*EAP1* mt). *HO* mRNA half life was then measured in each strain. When wild type Eap1p was expressed in *eap1* deletion cells, *HO* mRNA half-life was 7.5 minutes (Fig. 3.4A, Δ*eap1* + *EAP1*), a substantial reduction relative to 41 minutes in the *eap1* deletion and slightly shorter than the 12 minutes observed in wild type cells. These results, summarized in Figure 4E, support the conclusion that Eap1p promotes *HO* mRNA decay. Eap1p mt also accelerated decay of *HO* mRNA, resulting in a half life of 20 minutes (Fig. 3.4A, Δ*eap1* + *EAP1* mt). Thus, binding to eIF4E facilitates but is not absolutely required for Eap1p to enhance mRNA decay.

Figure 3.4.

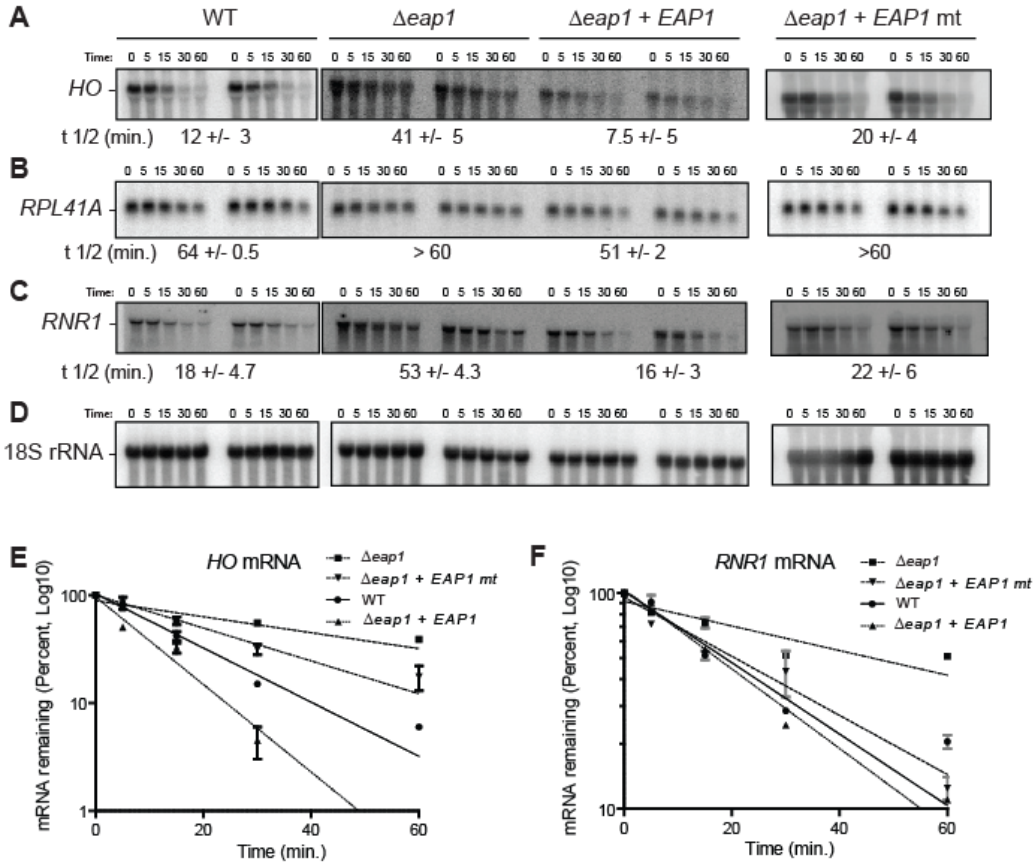

FIG. 3.4. Eap1p accelerates mRNA degradation. mRNA half-lives were measured by transcription shut-off with thiolutin. RNA samples were collected at the indicated time points, in minutes. Blots from duplicate samples are shown for each condition. Average mRNA half lives are indicated below each sample. **A)** Northern blot of *HO* mRNA from wild type (WT), *eap1* deletion (Δ*eap1*), or *eap1* deletion cells complemented with plasmids expressing wild type Eap1p (Δ*eap1+EAP1*) or eIF4E binding defective mutant Eap1p (Δ*eap1+EAP1* mt). **B)** Northern blots of *RPL41A* mRNA from samples in panel A. **C)** Northern blots of *RNR1* mRNA from samples in A. **D)** Northern blots of the stable ribosomal 18S rRNA from samples in panel A. **E)** Graph of *HO* mRNA half-lives in wild type, Δ*eap1*, Δ*eap1+EAP1* and Δ*eap1+EAP1* mt strains. **F)** Graph of *RNR1* mRNA half-lives in each strain.

To determine if the effect of Eap1p on mRNA stability was specific to PUF regulated mRNAs, we analyzed two mRNAs that are not regulated by PUFs, *RNR1* and *RPL41A*. *RPL41A* had a half-life of about 60 minutes that was not altered by deletion of *EAP1* or complementation with wild type or mutant *EAP1* (Fig. 3.4B). In contrast, the half-life of *RNR1* mRNA increased from 18 minutes in wild type cells to 53 minutes in the *eap1* deletion strain (Fig. 3.4C). Importantly, expression of wild type Eap1p in the deletion strain restored *RNR1* half life to 16 minutes (Δ*eap1* + *EAP1*, Fig. 3.4C). *EAP1* mt also restored *RNR1* decay to 22 minutes, albeit less effectively than wild type *EAP1* (Δ*eap1* + *EAP1* mt, Fig. 3.4C). These results are summarized in Figure 3.4F. The effect on *RNR1* demonstrates that Eap1p promotes degradation of an mRNA that is not a known PUF target. These results reveal a novel activity of Eap1p to promote mRNA degradation. Importantly, Eap1p binding to eIF4E facilitates decay but this interaction is not obligatory for enhanced mRNA degradation.

Eap1p promotes decapping of mRNAs. Having established that Eap1p accelerates mRNA degradation, we next investigated which step of decay is affected. mRNA degradation generally initiates by removal of the poly-adenosine tail (i.e. deadenylation). Once the tail is shortened to about 10 nucleotides (pA_{10}), the mRNA is decapped and degraded in a 5' to 3' direction or by the alternative 3'-5' decay pathway (Coller and Parker 2004). Previous research demonstrated that Puf5p and Puf4p enhance deadenylation (Goldstrohm, Hook et al. 2006; Goldstrohm, Seay et al. 2007; Hook, Goldstrohm et al. 2007). Because Eap1p serves as a Puf5p co-repressor, we speculated that it may affect deadenylation. To compare the rate of *HO* deadenylation in wild type and *eap1* deletion cells, transcription was inhibited with thiolutin and RNA samples were collected over time. To resolve the poly(A) tail length, *HO* mRNA was

cleaved with RNase H and a complementary DNA oligonucleotide to generate a 253 nucleotide, 3' fragment with a poly(A) tail of up to 80 nucleotides (Fig. 3.5A). Products were resolved by denaturing polyacrylamide gel electrophoresis and detected by northern blot (Fig. 3.5B). In wild type cells, *HO* 3'UTR had a poly(A) tails ranging from 80 to 10 adenosines (Fig. 3.5B, WT, time = 0 minutes, lane 2). Treatment with RNase H and oligo(dT) provided a marker for deadenylated *HO* mRNA (Fig. 3.5B, lane 1). The stable non-coding RNA, *SCR1*, served as a loading control (Fig. 3.5B). Following transcription shut-off, the tail was quickly shortened over the first ten minutes to a length of about 10 nucleotides. This oligo-adenylated intermediate subsequently decayed with a 6 minute half life (Fig. 3.5B, lanes 3-7), consistent with our past observations (Goldstrohm, Hook et al. 2006). *HO* mRNA was deadenylated within ten minutes in the *eap1* deletion strain, exhibiting the same kinetics observed in wild type cells (Fig. 3.5B, lanes 9-10). To more closely analyze the effect of Eap1p on *HO* deadenylation, we repeated the experiment using 3 minute intervals (Fig. 3.5C). In wild type and *eap1* deletion cells, *HO* poly(A) tails progressively shorten at equivalent rates (Fig.3.5C). Therefore, deadenylation does not appear to be affected by Eap1p. However, a major difference was observed in the *eap1* strain: the oligo-adenylated intermediate accumulated and persisted throughout the time course with a half life greater than 50 minutes (Fig. 3.5B, lanes 10-14; Fig.3.5C, lanes 9-14). This pattern of decay, wherein an oligo-adenylated mRNA accumulates, is identical to that caused by mutations in decapping factors (Beelman, Stevens et al. 1996; Tharun, He et al. 2000; Coller, Tucker et al. 2001; Fischer and Weis 2002).

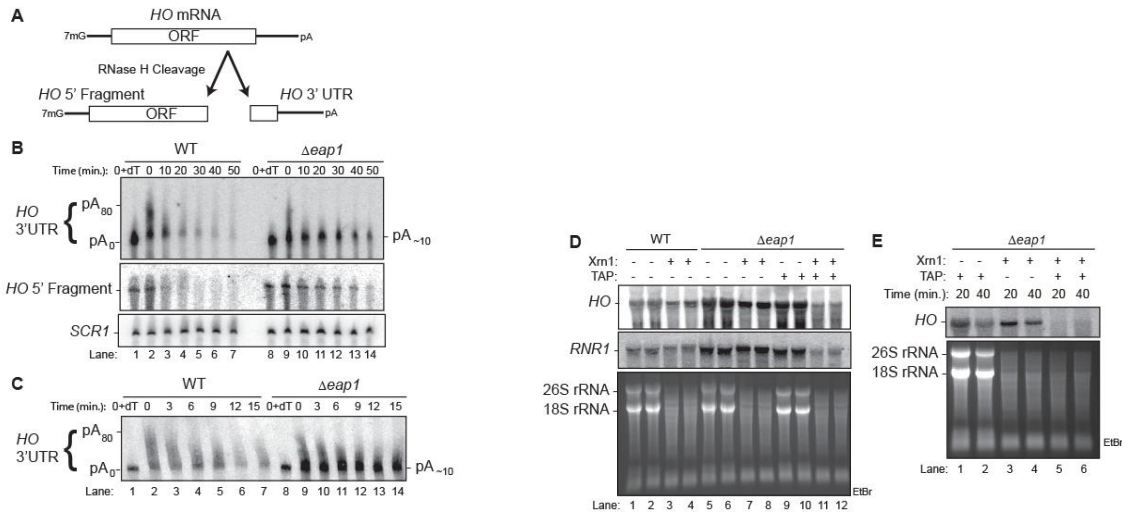

FIG. 3.5. Eap1p promotes decapping of *HO* mRNA. A) *HO* mRNA was cleaved with RNase H and a DNA oligonucleotide to produce a 1600 nucleotide 5' fragment and a 253 nucleotide 3' fragment with a poly(A) tail of up to 80 adenosines (pA_{80}). **B)** Northern blot analysis of *HO* mRNA decay in wild type (WT) or *eap1* deletion strain. RNA samples were collected over a time course (minutes) following addition of thiolutin and then cleaved as shown in panel A. The t=0 minute samples were also treated with RNase H and oligo dT_{15} (designated 0+dT) to remove the poly(A) tail (pA_0). Top panel: Northern analysis of poly(A) tail length and decay rate of the *HO* 3'UTR with a specific probe to the 3' fragment. The oligo-adenylated *HO* intermediate is indicated on the right ($pA\sim_{10}$). Middle panel: Northern blot of the *HO* 5' fragment. Bottom panel: *SCR1* RNA was detected by northern blot as a control for sample loading. **C)** Analysis of *HO* mRNA decay and deadenylation over the initial 15 minutes of decay following addition of thiolutin. **D)** Duplicate RNA samples from panel B were treated (as indicated by a "+") with recombinant Xrn1 or not treated ("-") to assess status of 5' cap. As a control, where indicated, samples were also treated with Tobacco Acid Pyrophosphatase (TAP) to remove the 5' cap. Northern blot for *HO and RNR1* mRNA as indicated on the left. Before transfer to membrane, the gel was stained with ethidium bromide (EtBr, bottom panel) to visualize degradation of uncapped 18S and 26S ribosomal RNA. **E)** Xrn1 sensitivity assay of *HO* mRNA decay intermediates from the 20 and 40 minute time points in panel B.

To further characterize the impact of Eap1p on *HO* mRNA decay, we detected the 5' *HO* mRNA fragment by northern blot (Fig. 3.5B, *HO* 5' fragment). In wild type cells, the 5' fragment began to rapidly disappear as the oligo-adenylated species appeared, consistent with the mRNA being degraded by the 5' decay pathway (Fig. 3.5B, lane 2-3). In contrast, when *EAP1* was deleted, the 5' fragment persisted throughout the time course (Fig. 3.5B, lanes 9-14). These results demonstrate that Eap1p accelerates degradation of *HO* mRNA at a step following deadenylation and preceding 5' decay.

We next sought to determine if the *HO* mRNA that accumulated in the *eap1* deletion retained a 5' cap or was decapped but not subsequently degraded by the processive, 5' to 3' exonuclease, Xrn1p. To assess the presence of the 5' cap, RNA was treated with recombinant Xrn1p. Decapped mRNA is sensitive to degradation by Xrn1p whereas capped mRNA is resistant. Ninety-five percent of *HO* mRNA in wild type cells was resistant to Xrn1p, consistent with the presence of a 5' cap (Fig. 3.5D, lanes 3 and 4). *HO* mRNA from *eap1* cells was fully resistant to Xrn1p and thus retained a 5' cap (Fig. 3.5D, lanes 7 and 8). Thus, deletion of *EAP1* causes accumulation of capped *HO* mRNA. We also observed that the *RNR1* mRNA that accumulated in *eap1* deletion cells was also resistant to digestion with Xrn1p, indicating that it too remained capped (Fig. 3.5D). Two controls were performed to verify the Xrn1p assay. First, RNA was decapped with tobacco acid pyrophosphatase (TAP) and then incubated with Xrn1p, resulting in a 64% reduction of *HO* and *RNR1* mRNAs (Fig. 3.5D, lanes 11 and 12) (Blewett, Coller et al. 2011). Second, ethidium bromide staining the RNA samples demonstrated that Xrn1p degraded the uncapped 26S and 18S ribosomal RNAs (Fig. 3.5D, lanes 3-4, 7-8, 11-12).

As observed in Figure 3.5B, the predominant *HO* mRNA decay intermediate in the *eap1* strain at 20 and 40 minutes after transcription shut-off has an oligo-adenylate tail. We used Xrn1p sensitivity to determine if this mRNA species possesses a 5' cap. At 20 minutes, 76% of the HO intermediate was resistant to Xrn1p. At the 40 minute time point, the *HO* intermediate was fully resistant to Xrn1p digestion (Fig. 3.5E, lanes 3 and 4). Removal of the 5' cap with TAP and then digestion with Xrn1p resulted in decapping and destruction of 95% of the oligo-adenylated *HO* intermediate (Fig. 3.5E, lanes 5 and 6). Collectively, these results support the conclusion that deletion of *EAP1* causes the accumulation of capped, oligo-adenylated *HO* mRNA. We conclude that Eap1p promotes decapping, a novel function for a 4E-BP.

Eap1p associates with Puf5p and Dhh1p. We next asked if Puf5p associates with Eap1p. FLAG tagged Eap1p (Eap1-FLAG), was co-expressed with T7 tagged Puf5p (Puf5-T7) in wild type cells. Eap1p was then immunoprecipitated with FLAG antibody resin, washed extensively and specifically eluted with FLAG peptide. Eluates were then analyzed by western blotting (Fig. 3.6A). As a negative control, a mock FLAG immunoprecipitation was performed on cells expressing only Puf5p-T7 (Fig. 3.6A). Puf5p was detected in the Eap1p immunoprecipitate (Fig. 3.6A). As a negative control, the Actin protein, which is abundant in the input extracts, was not detected in the FLAG eluates (Fig. 3.6A). Because these extracts were extensively treated with both RNase A and RNase One to degrade RNA prior to immunoprecipitation (Fig. 3.6B), we conclude that Puf5p likely associates with Eap1p via protein interactions, not by a bridging RNA.

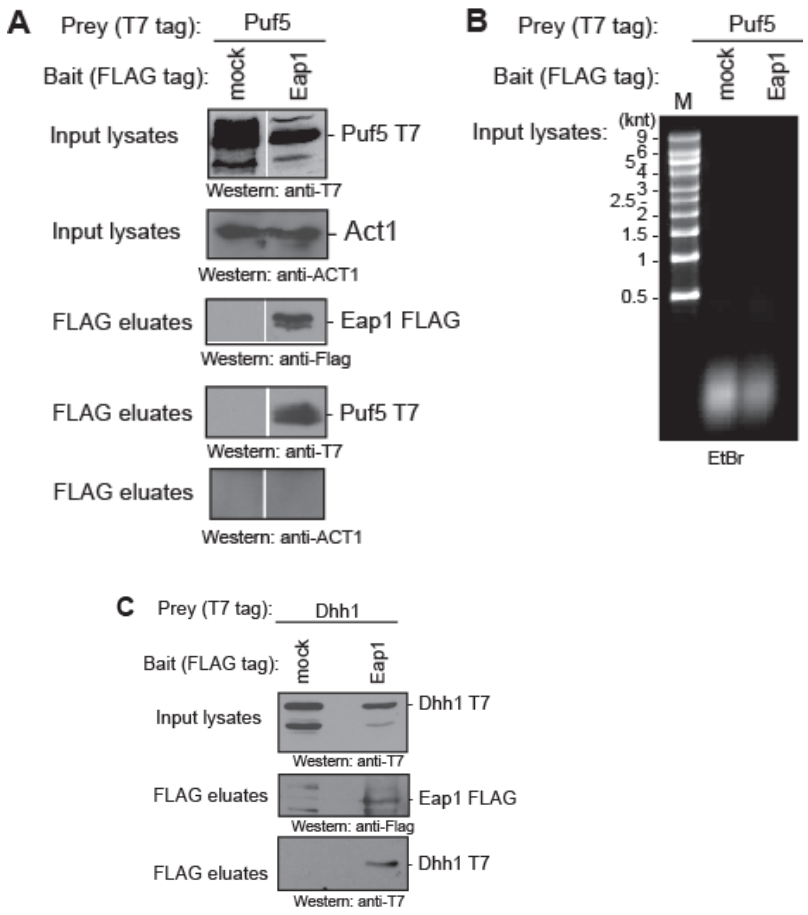

FIG. 3.6. Eap1p associates with Puf5p and Dhh1p. A) T7-tagged Puf5p co-immunoprecipitates with FLAG-tagged Eap1p from cell extracts (input) treated with RNases A and One. Western blot detection of input lysates and FLAG peptide eluates from mock or Eap1-FLAG immunoprecipitations. **B)** RNase mediated destruction of RNA in extracts from panel A was confirmed ethidium bromide (EtBr) staining of nucleic acids. RNA size markers are shown on the left (M). **C)** T7-tagged Dhh1p co-immunoprecipitates with Eap1-FLAG from RNase treated cell lysates (input).

The observation that Eap1p enhanced decapping suggested that it may physically associate with the decapping machinery. The Dhh1 protein, a DExD/H box helicase, is a well known activator of decapping (Coller and Parker 2004). T7 tagged Dhh1p coimmunoprecipitated with Eap1p-FLAG but was not present in mock immunoprecipitate (Fig. 3.6C). These extracts were also RNase treated prior to immunoprecipitation; therefore, association of Eap1p and Dhh1p is not dependent on RNA. This result provides a physical link between Eap1p and the decapping machinery. In addition to this physical interaction, the mRNA decay phenotypes caused by deletion of *EAP1* (Fig. 3.5A) and *DHH1* (Fig. S3)(Coller, Tucker et al. 2001) were remarkably similar; *HO* mRNA was stabilized ($t_{1/2}$ > 50 minutes) and accumulated as an oligo-adenylated species.

Eap1p associates with *HO* mRNA in a Puf5p dependent manner. Our data show that Eap1p participates in Puf5p mediated degradation of *HO* mRNA. Puf5p binds directly to the *HO* 3'UTR and may recruit Eap1p to the message. Alternatively, Eap1p may associate with *HO* mRNA by binding to eIF4E. To test these models, we expressed FLAG tagged Eap1p or the eIF4E binding defective Eap1p mt and asked if *HO* mRNA coimmunoprecipitated with each protein. To assess the role of Puf5p in recruiting Eap1p, wild type Eap1p-FLAG was immunoprecipitated from the *puf5* deletion strain. As a negative control, a mock immunoprecipitation was performed using extract from wild type cells. The FLAG eluates were analyzed by western blotting to confirm purification of Eap1p and Eap1 mt (Fig. 2.7A). *HO* mRNA was measured in the eluates by reverse transcription and quantitative polymerase chain reaction. *HO* mRNA was nearly undetectable in mock eluates whereas it was enriched 1400 fold

in the Eap1p FLAG eluates (Fig. 3.7B). This demonstrates that Eap1p associates with *HO* mRNA.

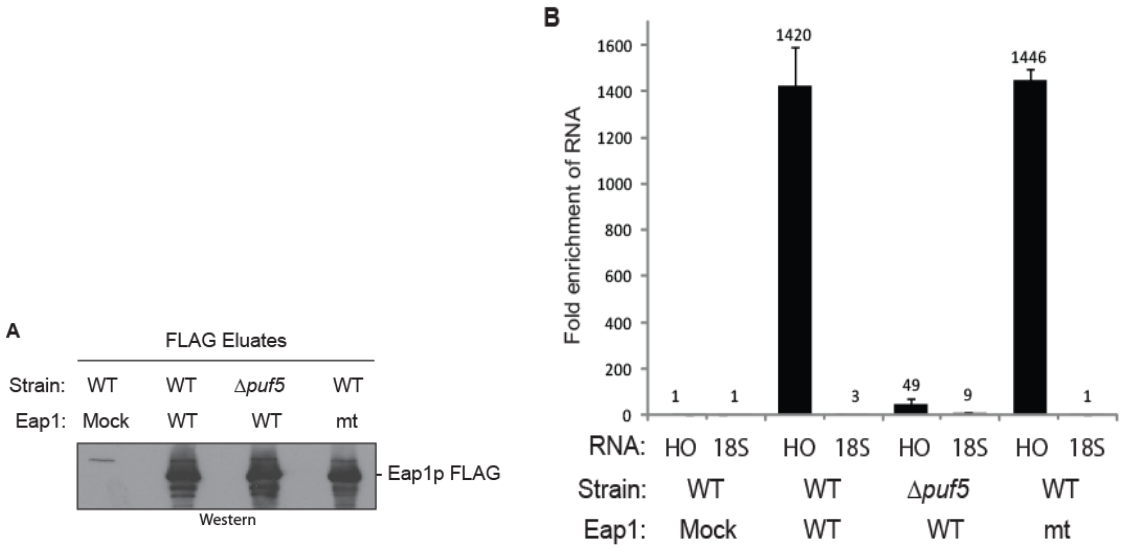

FIG. 3.7. Eap1p associates with *HO* mRNA, dependent on Puf5p. A) FLAG-tagged wild type Eap1p (WT) or eIF4E binding defect mutant Eap1p (mt) were expressed and immunopurified from wild type or Δ*puf5* cells. Negative control Mock immunoprecipitation was performed form cells that did not express tagged Eap1p. Anti-FLAG western blot of FLAG peptide eluates. **B)** Graph of fold enrichment of *HO* mRNA purified from eluted samples in panel A, detected using qRT-PCR. Fold enrichment was calculated relative to mock immunoprecipitation, normalized to input levels. As a negative control, 18S rRNA was also measured. Note that conditions used in this assay did not preserve poly-ribosomes.

Purification of Eap1p from a *puf5* deletion strain reduced its association with *HO* mRNA by 35-fold relative to wild-type strain (Fig. 2.7B, 49 fold enrichment); therefore, Puf5p facilitates Eap1p association with *HO* mRNA. We next tested the contribution of Eap1p interaction with eIF4E. No significant change was observed relative to wild type Eap1p; *HO* mRNA was enriched 1400 fold in the Eap1 mt FLAG eluates (Fig. 3.7B). As a negative control, the non-coding 18S ribosomal RNA was not enriched in these immunoprecipitates. These findings demonstrate that Eap1p associates with *HO* mRNA, mediated by Puf5p.

3.3 DISCUSSION

Eap1p is required for Puf5p-mediated repression. Yeast PUF proteins have a well documented role in accelerating mRNA degradation (Olivas and Parker 2000; Jackson, Houshmandi et al. 2004; Houshmandi and Olivas 2005; Goldstrohm, Hook et al. 2006; Seay, Hook et al. 2006; Goldstrohm, Seay et al. 2007; Hook, Goldstrohm et al. 2007; Ulbricht and Olivas 2008) and deadenylation plays an important role. Both Puf4p and Puf5p enhance deadenylation of *HO* mRNA *in vivo* and *in vitro* (Goldstrohm, Hook et al. 2006; Goldstrohm, Seay et al. 2007; Hook, Goldstrohm et al. 2007). Puf4p repression depends on both *POP2* and *CCR4* genes, which encode subunits of the Ccr4-Not deadenylase complex, and the catalytic activity of Ccr4p deadenylase (Goldstrohm, Seay et al. 2007; Hook, Goldstrohm et al. 2007). That said, several clues indicate that additional mechanisms are utilized by specific PUFs. First, Puf5p represses a target mRNA even when deadenylation is genetically blocked by removal of the *CCR4* gene (Goldstrohm, Hook et al. 2006). Further evidence of a deadenylation independent mechanism was revealed from analysis of *HO* mRNA half-lives in different genetic backgrounds. *HO* mRNA is stabilized ten-fold when both *PUF4* and *PUF5* are deleted, whereas deletion of *CCR4* stabilizes *HO* only three-fold (Goldstrohm, Hook et al. 2006; Goldstrohm, Seay et al. 2007; Hook, Goldstrohm et al. 2007). While deadenylation of *HO* is blocked by the absence of Ccr4p, the mRNA is still degraded (Goldstrohm, Seay et al. 2007), indicating that another step of decay is promoted by Puf5p.

We hypothesized that Puf5p recruits additional co-repressor proteins (Goldstrohm, Hook et al. 2006; Goldstrohm, Seay et al. 2007; Hook, Goldstrohm et al. 2007). In the present work, we provide strong evidence that the eIF4E binding protein, Eap1p, participates in Puf5-mediated repression. Deletion of *EAP1* blocks the repression by Puf5p (Fig. 3.1). In reciprocal tests, Eap1p represses an *HO* reporter mRNA, dependent on the *PUF5* gene. Together, these results indicate that Eap1p is a Puf5p co-repressor. The requirement of Eap1p is specific to Puf5p, as Puf4p repression is not *EAP1* dependent (Fig. 3.1). Additionally, Eap1p and Puf5p associate with each other (Fig. 3.6) and *HO* mRNA (Fig. 2.7), biochemically connecting both regulators to the target mRNA.

Eap1p is one of two 4E-BPs encoded by the *S. cerevisiae* genome (Altmann, Schmitz et al. 1997; Cosentino, Schmelzle et al. 2000). The second 4E-BP, Caf20p, was reported to associate with Puf4 and Puf5p in an RNA dependent manner (Cridge, Castelli et al. 2010), though the function was not tested. Our functional analysis demonstrates that *CAF20* is dispensable for repression by Puf4p and Puf5p (Fig. 3.1). Thus, a general 4E-BP function is not essential for PUF repression. Instead, our data indicate that Puf5p specifically utilizes Eap1p to elicit repression. We conclude that Puf4p and Puf5p exert their repressive effects through distinguishable mechanisms. Both PUFs enhance deadenylation while Puf5p also promotes Eap1p dependent repression (Fig. 3.8) (Goldstrohm, Hook et al. 2006; Goldstrohm, Seay et al. 2007; Hook, Goldstrohm et al. 2007). The features of Puf5p that confer Eap1p dependence are currently not known. While the conserved RNA binding domains of Puf4p and Puf5p bind to the Pop2p-Ccr4p deadenylase (Fig. 3.8) (Goldstrohm, Hook et al. 2006; Goldstrohm, Seay et al.

2007; Hook, Goldstrohm et al. 2007), unique domains of Puf5p may dictate specificity for Eap1p.

The physical association of Eap1p with Puf5p and the dependence of Puf5p for Eap1p interaction with *HO* mRNA support a model wherein Puf5p binds *HO* mRNA and recruits Eap1p (Fig. 3.8). How might Eap1p be recruited? We have not detected a direct protein interaction between Eap1p and Puf5p, which could be a purely technical issue as both full length proteins are difficult to purify. Alternatively, a factor that bridges the interaction may exist. Because Puf5p and Eap1p co-immunoprecipitate from extracts extensively treated with RNases, RNA is not a likely bridging factor (Fig. 3.6). Decapping factors may interconnect Eap1p and Puf5p, because decapping proteins associate with both regulators (Fig. 3.6)(Goldstrohm, Hook et al. 2006). Future biochemical analysis of Eap1p and Puf5p complexes may illuminate this aspect.

Eap1p does not inhibit *HO* poly-ribosome association. The discovery that Eap1p is necessary for Puf5p repression suggested a mechanism based on the existing model of 4E-BP molecular function: Puf5p recruitment of Eap1p may block translation initiation, thereby reducing loading of ribosomes onto target mRNAs. If accurate, then *HO* mRNA should inefficiently associate with ribosomes, resulting in accumulation of *HO* mRNA in the ribosome free fractions of sucrose gradients. Our findings contradict this hypothesis. First, nearly all *HO* mRNA associates with poly-ribosomes in wild type cells, indicating efficient translation (Fig. 3.2). *HO* mRNA remains associated with poly-ribosomes when *EAP1* is deleted. Instead of the predicted increase in ribosome density, *eap1* deletion slightly reduced the density of poly-ribosome associated *HO* mRNA. These findings argue against Eap1p mediated translational

inhibition of *HO*. The predominant effect of *eap1* deletion was to increase the total amount of *HO* mRNA and increase its half-life, pointing towards a role of Eap1p in promoting mRNA decay. The small reduction of *HO* ribosome density caused by the absence of Eap1p may reflect the accumulation of *HO* mRNA with short poly(A) tails in the *eap1* deletion strain (Fig. 3.5).

If Eap1p inhibits translation initiation, then Eap1p would be predicted to be found in ribosome-free fractions at the top of the sucrose gradient. Contrary to this, a significant portion of Eap1p associates with poly-ribosomes (Fig. 3.3). Because poly-ribosomal mRNAs have undergone multiple rounds of initiation, poly-ribosome associated Eap1p cannot have blocked initiation. Our data indicate that interaction of Eap1p with eIF4E mediates its association with poly-ribosomes. This conclusion is supported by the observation that eIF4E was distributed across the gradient, including poly-ribosome fractions (Fig. 3.3). Furthermore, mutations in Eap1p that disrupt binding to eIF4E cause a complete loss of Eap1p poly-ribosome association (Fig. 3.3). Currently the functional significance of poly-ribosomal Eap1p remains unknown.

Eap1p is also present in two other peaks of the sucrose gradient. One peak, in the ribosome free fractions at the top of the gradient, increases upon EDTA treatment, ribosome run-off, and mutation of the eIF4E binding motif (Fig. 3.3). These observations indicate that this pool of Eap1p is not bound to ribosomes or eIF4E. An Eap1p species with slower electrophoretic mobility is present in this peak, suggesting that Eap1p may be modified post-translationally. This idea is supported by proteomic identification of multiple phosphorylation sites in Eap1p (Ptacek, Devgan et al. 2005). Eap1p phosphorylation could block its interaction with eIF4E in manner similar to other 4E-BPs (Sonenberg and Hinnebusch 2009). A third peak

of Eap1p cofractionates with 60S ribosomal subunits. This peak shifts to the ribosome free fractions upon ribosome run-off and mutation of the eIF4E binding motif; therefore, it might represent an intermediate in translation. Future biochemical analysis of Eap1p complexes will be necessary to understand their composition and functions.

Deletion of *EAP1* does not alter global translation state, as deduced from the identical chromatograms of poly-ribosomes from wild type and *eap1* deletion strains (Fig. 3.2)(Ibrahimo, Holmes et al. 2006). This conclusion is supported by analysis of ribosome association of *RNR1* and *RPL41A* mRNAs, which like *HO*, were not inhibited by Eap1p. That said, based on the available data, we do not exclude the prospect that specific mRNAs may be translationally inhibited by Eap1p. In the study that identified Eap1p, an *in vitro* translation assay indicated that Eap1p inhibits translation (Cosentino, Schmelzle et al. 2000); however, the role of eIF4E binding and impact on mRNA stability were not addressed. More recently, a micro-array based study found that deletion of *EAP1* changed the translation state of 329 mRNAs by greater than 1.8 fold, as measured by the ratio of mRNA in poly-ribosomes to mono-ribosomes. Of these, the ratios of 176 mRNAs increased, suggesting that Eap1p inhibits their translation. In our analysis of *HO* mRNA, deletion of *EAP1* caused a 1.6 fold increase in poly- to mono-ribosome ratio; however, this change reflects the 1.7 fold increase in *HO* abundance. Moreover, *eap1* deletion did not increase *HO* ribosome occupancy and density (Fig. 3.2). It remains to be investigated whether Eap1p and Puf5p function together to regulate additional mRNAs. The mRNAs affected by *eap1* deletion did not correlate with those the co-immunoprecipitate with Puf5p (Cridge, Castelli et al. 2010). Cridge et al. also reported that deletion of *EAP1* altered steady state levels of 99 mRNAs more than two-fold, and of these, 56 increased, hinting that Eap1p may

affect stability of additional mRNAs (Cridge, Castelli et al. 2010). Whether the observed effects of *eap1* deletion on translation state and mRNA levels are direct remains to be established. Germane to the challenge of discerning direct Eap1p effects from indirect effects, our demonstration that an Eap1p regulated mRNA (i.e. *HO*) coimmunoprecipitates with Eap1p provides proof of principle for future ribonomic approaches to identify Eap1p target mRNAs.

In summary, our findings do not support a role of Eap1p in inhibition of translation initiation of Puf5p targeted *HO* mRNA. Instead, our results argue that Eap1p elicits a mode of repression that is divergent from the canonical 4E-BP mechanism of translation inhibition.

Eap1p accelerates mRNA decay. We discovered a novel function for Eap1p in promoting mRNA degradation. Deletion of *EAP1* stabilizes *HO* mRNA more than three-fold. Conversely, over-expression of Eap1p enhances decay of *HO* mRNA beyond that observed in wild type cells. Targeting of *HO* by Eap1p is likely directed by Puf5p, a hypothesis supported by their mutual interdependence for repression (Fig. 1) and the finding that association of Eap1p with *HO* mRNA depends on Puf5p (Fig. 3.7).

Enhancement of mRNA decay by Eap1p is not likely to be solely dependent on Puf5p, because we also observed an effect on *RNR1* mRNA, which is not regulated by Puf5p (Goldstrohm, Hook et al. 2006; Seay, Hook et al. 2006) and is not known to associate with other PUF proteins (Gerber, Herschlag et al. 2004). The factors that control *RNR1* mRNA remain to be discovered in future work. Other mRNAs, such as *RPL41A*, are unaffected by Eap1p, suggesting that Eap1p-enhanced mRNA decay may be restricted to specific messages.

Is the eIF4E binding activity of Eap1p necessary for mRNA degradation? An Eap1p mutant that cannot bind eIF4E exhibits half of the mRNA decay activity of wild type protein (Fig. 4); therefore, we conclude that binding to eIF4E facilitates, but is not essential for, Eap1p mRNA decay activity. Binding to eIF4E could promote decay by displacing eIF4G (Cosentino, Schmelzle et al. 2000), destabilizing the eIF4E-5' cap interaction and facilitating access of mRNA degradation enzymes (Fig. 3.8). This idea is supported by data showing that mutations in translation initiation factors, including eIF4E and eIF4G, increase mRNA decay (Schwartz and Parker 1999). However, our data also indicate that this explanation in itself is not sufficient. First, the Eap1p mutant does not bind eIF4E (Fig. 3.3), nor does it associate with poly-ribosomes (Fig. 3.3), yet it still stimulates mRNA decay (Fig. 3.4), albeit with reduced efficiency. We interpret this as evidence that Eap1p promotes mRNA decay by another means, perhaps by affecting decapping (Fig. 3.8), as discussed below.

Eap1p promotes decapping. Degradation of yeast mRNAs typically initiates by shortening of the poly(A) tail to an oligo-adenylated length, followed by decapping (Coller and Parker 2004; Goldstrohm and Wickens 2008). Decapped mRNA is then rapidly degraded in by Xrn1p. As Puf5p enhances deadenylation of *HO* mRNA, we examined the effect of Eap1p. Loss of Eap1p does not affect poly(A) removal, which occurs rapidly in both wild type and *eap1* deletion cells (Fig. 3.5). Instead, Eap1p dramatically affects the fate of the oligo-adenylated intermediate. In wild type cells this species is rapidly degraded, coincident with disappearance of the 5' end of the mRNA (Fig. 3.5). When *EAP1* is deleted, the oligo-adenylated mRNA is highly stabilized, as is the 5' end of *HO* (Fig. 3.5). The oligo-adenylated *HO* that accumulates is resistant to Xrn1p and thus remains capped (Fig 3.5). We conclude that Eap1p promotes

decapping of *HO* mRNA. Our data support that *HO* is degraded by the 5' decapping pathway; deletion of decapping factor genes greatly stabilize *HO* mRNA including Δ*pat1*, $t_{1/2}$ = 55 minutes, and Δ*dcp2*, $t_{1/2}$ > 60 minutes (unpublished data) and Δ*dhh1*, $t_{1/2}$ > 50 minutes (Fig. 3.S3). Additionally, accumulation of deadenylated, capped mRNA species is identical to the effect of mutations in decapping factors including Dhh1p (Fig. 3.S3), Pat1p, and the Lsm1-7p complex (Beelman, Stevens et al. 1996; Tharun, He et al. 2000; Coller, Tucker et al. 2001; Fischer and Weis 2002). We note that deletion of genes encoding the 3' to 5' exosome complex did not increase *HO* mRNA levels (Fig. S4), nor abrogate Puf5p repression (Goldstrohm, Hook et al. 2006); therefore, the 3' decay pathway does not impact *HO* mRNA degradation.

Eap1p associates with the decapping factor Dhh1p. This finding suggests that Eap1p recruits decapping factors or alters their activity (Fig. 3.8). Puf5p also associates with decapping factors including Dhh1p and Dcp1p (Goldstrohm, Hook et al. 2006). These associations do not depend on RNA, indicating that the proteins were not simply tethered to the same mRNA, though the direct protein contacts remain to be delineated.

We propose a model of post-transcriptional regulation of *HO* mRNA that integrates past and new data (Fig. 3.8). Both Puf4p and Puf5p bind to their respective recognition sequence in the 3'UTR of *HO* and recruit the Ccr4-Not complex via direct contact with the Pop2p subunit, thereby enhancing deadenylation. Puf5p also recruits Eap1p and decapping factor Dhh1p and decapping enzyme Dcp2-Dcp1 to promote removal of the 5' cap. Eap1p binding to eIF4E facilitates decay. This model provides a useful framework for future research on PUF repression.

Figure 3.8

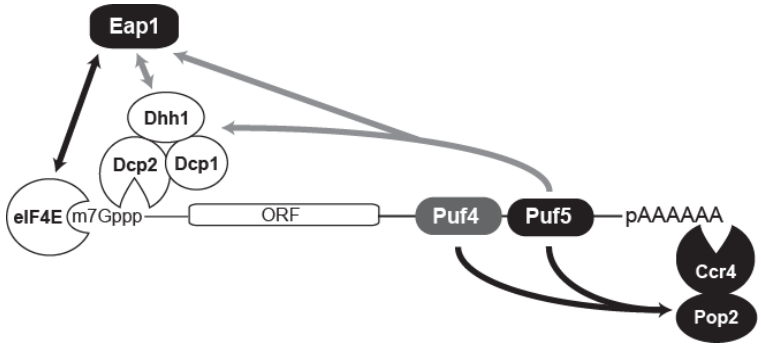

Model of post-transcriptional regulation of *HO* mRNA by PUFs and Eap1p. Puf4p and Puf5p bind to respective sites in the 3'UTR of *HO* mRNA. Both proteins recruit the Pop2p-Ccr4p deadenylase complex to accelerate deadenylation. Puf5p also recruits Eap1p and decapping factors Dhh1p and decapping enzyme Dcp1-Dcp2 to enhance decapping. Eap1p interacts with 5' cap bound eIF4E to facilitate mRNA decay. Direct protein interactions are shown by black lines. Grey lines indicate protein associations; direct protein-protein contacts remain unknown.

Recent evidence indicates that mRNA decay can occur co-translationally on poly-ribosomes (Hu, Sweet et al. 2009; Hu, Petzold et al. 2010). It is tempting to speculate that decay of *HO* mRNA, promoted by Eap1p, might occur on poly-ribosomes; however, because eIF4E binding defective Eap1p retains partial activity but does not associate with poly-ribosomes, ribosome association is unlikely to be an essential feature.

Our analysis does not exclude the possibility that PUFs block translation by additional mechanisms. Chritton et al. reported that the Puf5p inhibits translation of a capped, poly-adenylated reporter mRNA *in vitro* (Chritton and Wickens 2010). Eap1-mediated decapping

may account for the observed regulation. Alternatively, Puf5p may have an independent direct effect on translation. Dhh1p can inhibit translation (Coller and Parker 2005); therefore, Puf5p recruitment of Dhh1p may impact translation.

Do other 4E-BPs affect mRNA decay? Multiple 4E-BPs have been identified in eukaryotes (Pause, Belsham et al. 1994; Mader, Lee et al. 1995; Altmann, Schmitz et al. 1997; Poulin, Gingras et al. 1998; Stebbins-Boaz, Cao et al. 1999; Cosentino, Schmelzle et al. 2000; Wilhelm, Hilton et al. 2003; Matsuo, Muramatsu et al. 2004; Nakamura, Sato et al. 2004; Nelson, Leidal et al. 2004; Ferraiuolo, Basak et al. 2005; Jung, Lorenz et al. 2006). The finding that Eap1p is required for repression by Puf5p is reminiscent of other examples wherein an RNA binding protein utilizes a 4E-BP to repress an mRNA (Stebbins-Boaz, Cao et al. 1999; Wilhelm, Hilton et al. 2003; Nakamura, Sato et al. 2004; Nelson, Leidal et al. 2004; Sonenberg and Hinnebusch 2009). In these cases, translation inhibition is thought to be the means of repression. Our results showing that Eap1p enhanced decay and decapping were therefore unanticipated in the context of current understanding of 4E-BP repression. Furthermore, Puf5p may not be the only RNA binding factor to use Eap1p as a co-repressor, as the yeast Vts1p protein employs Eap1p to enhance mRNA decay (Craig Smibert, University of Toronto, personal communication).

Additional clues are emerging that implicate specific 4E-BPs as versatile regulators that can influence steps of gene expression other than translation initiation. The human eIF4E-Transporter was implicated in the destabilization of ARE-containing mRNAs (Ferraiuolo, Basak et al. 2005). A recent analysis of the *Drosophila* 4E-BP, Cup, found that it represses mRNAs by

specifically enhancing deadenylation (Igreja and Izaurralde 2011). Interestingly, Cup subsequently stabilizes the deadenylated mRNA by blocking decapping (Igreja and Izaurralde 2011). These findings suggest the exciting possibility that each 4E-BP may have unique activities to control translation, localization, and degradation of distinct groups of mRNAs.

ACKNOWLEDGEMENTS

A.C.G. gratefully acknowledges support by Dr. Marvin Wickens, University of Wisconsin, during the initial phase of this research. We appreciate advice from Dr. Trista Schagat, Jamie Van Etten, Chase Weidmann, Nathan Raynard and Joel Hrit. We thank Dr. Brad Hook, Dr. Daniel Seay, Dr. Jeff Coller and May Tsoi for technical assistance, and Dr. Eric Wagner for comments on this manuscript. Pfizer generously supplied thiolutin. Nathan Blewett was supported by the NIH Cellular and Molecular Biology Training Grant T32-GM007315.

3.4 MATERIALS AND METHODS

Yeast strains. Yeast strains were obtained from Open Biosystems unless otherwise noted.

AGY111: BY4741 Mata *his3Δ1 leu2Δ0 met15Δ0 ura3Δ0*

AGY153: BY4741 Mata *eap1::KanR*

AGY152: BY4741 Mata *caf20::KanR*

AGY150: BY4741 Mata *puf5::KanR*

AGY109: BY4741 Mata *puf4::KanR*

AGY151: BY4741 Mata *dhh1::KanR*

Plasmids.

ACG858: YCp33 *HIS3 HO* 3'UTR was previously described by Goldstrohm et al, 2006.

ACG399:YCp33 LacZ *HO* 3'UTR was derived from ACG858 by replacing the *HIS3* open reading frame with the coding sequence for β-galactosidase.

ACG441: YEp181 *PUF5*-T7 was previously described by Goldstrohm et al, 2006.

ACG705: p415 GPD *PUF4*-T7 was previously described by Hook et al, 2007.

ACG137: pACG1 NTB contains the *ADH1* promoter and 3'UTR. The plasmid has a 2μ origin of replication and Zeocin selectable marker.

ACG693: pACG1 NTB-*EAP1* was created by inserting the *EAP1* open reading frame into Kpn1 and Not1 sites in pACG1 NTB.

NB1: YEp181 *EAP1*-FLAG: *EAP1* was PCR-amplified from S288C genomic DNA, and cloned into Xma1 sites of YEp181. The C-terminal FLAG epitope was added by inverse PCR using primers NB85/86.

NB2: YEp181 *EAP1* mt Y109A/L114A-FLAG: Quickchange PCR (Stratagene) was performed on plasmid NB1 with primers AG787/788 to mutate Y109A and L114A.

NB3: pACG1-eIF4E-T7: The *CDC33* ORF, encoding eIF4E, was PCR-amplified from S288C genomic DNA, and cloned into KpnI and NotI sites of pACG1 plasmid. All plasmids were verified by restriction digests and DNA sequencing.

Oligonucleotides.

Synthetic oligonucleotides were purchased from Integrated DNA technologies.

NB64: 5' TCCATTCCCGGGGTTTTAATGTATTGAAAATCACTTAGTTGTATATAGCC-3'

NB65: 5'-GCAAGGCCCGGGGCTTTCAGGCGCAGAAAACCTGAAAA-3'

NB85: 5'-GATGCGTAACGAGCGAGTACTTGACAGG-3'

NB86: 5'-
TCACTTGTCATCGTCATCCTTGTAATCGATGTCATGATCTTTATAATCACCGTCATGG
TCTTTGTAGTCTTT
TATATTCTTTTTAGAG-3'

AG787: 5'-
GCAATACAAGACATATGCAGCGTCCATGAATGAAGCGTATCATTTGAAACCATCTTT
GGC-3'

AG788: 5'-
GCCAAAGATGGTTTCAAATGATACGCTTCATTCATGGACGCTGCATATGTCTTGTAT
TGC-3'

AG1029: 5’-GCACGGTACCTATGTCCGTTGAAGAAGTTAGCAAG-3’

AG1030: 5’-GCACGCGGCCGCTTACAAGGTGATTGATGGTTGAGGG-3’

HO ORF riboprobe T7 transcription template PCR primers:

NB22:

5’GGATCCTAATACGACTCACTATAGGGAGAACCTGCGTTGTTACCACAACTCTTATG

A3’

NB23: 5’-AAGTGGTCACAAAACAAGAGAAGTTCCG-3’

HO 3’UTR riboprobe T7 transcription template PCR primers:

NB92:

5’GGATCCTAATACGACTCACTATAGGGAGACATCCAAAATATTAAATTTTACTTTTA

TTAC-3’

NB98: 5’-GCAAGTATGTACCAGAAGCACGTGAA-3’

LacZ 3’UTR riboprobe T7 transcription template PCR primers:

NB92:

5’GGATCCTAATACGACTCACTATAGGGAGACATCCAAAATATTAAATTTTACTTTTA

TTAC-3’

NB115: 5’- CATCAGCCGCTACAGTCAACAGCAA-3’

***HO* 3’UTR RNase H cleavage:**

NB99: 5’-ATACAGTGATGACCGCTG-3’

***LacZ* 3’UTR RNase H cleavage**

NB116: 5’-AACTGGAAGTCGCCGCGCCAC-3’

***RNR1* probes:**

pNB5: 5’-AAAGCACATTCCTTCAAGGTGTCGTAAATCCCCTCGATAGAGTCCTCCTTC-3’

pNB6:

5’ AAGAGGACATTTGAGGTTTTGGAGTACCGGCATTGAACAACGTTGGAGAGG-3’

***RPL41A* probe:**

pNB76: 5’-CCGCTTATTTGGATCTGGCTCTCACCTTCCGTCTCTTTCTCTTAAG-3’

***SCR1* probe:**

pNB79: 5’-CGCCTCCATCACGGGTCACCTTTGCTGAC-3’

***HO* qRT-PCR primers:**

NB36: 5’-CCTCATAAGCAGCAATCAATTCTATCTAT-3’

NB90: 5’-TTTAATTTCACCGTTAGCCATCAGAA-3’

***18S* rRNA qRT-PCR primers:**

NB69: 5’-ACGGAAGGGCACCACCA-3’

NB70: 5’-CCACCCACAAAATCAAGAAAGAGCTCTC-3’

PUF repression assay. Yeast growth assays were performed to detect repression by Puf4p and Puf5p as described in Goldstrohm et al, 2006, with the following modifications. Wild type yeast strain BY4741 or gene-specific deletion strains were transformed with the reporter gene YCp33 HOp *HIS3-HO* 3’UTR and either empty vector YEp181 or the *PUF5* expression plasmid YEp181 *PUF5* or p415 GPD *PUF4.* Colonies were isolated and grown to mid-log phase at 30°C and the indicated number of cells was spotted onto selective minimal media with or without histidine. The His3p competitive inhibitor 3-aminotriazole was added at 1 mM final concentration to increase stringency. For assays presented in Figure 1C, media was

supplemented with 300 µg/ml Zeocin to select for pACG1 NTB *EAP1* or the negative control plasmid pACG1.

β-galactosidase reporter assay. Wild type or gene specific deletion strains were transformed with the YCp33 LacZ-HO3'UTR reporter gene. Each strain was then grown to mid log phase and 3 O.D. units (8.9 x 10^7 cells) from each sample were harvested and resuspended in 100 µl of fresh media. An equal volume of room temp Beta-Glo (Promega) reagent was added to each tube. Samples were transferred to 96-well plate and incubated for 1 hour at 25°C. Luminescence measurements were made using a GloMax Multi+ detection system (Promega). Specific signals were 2 orders of magnitude above the background measured with Beta-Glo reagent, media or empty wells. Each assay was performed with five biological replicates and data are plotted as the mean value of relative light units with standard error of the mean.

Poly-ribosome fractionation. Yeast cultures were seeded in 250 mL of the appropriate media at an Optical Density at 600nm (OD_{600} nm) of 0.2 and grown to an OD_{600} nm of 0.8. Cells were rapidly harvested at 4°C and all subsequent steps were carried out in a cold room. When indicated, cycloheximide (60 µg/ml) or EDTA (50 mM) was added to cultures, which were immediately poured into cold centrifuge bottles with one-third volume of crushed ice. Cells were pelleted for five minutes at 3200 x g. Media was decanted, cells were washed with 10 ml ice-cold 50 mM Tris-Cl pH 6.8, 100 mM NaCl, 30 mM $MgCl_2$, and 50 µg/ml cycloheximide, (or when indicated, 50 mM EDTA was added in lieu of cycloheximide). Cells were pelleted again and resuspended in 650 µl ice-cold 50 mM Tris-Cl pH 6.8, 100 mM NaCl, 30 mM $MgCl_2$, and 50 µg/ml cycloheximide, (or 50 mM EDTA was added in lieu of cycloheximide) with 20 Units/mL RNasin, and 2X protease inhibitors (2 mM PMSF, 100 µg/mL aprotinin, 100 µg/mL pepstatin, 100 µg/mL leupeptin) in 1.5 mL tubes containing 650 µl glass beads. Cells were lysed

in a FastPrep (MP) 2 times for 60 seconds at 6.5 m/s. Cell debris and beads were removed from the extract by centrifugation for 5 minutes at 1400 x g. The extracts were diluted 1/200 and the absorbance at 260 nm (A_{260}nm) was measured with a NanoDrop spectrophotometer (Thermo Scientific). Twenty A_{260}nm units of extract were loaded onto each sucrose gradient. Ribosome run-off was performed as above, except that cycloheximide was omitted from all steps.

To fractionate ribosomes and poly-ribosomes, 7-47% sucrose gradients were prepared using a Gradient Master (BioComp). Samples were applied to the top of each gradient. For Figure 2, gradients were centrifuged 2 hours and 30 minutes at 28,000 rpm in an SW41 Ti rotor at 4°C. For Figure 3, gradients were centrifuged 4 hours to resolve 40S, 60S, 80S, and poly-ribosome peaks. Gradients were fractionated using a Biologic DuoFlow system with an Econo Gradient peristaltic pump (Bio-Rad) at a rate of 1.75 ml/min. while collecting 500 µl fractions. Gradient tubes were pierced with a gradient fractionation device (Brandel), and gradients pumped from the bottom of the tube using Fluorinert. A_{260}nm readings were made continuously during fractionation using a Bio-Rad Quadtec spectrophotometer. Samples were stored at -80°C after fractionation. RNA was extracted from a total of 460 µl of each gradient fraction using the Maxwell RNA purification system and 16 cell LEV RNA purification kit (Promega). The percentage of each mRNA in each fraction was calculated relative to the total detected by northern blot in all fractions. Values from each fraction were represented as the mean value of multiple replicates. For western blot analysis of fractions, 45 µl of each fraction was boiled 5 minutes in 1xSDS-PAGE loading buffer and then separated in a 4-12% SDS-PAGE.

Northern blotting. RNAs was separated on 1.4% agarose - formaldehyde denaturing gels with 1x MOPS running buffer and transferred to Immobilon NY+ membrane (Millipore) using downward transfer method. Membranes were UV cross linked with a UVP CL1000. Membrane

blocking and hybridization was performed using oligo-hyb or ultra-hyb buffers (Ambion). End-labeled oligonucleotide probes were hybridized in oligo-hyb buffer, overnight at 42°C, and washed 2 x 30 minutes in 2X SSC with 0.5% SDS at 42°C. Body-labeled riboprobes for *HO* mRNA were hybridized in ultra-hyb at 68°C, and washed 2 x 5 minutes in 2X SSC with 0.1% SDS, then 2 x 15 minutes in 0.1X SSC with 0.1%SDS at 68°C. Membranes were exposed to phosphor screens and scanned using a Typhoon Trio phosphorimager (General Electric).

Measurement of mRNA half-life. Transcription shut-off using thiolutin (Pfizer) and RNA purification was performed as described previously (Blewett, Coller et al. 2011). Specific northern blot bands were quantitated on a Typhoon phosphorimager using ImageQuant TL software. Each time point was normalized to the *SCR1* RNA in that same sample and decay was calculated relative to the time of drug addition. mRNA half-lives were calculated with GraphPad Prism software using non-linear regression, one-phase decay analysis of biological replicate samples.

Poly-adenosine tail length analysis. Forty micrograms of total RNA was first treated with Turbo DNase (Ambion). RNA was precipitated with 1/10 volume 3M sodium acetate and 3 volumes of 100% ethanol at -20°C. Pellets were washed with 70% ethanol and resuspended in 24 µl Buffer A (20 mM KCl, 1 mM EDTA), 20 pmol of cleavage oligonucleotide NB99, and either 5 µl of water, or 5 µl of oligo dT (500 ng/ul). Samples were heated 5 minutes at 90°C, then cooled for 5 minutes at 65°C, then 20 minutes at room temperature. To each sample, 30 µl of Buffer B (40 mM Tris-Cl pH8.0, 56 mM $MgCl_2$) was added, along with 1 unit of RNase H (NEB), and 1 unit of RNasin Plus (Promega). Samples were incubated for 1 hour at 37°C. RNA was then precipitated with 1/10 volume 3M sodium acetate, and 3 volumes ethanol at -20°C. RNA pellets were washed with 70% ethanol and resuspended in denaturing polyacrylamide

northern loading buffer. After heating for 5 minutes at 95°C, the RNA was separated in a 6% polyacrylamide, 7M urea denaturing gel and transferred to Immobilon NY+ with a transblotter (Bio-Rad). Northern blots were performed as described above.

Xrn1 sensitivity assay. 20 µg of total RNA extracted from wild type and *eap1* strains was used for each reaction. Where indicated, control samples were treated with 15 units of Tobacco Acid Pyrophosphatase (Epicentre) to remove 5' cap structures using the supplied TAP reaction buffer for 1 hour at 37°C. RNA was precipitated, pelleted and washed with 70% ethanol. RNA was then digested with 10 units of Xrn1 (NEB) in reaction buffer with 1 unit RNase Inhibitor Plus for 1 hour at 37°C. The RNA was precipitated, washed with 70% ethanol, and resuspended in northern loading buffer.

Protein co-immunoprecipitation. Yeast expressing FLAG-*EAP1*, or empty vector (mock) as bait, and T7-tagged prey were grown overnight in appropriate media. The next day yeast were seeded to an optical density, OD_{600} nm, of 0.2 in 1L of media and then grown to OD_{600} nm 0.8. Cells were then harvested, washed with TNMT250 (50 mM Tris-Cl pH 8.0, 250 mM NaCl, 2 mM $MgCl_2$, 0.1% Tween-20), pelleted and stored at -80°C. Anti-FLAG M2 agarose (Sigma), 50 µl bed volume of beads, was pre-equilibrated in 10 ml TNMT250 with 300 µg/ml denatured salmon sperm DNA and 500 µg/ml BSA for 1 hour at 4°C. Beads were then washed twice for 10 minutes with TNMT250. Cell pellets were thawed on ice, suspended in an equal volume of TNMT250 with 10 µg RNase A (Fermentas), 100 units of RNase One (Promega), and 2 x protease inhibitors. Cells were transferred to 15 ml tubes containing 700 µl acid-washed glass beads. Lysis was performed with a FastPrep (MP) with three 60 second pulses at 6.5 m/s. Cell debris was pelleted 10 min. at 6000 x g, supernatant was removed to fresh tube, and pelleted 10 min again at 12000 x g. The resulting lysate was pre-cleared by incubation with IgG-agarose to

remove non-specific interactions. After pre-clearing, RNase-treated lysates were applied to Anti-FLAG M2 affinity agarose (Sigma) and incubated for 2 hours at 4°C. Beads were pelleted 5 min. at 1000 x g, supernatant was removed, and beads were washed 5 times for 15 minutes with 10 mL TNMT250. After final wash, beads were transferred to a microfuge tube. Beads were resuspended in 100 µl of TNMT250 and 150 ng of FLAG peptide (Sigma). Elution was performed 30 minutes at 4°C with end-over-end rotation. After incubation, the supernatant was passed through a Bio-Rad mini-spin column to remove beads. Eluates were then separated by 4-12% SDS-PAGE gels and probed with anti-FLAG antibody (Sigma) and anti-mouse HRP conjugate monoclonal antibody (Thermo Scientific), anti-T7 monoclonal antibody linked to HRP (Novagen), or anti-Actin monoclonal antibody (MP Biomedical).

RNA co-immunoprecipitation. Co-immunoprecipitation of mRNA with Eap1p was performed as described above, with the following alterations. Yeast were lysed in TKNM140 buffer (40 mM Tris-Cl pH 8.0, 140 mM KCl, 0.1% NP-40, 2 mM $MgCl_2$, 40 units/ml RNasin Plus with 2X protease inhibitors). Beads were washed 5 x 10 min. in TKNM140, then protein and RNA were eluted as above with 150 ng of FLAG peptide.

Quantitative PCR detection of *HO* mRNA immunoprecipitation. Input and elution samples were first treated with 4 units of Turbo DNase (Ambion) in 1X Turbo buffer at 37°C for 30 minutes. RNA was precipitated with 1/10 volume sodium acetate and 3 volumes ethanol 1 hour at -20°C and pellets were washed with 70% ethanol. qRT-PCR was carried out as described previously (Blewett, Coller et al. 2011). Briefly, *HO* cDNA was generated with GoScript Reverse Transcriptase (Promega) using 20 pmol of primer NB90. Amplification of PCR products was measured using GoTaq qPCR master mix (Promega) with 200 nM of each primer in 50 µL reactions. A Bio-Rad CFX 96 C1000 real-time PCR instrument was used for all assays.

Each immunoprecipitation was performed in triplicate and the elution C(t) was normalized to *HO* input C(t) for each sample. Fold enrichment was then calculated relative to the mock immunoprecipitation samples using the ΔΔC(t) method (Livak and Schmittgen 2001; Schmittgen and Livak 2008).

3.5 Chapter 2 Supplemental Material:

Figure S2.1.

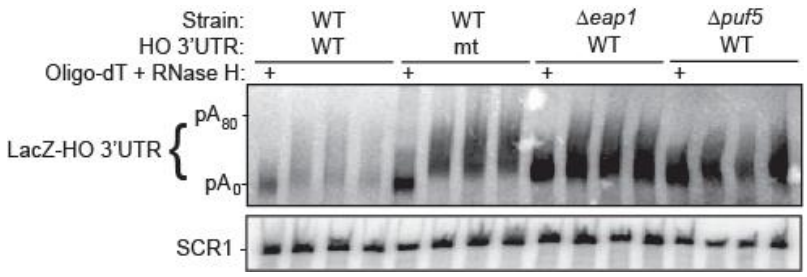

Northern blot detection of wild type and mutant *LacZ-HO* reporter mRNAs in wild type (WT), *eap1* deletion, and *puf5* deletion strains. SCR1 RNA was also detected as to normalize for variations in sample loading. To resolve poly(A) tail lengths of the reporter, the mRNA was cleaved with RNase H and a specific oligonucleotide. RNA was then separated by denaturing poly-acrylamide gel electrophoresis and detected with a specific northern probe. Three biological replicates were analyzed for each test condition.

Figure S2.2

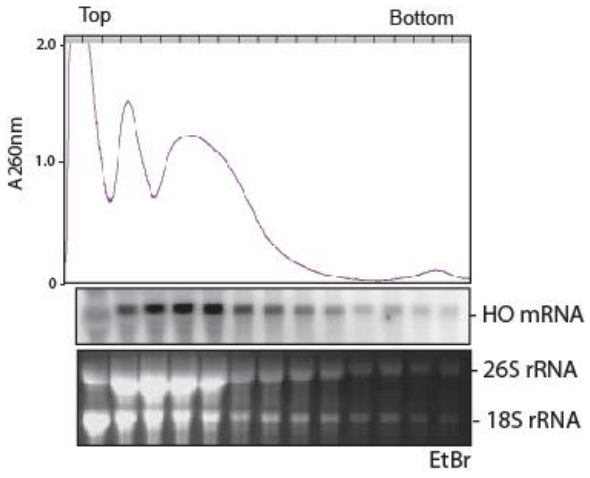

Fig. S2. Dissociation of poly-ribosomes causes *HO* mRNA to shift to the top of the gradient. Cell extract from wild type yeast was treated with EDTA to dissociate poly-ribosomes and then fractionated by sucrose density gradient. The chromatogram is shown in the top panel. Northern blot of *HO* mRNA is shown in the middle panel. The bottom panel shows ethidium bromide staining of the ribosomal RNAs.

Figure S2.3

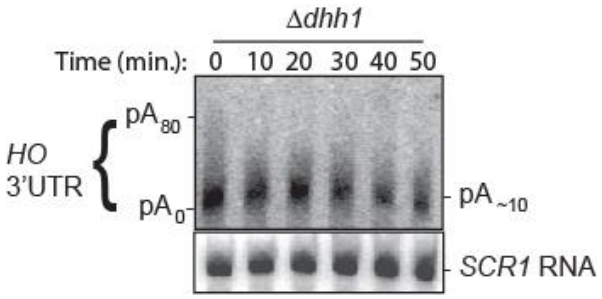

Deletion of *DHH1* gene causes accumulation of deadenylated, decapped *HO* mRNA. Thiolutin was used to inhibit transcription and samples were collected over a time course, indicated at the top. *HO* mRNA was cleaved with RNAse H as shown in Fig. 5A. Northern blot was probed to detect the 3' end of *HO* mRNA and, as a loading control, *SCR1* noncoding RNA.

Chapter Four

Mechanisms of mRNA Regulation by *D. melanogaster* Pumilio

Work in this chapter was accomplished through collaboration with Chase Weidmann. C.W. performed drosphila cell culture, transfections, and luminescent assays.

4.1 Introduction: Pumilio (PUM) is the founding member of the PUF protein family, its function has been studied extensively in the developing fly through genetic identification of factors involved in PUM regulation of the anterior-posterior body axis (Lehmann and Nusslein-Volhard 1991; Barker, Wang et al. 1992; Cho, Gamberi et al. 2006), as well as through more direct biochemical analysis to identify the conserved high-affinity PUM Recognition Element (PRE)(Zamore, Bartel et al. 1999). The majority of this work has been performed at the level of the whole organism, or *in vitro*, which highlights the need for mechanistic dissection of PUM-mediated repression to define what co-factors contribute to, and are necessary for PUM repression *in vivo*.

The PUM RNA Binding Domain (RBD) is highly conserved in all eukaryotes studied, as such; much effort has been put into defining a conserved mode of repression via the PUM RBD. Over the last twenty years there has been significant debate over the mechanism of repression, proposed mechanisms range from: recruitment of proteins which inhibit translation initiation, recruitment of the deadenylase machinery and mRNA decay machinery, deadenylation-mediated translation repression, and most recently, inhibition of translation elongation. The mechanism

involving elongation proposes a requirement for the microRNA (miRNA) pathway Argonaute (Ago) proteins. Traditionally miRNA repression involves Ago, and several other factors that complex with a 22-23nt RNA that directs the complex to specific mRNAs via base-pairing between the miRNA, and target mRNA.

In the case of RBD-Ago mediated repression, the authors suggest that the miRNA pathway is not involved. Along with the proposed Ago association, both nematode FBF-1 and human PUM2 were shown to associate with orthologues of the translation elongation factor eEF1A; eEF1A hydrolyzes GTP during ribosome translocation and this promotes elongation. *In vitro* GTP hydrolysis, as well as separate translation assays indicated that the RBD inhibits GTP hydrolysis and that the RBD causes ribosomes to stall immediately after initiation. This work also identified conserved residues in the RBD that are required for interaction with Ago and eEF1A respectively. Repression was exerted on both polyadenylated and non-adenylated targets; this suggests the mechanism of repression does not require deadenylation.

Arguing for an alternate mechanism of repression is work by Weidmann et. al., 2012, which showed in a *drosophila* S2 cell culture model, that the conserved PUM RBD represses target mRNA expression via an unknown mechanism involving reduction of reporter mRNA levels. Work in *drosophila* embryos indicates that PUM represses the *hb* mRNA via repression of translation through association with two factors: Brat and 4EHP. Brat is an NHL domain protein that has been implicated in post-transcriptional mRNA regulation, but little is known about the mechanism (Slack 2000). 4EHP is similar to eIF-4E in that it specifically binds the 5' cap, unlike eIF-4E, 4EHP doesn't bind eIF-4G and instead forms a complex on the 5' cap that

represses translation initiation. Both Brat, and 4EHP mutant flies exhibit defects in Hunchback gradient formation. Also, PUM binding to a PBE in an mRNA has the ability to form a ternary complex with Brat and 4EHP (Sonoda, Wharton 2001) (Cho Sonenberg, 2006) (Weidmann and Goldstrohm 2012). Traditionally, much of PUMs' repressive activity has been thought to occur through inhibition of translation, but the story may be more complicated than one single pathway(Parisi and Lin 2000).

We report here that the conserved PUM RBD does not require Ago or eEF1A, but rather accelerates deadenylation through a Poly(A) Binding Protein (Pabp)-dependent mechanism. Interestingly, while Pabp promotes RBD activated deadenylation, the repressive activity of Pabp appears to function at the level of translational inhibition, at step preceding deadenylation. Furthermore, we demonstrate that deadenylation of a PUM-targeted mRNA is catalyzed by the Ccr4-Pop2 complex. We also found that mRNA decapping is involved in PUM-activated mRNA decay as well as repression. In summary, our data suggest that post-transcriptional repression by the PUF RBD is exerted through inhibition of translation via PABP, which then activates subsequent deadenylation and destruction of the target mRNA.

4.2 RESULTS:

The PUM RBD, and Mutant RBDs that Abolish Ago and eEF1A-Binding all Reduce Reporter mRNA Levels to Similar Extent: The PUM RBD was previously shown to reduce reporter mRNA levels via qRT-PCR(Weidmann and Goldstrohm 2012), we first sought to monitor the ability of the RBD to reduce reporter mRNA levels, testing mutations in the RBD that were reported to abrogate binding to Ago and eEF1A respectively. Reporter mRNA levels were quantified via northern analysis, and reporter protein output was monitored with the DualGlo luciferase assay, a quantitative luminescence assay. To assess PUM repression of the PBE, reporter constructs expressing PUM-targeted Renilla luciferase and a control firefly luciferase are transfected with a PUM RBD expression vector. Percent repression is calculated by normalizing the PUM-targeted renilla luciferase to the untargeted firefly luciferase luminescence, after normalization the normalized relative response ratio is then divided by the normalized renilla signal from samples that were transfected a PUM RBD mutant which is unable to bind RNA and repress. This allows quantitation of the specific repressive effects generated from PUM RBD binding to the targeted reporter mRNA.

To test the involvement of Ago and eEF1A, mutations were made on conserved residues in the PUM RBD that are required for binding to Ago and eEF1A respectively. Plasmids were transfected that express either wild-type PUM RBD, a Threonine to Glutamic Acid mutation (T752E Ago binding defective, or a phenalanine to arginine mutation that disrupts binding to eEF1A (F868R eEF1A binding defective), or a mutant in which the PUM repeat 7 is mutated

(R7mut); destroys the ability of the RBD to bind its' target sequence, inactivating repression. Two days post-transfection, the cells were harvested, and aliquots were removed to perform the DualGlo luciferase assay. Repression relative to R7mut expression was compared between the Ago binding mutant, eEF1A binding mutant and wild-type RBD. RNA was also extracted from the same cells, and the levels of the Renilla-3X PBE mRNA were measured via northern blot.

Figure 4.1.

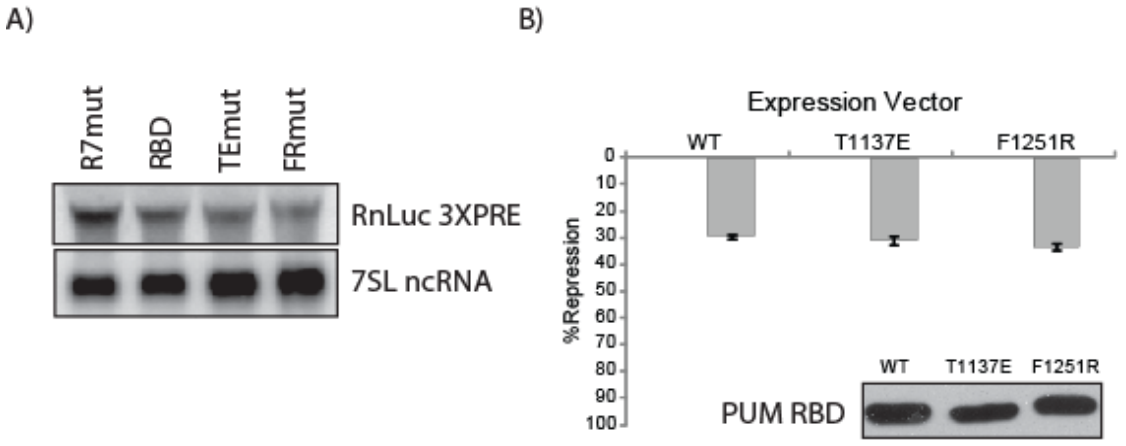

PUM RBD and Mutant RBDs Each Reduce Reporter Levels. A) Northern blot, assaying the levels of RnLuc3XPRE mRNAin response to RBD and mutant RBD expression, and the loading control 7SL ncRNA. **B)** Dual Glo luminescence assay from four biological replicates. Renilla-PRE luminescence was normalized to control Firefly, the % repression was calculated relative to R7mut expression.

Figure 4.1A shows that expression of the PUM RBD, as well as both the Ago and eEF1A binding defective mutants all reduce reporter mRNA levels. Figure 3.1B shows the percent repression of PUM-targeted reporter for each mutant. This also showed that repression at the level of protein is robust for the RBD mutants which cannot bind Ago, or eEF1A respectively. To further test the involvement of *Ago-1* and *Ago-2*, they were knocked-down via double-stranded siRNA, and the ability of the RBD repress was monitored via luminescent assay. Again, in the case of both *ago-1* and *ago-2* knock-down, the RBD consistently repressed the

reporter to the same extent, demonstrating that 80% reduction of Ago does not impair PUM RBD-mediated repression(data not shown). Because mutants which are unable to bind Ago or eEF1A, and siRNA knock-down of Ago had no impact of RBD-mediated repression we conclude that Ago and eEF1A are not required for PUM repression *in vivo*. These results also indicate that repression via the PUM RBD may be exerted at the level of mRNA destruction, rather than a translational mechanism as suggested above. However, these results only show that a reduction in mRNA levels is correlated with the reduction in reporter luminescence; it is possible that PUM is inhibiting translation of the reporter, leading to its' destabilization.

The PUM RNA Binding Domain Activates Reporter mRNA Deadenylation:

The degradation of most mRNAs is initiated primarily through removal of the poly(A) tail, this is usually followed by decapping and 5'-3' destruction of the message. PUF proteins are known to associate with deadenylases in other organisms, and have been demonstrated to increase the rate of deadenylation on targeted mRNAs. We asked whether this mechanism is conserved by the *drosophila* PUM RBD and accounts for the PUM-RBD mediated reduction in mRNA levels. To begin to address this question, empty vector, the R7mut, or RBD were expressed along with either wild-type or a mutant 3X-PBE which the first UGU is mutated to ACA abolishing RBD recognition. The poly(A) tail status of the reporter was then assessed via Rnase H cleavage of the message, directed with a DNA oligonucleotide, to liberate a 500 nt 3' cleavage product. RNA was separated in a high-resolution polyacrylamide gel, and probed for the reporter mRNA as well as the loading control 7SL ncRNA.

It should be noted that there is a small amount of endogenous Pumilio expressed in *D. melanogaster* S2 cells, however, optimal repression by the PUM RBD requires higher expression levels(Weidmann and Goldstrohm 2012); Figure 3.2 shows that there is a some amount of activity coming from endogenous PUM (compare empty vector with wild-type PBE vs. empty vector with mutant PBE, Figure 3.2). Mutation of the PBE abolishes PUM binding to the reporter, and this results in a dramatic stabilization of the poly(A) tail when compared to the wild-type PBE reporter. Expression of the RBD results in an increase of deadenylated reporter mRNA, and a decrease in fully-adenylated mRNA; this is consistent with the PUM RBD lowering target mRNA levels by activating deadenylation.

Figure 4.2

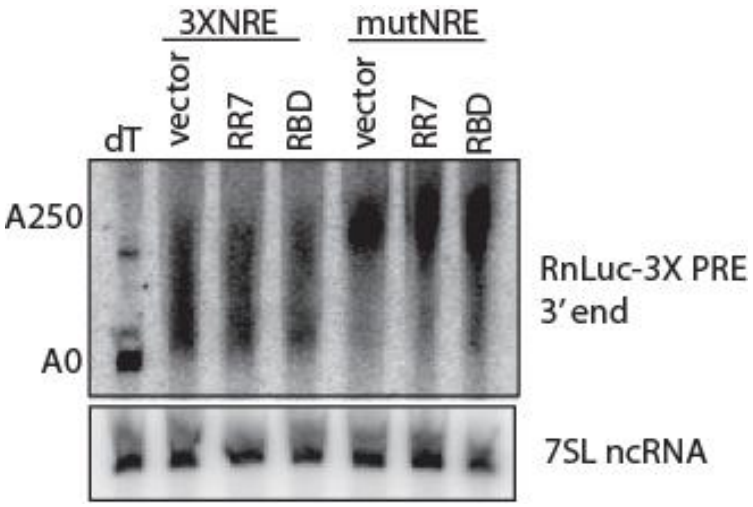

Figure 2. The PUM RBD Binds the 3X PRE and Activates Deadenylation. Empty vector, R7mut and RBD were transfected along with wild-type PRE reporter, or a reporter in which the PBE is mutated to abolish PUMs ability to recognize the target. This was followed by RNase H cleavage of the reporter mRNA and high-resolution PAGE, RNAs were detected with probes specific for the transcripts indicated. The A0 sample was generated using the same oligo to cleave, in addition to oligo dT to cause the degradation of the poly(A) tail by RNase H *in vitro*.

The PUM RBD Accelerates the Rate of Poly(A) Tail Removal: We next asked whether the RBD in fact increases the rate of deadenylation for a target mRNA. To do this, we expressed R7mut or the RBD along with the 3X-PBE reporter, and transcription was inhibited via addition of Actinomycin D. An aliquot of cells was taken immediately after drug addition and frozen, and then time points were taken at half-hour intervals out to two hours. RNA was extracted from these time points, cleaved with Rnase H and the poly(A) status of the reporter mRNA was monitored via northern blot. Figure 3 shows that very little deadenylation occurs on the reporter when the R7mut is expressed. Expression of the wild-type PUM RBD results in a dramatic acceleration of deadenylation, where the reporter is nearly fully deadenylated at the 1.5 hour time point; this result demonstrates that the PUM RBD accelerates the rate of deadenylation for a target mRNA.

Figure 4.3.

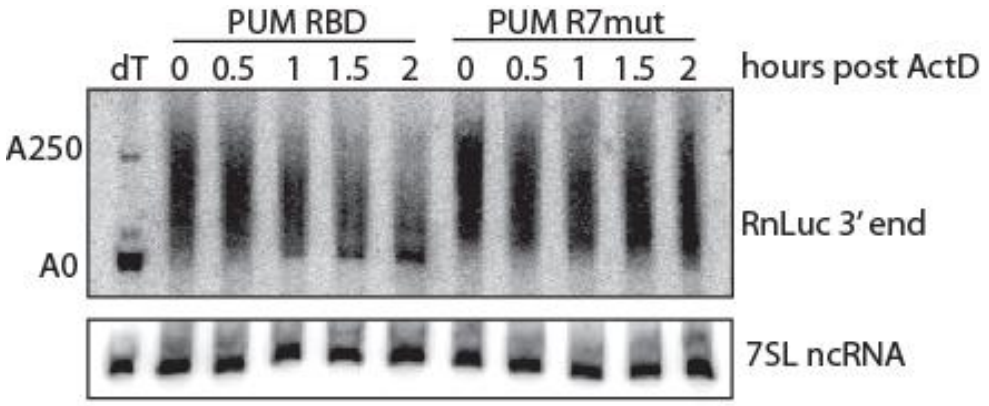

Figure 3. The PUM RBD Accelerates the Rate of Deadenylation. S2 cells expressing the 3X-PRE reporter and wild-type RBD or R7mut were treated with the inhibitor of transcription, actinomycin D. An aliquot of cells was taken immediately after drug was administered, and at the time points indicated. RNA was extracted, and the PBE reporter cleaved with RNase H as in Figure 2. Northern analysis was then performed to visualize the indicated RNAs.

Activation of Deadenylation: The enzyme in *D. melanogaster* that is responsible for the bulk of cytoplasmic deadenylation is Pop2, and its' associated co-factor Ccr4. In *S. cerevisaie*, Puf5p has been demonstrated to bind to Pop2p, also in *drosophila* PUM is able to bind to Pop2 (Kadyrova 2007), so we chose to test whether the Ccr4/Pop2 complex was involved in RBD-mediated activation of deadenylation in S2 cells. To ask this question S2 cells were bathed in double stranded RNAs that target *ccr4* and *pop2* respectively, or non-targeting siRNAs, which should have no effect. R7mut or RBD were also expressed along with the 3X-PBE reporter, and transcription was inhibited using Actinomycin D to monitor deadenylation over time. Figure 4.4 shows that siRNA knock-down of *ccr4*/pop2 results in a dramatic 3-4 fold increase in the reporter mRNA at the zero time point, strongly suggesting that deadenylation via Ccr4/Pop2 is important for the decay of this message. RBD expression in the context of the non-

Figure 4.4

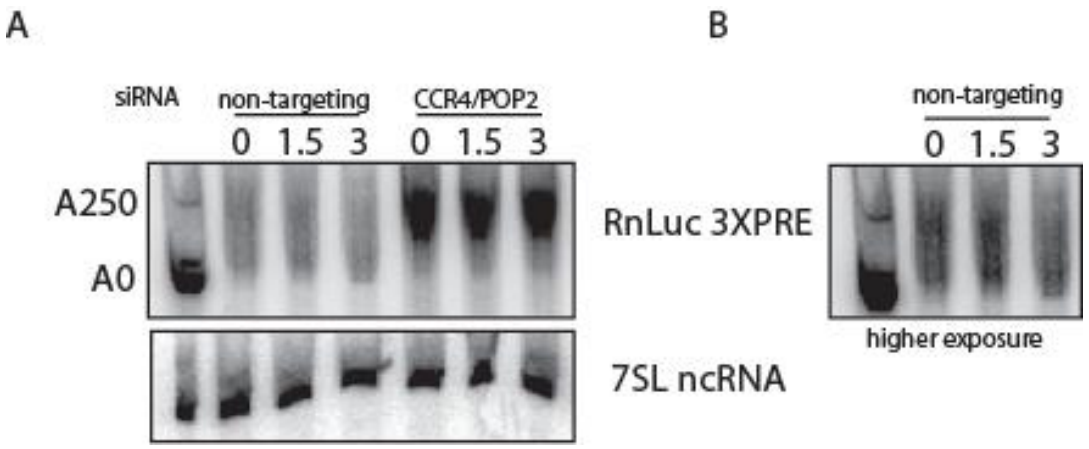

Figure 4. CCR4/POP2 are Important for PUM RBD-Mediated Deadenylation. A) siRNAs targeting CCR4 and POP2, or a non-targeting siRNA were transfected along with PUM RBD and the 3X PBE reporter in to S2 cells. 2 days post-transfection RNA was harvested, cleaved with Rnase H as described above, and separated with high-resolution PAGE. **B)** Is same gel with a higher gain level to visualize the reporter at a much lower level, due to PUM RBD mediated deadenylation and degradation.

targeting siRNA showed robust activation of deadenylation as shown in figure 4.3, however, knock-down of *ccr4/*pop2 resulted in an almost complete inhibition of deadenylation mediated by the PUM RBD; these results show that the PUM RBD is utilizing the Ccr4/Pop2 complex to activate deadenylation.

Decapping and Deadenylation are Involved in PUM-Mediated Degradation of the Reporter mRNA: The above result suggested that the canonical decay pathway involving deadenylation activated decapping and 5' – 3' degradation may be the pathway to destruction for a PUM-targeted mRNA. To test this, *ccr4/pop2*, and the decapping co-factor *dcp1* were knocked down individually, and in combination to determine the relative inputs of deadenylation and decapping on the PUM reporter mRNA. It is important to note that siRNA knock-down is not 100% effective; however knock-down efficiency was monitored at the mRNA level, and routinely reduced mRNA levels for targets by 80-90%. Also, knock-down of *dcp2* has been difficult, however, Dcp1 which catalytically activates Dcp2, and couples decapping to 5'-3' degradation, can be knocked-down. Figure 5 confirms that knock-down of *ccr4/*pop2 does result in a 4 fold increase in the mRNA level; strikingly PUM RBD expression still reduces the level of the reporter by 27% (Figure 4.5, lane 3 vs. lane 4). Knock-down of *dcp1* resulted in a 2-fold increase in mRNA levels, and in this case the RBD was slightly impaired in its' ability to reduce the reporter levels. *ccr4/pop2* and *dcp1* simultaneous knock-down caused an additive 10-fold increase in reporter mRNA levels, and the PUM RBD was only able to reduce the mRNA levels by 21%, compared to 30% in the non-targeting control siRNA. Taken together, these results indicate that decapping may play a role in the regulation of PUM-targeted mRNA levels, and that deadenylation is accelerated by the PUM RBD. As mentioned above, decapping is impaired but

still occurring, and the knock-down does not remove all target enzyme, given the inhibited ability of the PUM RBD to cause reporter mRNA degradation in the context of dcp1 knock-down.

Figure 4.5

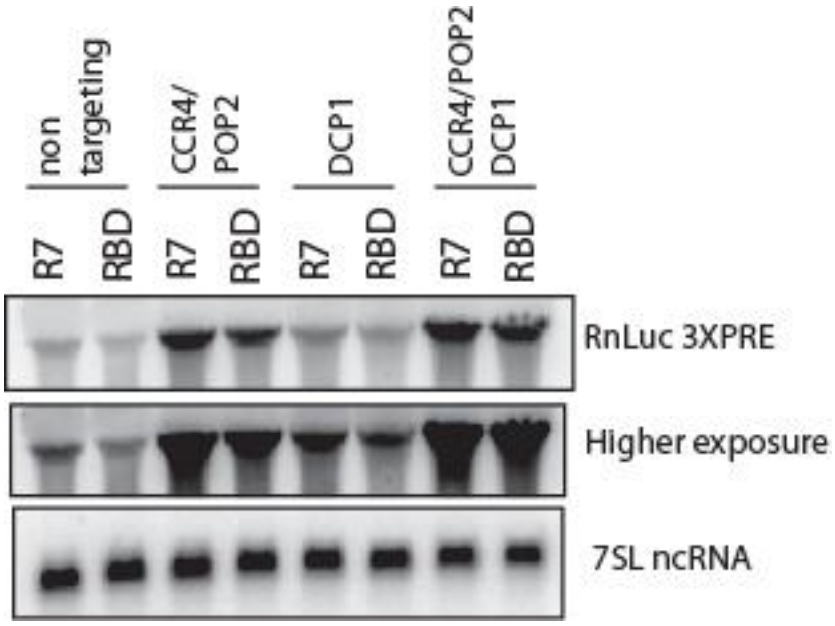

Figure 5. Deadenylation and Decapping Contribute to PUM RBD Mediated mRNA Degradation. Either non-targeting, or siRNAs targeting the indicated factors were transfected with with R7mut, or RBD and the 3XPRE reporter. RNA was harvested and separated on agarose MOPS/formaldehyde gel and probed for the indicated RNAs. The middle panel is the same gel as top panel with higher exposure level again to allow visualization of the lower abundance lanes.

We conclude that decapping is potentially involved in RBD-mediated regulation of target mRNA levels. Knock-down of the decapping and deadenylation machinery together impaired the ability of the RBD to reduce mRNA levels, however, percent repression of reporter protein remains at 27%, this may suggest that the PUM RBD is capable of exerting translational repression as well as activating mRNA decay. Removal of the poly(A) tail is known to result in decreased translation (Wiederhold and Passmore 2010), so it is likely that RBD-mediated

acceleration of deadenylation results in decreased translational efficiency for the reporter, and the RBD is also activating downstream decay steps which also serve to reduce protein output through reduction in mRNA levels. It is also possible that the 3' -5' decay pathway is important for PUM RBD repression

Poly(A) Binding Protein is Required for PUM RBD-Mediated Deadenylation and Contributes Strongly to Overall Repression at the Level of Protein Output: Several lines of evidence led us to question whether Pabp might be involved in repression by the PUM RBD. In *S. cerevisiae*, Pab1p has been reported to bind internal poly(A) tracts and be important for the ability of *PUF5* to repress the expression of reporter mRNAs in an *in vitro* translation extract (Chritton and Wickens 2011). Also, mammalian miRNA-mediated repression of targets has recently been demonstrated to involve deadenylation, and the recruitment of PABP was shown to be important for repression (Fabian, Mathonnet et al. 2009). To test the involvement of Pabp in RBD-mediated repression, *pAbp*-targeting dsRNAs were used, and either the R7mut, or RBD expression constructs were transfected along with the 3XPBE reporter. Cultures were treated with Actinomycin D to inhibit transcription, and deadenylation was monitored over a 2 hour time course as above.

Remarkably, *pAbp* knock-down completely abolished acceleration of deadenylation by the PUM RBD. There is no discernible difference in the rate of poly(A) tail removal comparing R7mut expression to RBD expression; this strongly implies a role for *pAbp* in the execution of RBD-mediated deadenylation. We also assayed the repression at the level of reporter protein output, and compared siRNAs which target *ccr4/pop2*, *pAbp*, or a non-targeting siRNA control.

As seen previously, *ccr4/pop2* knock-down had no effect on the ability of the RBD to reduce reporter protein output. Remarkably, knock-down of *pAbp* resulted in a 50% loss of repression

Figure 4.6

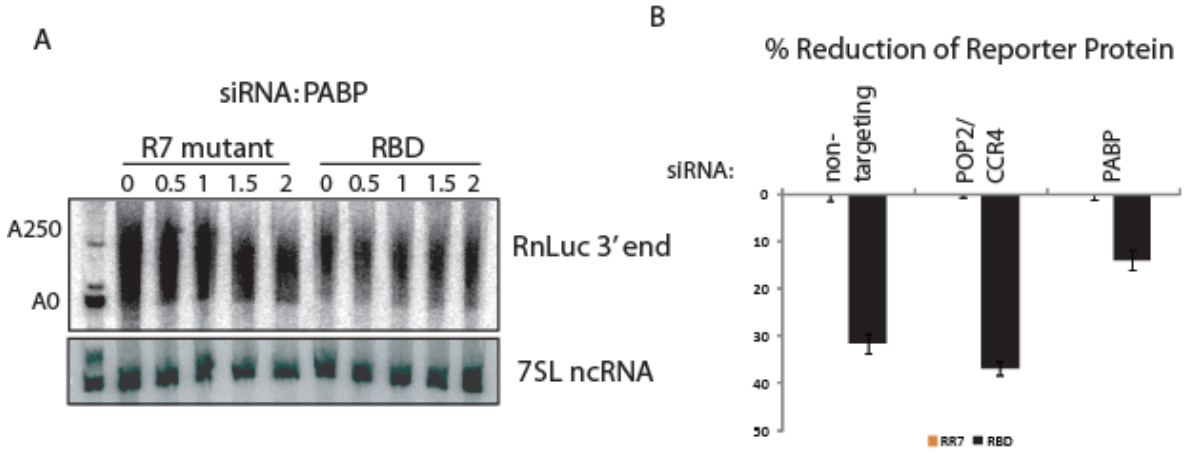

PABP is Required for RBD-mediated Acceleration of Deadenylation, and Contributes Strongly to Repression by PUM. A) siRNAs targeting PABP were transfected along with the 3X PRE reporter and either the R7mut, or RBD. Rnase H cleavage was performed and the RNAs indicated were analyzed via high-resolution northern blot. **B)** Dual-Glo luminenscence assay from biological quadruplicate samples. Renilla-3XPRE signal was normalized to non-regulated Firefly luciferase signal, then reduction in reporter output was calculated relative to R7mut expression. S.E.M. is plotted to indicate error.

by the RBD at the protein level; the RBD reduced protein output by 30% in the non-targeting control and only 12% with PABP knock-down. As knock-down is not completely effective, and Pabp is fairly abundant, is possible that the residual repression by the RBD is still coming through Pabp-mediated effects. Alternatively, it is equally possible that there remain additional effectors that the PUM RBD utilizes to direct repression, it is notable that the RBD does still reduce the reporter mRNA levels at time zero (Figure 3.5, compare R7 t0 vs. RBD t0). It seems plausible that the PUM RBD directs both *pAbp*-dependent translational repression, as well as decay dependent repression. While *pAbp* knock-down does not impair the ability of the RBD to reduce mRNA levels, repression at the level of reporter protein is compromised by 50%; this

suggests that *pAbp*-dependent deadenylation impairs translation of the message but does not necessarily lead to destruction. Nonetheless, a portion of the repressive activity from the conserved PUM RBD may also stem from activation of mRNA decay.

4.3 DISCUSSION

The Conserved PUM RBD Does not Require Ago or eEF1A to Reduce Reporter mRNA Levels or Exert Repression Overall. To confirm previous findings(Weidmann and Goldstrohm 2012) and extend the investigation into the mechanism utilized by PUM RBD to repress target mRNA expression we first compared reporter mRNA levels by northern blot to reporter luminescence output. In agreement with previous data, the PUM RBD reduced reporter mRNA levels to nearly the same extent as seen at the level of reporter protein. Mutation to residues reported to be required for interaction with Ago and eEF1A, and be important for *in vitro* repression had no effect on the ability of the RBD to repress the target mRNA. *ago-1* and *ago-2*, were knocked-down with dsRNAs to approximately 10% of original levels (measured by qRT-PCR), and this too had no impact on RBD-mediated repression. These results demonstrate through both mutations that abrogate binding, and siRNA knock-down that Ago and eEF1A are not important for PUM RBD-mRNA regulation in *D. melanogaster* cells. Also, the PUM RBD causes a reduction in mRNA levels, and it appears that the mechanism of repression is intimately linked to mRNA decay. Conversely, decapping and destruction of an mRNA is the ultimate translational inhibition, as the mRNA is no longer present to be translated

PUM RBD Activates Reporter mRNA Deadenylation, and this Requires the 3X PBE and RNA Binding by the RBD. PUF proteins activate deadenylation in yeast, flies, humans, and worms (Wreden, Verrotti et al. 1997; Goldstrohm, Seay et al. 2007; Suh, Crittenden et al. 2009; Van Etten, Schagat et al. 2012) While PUM activation of deadenylation has been

demonstrated in the developing fly embryo, it was important to mechanistically assess poly(A) regulation by PUM in our S2 cell culture model because it allows functional dissection of elements important for regulation. We found that PUM does robustly accelerate deadenylation of a PBE reporter, and this activity was largely blocked by mutation of the PBE.

We also wished to determine which enzymes are responsible for deadenylation of the PBE reporter. *D. melanogaster* encodes six known deadenylase enzymes, Pop2, Pan, Ccr4, Nocturnin, Angel, and 2-PhosphoDiesterase. We chose to test Ccr4 and Pop2 for their involvement in PUM-mediated deadenylation as PUFs in yeast, humans, and worms all are known to associate with Ccr4 and Pop2 orthologs, as well as functionally promote deadenylation via these enzymes. We found that Ccr4 and Pop2 are required for PUM-activated deadenylation of the PBE reporter; dsRNAs targeting *ccr4/pop2* completely abolished deadenylation of the PBE reporter. While we have not tested the involvement of the other poly(A) nucleases, the activity of Ccr4 and Pop2 are necessary for PUM-mediated acceleration of deadenylation.

The Deadenylation and Decapping Pathways are Important for PUM-mediated Degradation of a Targeted mRNA. All poly-adenylated mRNAs are subject to deadenylation, but at varying rates that tend to correlate well with mRNA stability. Because the Ccr4/Pop2 deadenylase machinery acts on all messages, perturbation of their activity can lead to global changes in post-transcriptional mRNA regulation. Knock-down of *ccr4/pop2* increased reporter mRNA levels by 6-fold when R7mut was expressed, and 4-fold when the RBD was expressed; the data suggest that Ccr4/Pop2 contribute to PUM-mediated reduction in mRNA

levels, and that the PUM RBD is also capable of reducing mRNA levels when deadenylation is impaired.

Knock-down of the decapping co-factor, Dcp1 impaired PUM-mediated mRNA decay activity. This is striking, because knock-down of Dcp1 reduces Dcp1 levels by 80%, but there is still some residual Dcp1 present in the cells. Also, the decapping enzyme, Dcp2, was not targeted, so it is likely that decapping catalysis is still being stimulated by the small amount of Dcp1 which remains after dsRNA treatment. Because Dcp1 knock-down impairs PUM repression by 10% it is very likely that decapping is an important regulatory step that is targeted by the PUM RBD. This is particularly relevant in light of data from *S. cerevisiae* Puf5p, which is known to recruit Ccr4p/Pop2p and accelerate deadenylation. *PUF5* can also repress its target mRNA when deadenylation is genetically abolished; *PUF5* is able to circumvent the general requirement for deadenylation and directly recruits activators of decapping and the decapping enzyme (Goldstrohm, Hook et al. 2006; Hook, Goldstrohm et al. 2007). Repression at the protein luminescence level was monitored for each of these experiments, and while *ccr4/pop2* knock-down had no effect on overall repression, *dcp1* knock-down actually reduced repression by a modest 10 %(data not shown). So, while the effects of *dcp1* knock-down are likely partial, these results indicate a potential role for PUM RBD to impact 5' cap removal.

One conclusion reached from this experiment is that both deadenylation and decapping activities have additive effects on PUM-targeted mRNA levels, and that the PUM RBD activation of decay was is impaired by inhibiting mRNA decapping.

Poly(A) Binding Protein (PABP) is Required for RBD-Mediated Acceleration of Deadenylation, and Accounts for 50% of Overall RBD Repression. Pabp, as its name suggests, binds stretches of A residues at least 5 bases in length. It is commonly found in the context of a circularized mRNA, and is known to contact the initiation factor eIF-4G, which binds to cap-bound eIF-4E. It's function in this case is thought to play a protective role for the poly(A) tail, and also promote translation initiation by assisting forming of the eIF-4F complex (Mangus, Evans et al. 2003).

So how then does PABP promote PUM-mediated deadenylation, and also promote mRNA stability and translation initiation? There are reports that Pabp has a conserved function in promoting the formation of repressed RNPs, as well as in activation of deadenylation. Pab1p is important for post-transcriptional mRNA repression by: Puf5p, the miRNA RISC machinery, the RBP Sex Lethal, as well as a neuronal RBP known as Musashi (Kawahara, Imai et al. 2008; Duncan, Strein et al. 2009; Fabian, Mathonnet et al. 2009; Chritton and Wickens 2011; Huntzinger, Kuzuoglu-Ozturk et al. 2013). The mechanism of repression via PABP generally involves an RBP associating with PABP, which inhibits formation of the translation pre-initiation complex. Those activities, when viewed in the context of the results presented in Figure 6 provide a hint as to how PABP seems to retain both inhibitory and activating qualities for mRNA regulation. In the case of Puf5p, Pab1p binding in close proximity to Puf5p strongly increased repression in an *in vitro* translation system. .

There has been significant argument over the mechanism miRNA repression, specifically, what roles do deadenylation, translational repression, and mRNA decay play in the overall repression of a target message. This situation is remarkably similar to the PUF protein story, with many of the same actors taking the stage. One piece of evidence Figure 6 demonstrates is that *pabp* knock-down almost completely inhibits PUM activation of deadenylation, and also reduces overall repression by 50 %. There is no reason to suspect that Pabp has exo-nuclease activity, and, as noted above, siRNAs against *ccr4/pop2* completely block deadenylation. Therefore, it is likely PUFs target PABP to inhibit translation, and this activity acts as a signal to promote deadenylation, possibly through association of the PUM RBD, PABP, and the Ccr4/Pop2 complex. In this model, PUM bound in proximity to Pabp results in de-stabilization of the eIF-4F complex, which immediately exposes the 3' end of the mRNA to deadenylases in recruited by PUM. This result shows that the PUF RBD retains a conserved function to utilize PABP to direct translational represson, and the Ccr4/Pop2 deadenylase complex to elicit deadenylation

While *pAbp* knock-down resulted in a 50% loss or repression, the RBD still retains half of its' repressive activity. It is clear that the canonical deadenylation and decapping pathways are acting on the PUF-targeted mRNA. It is enticing to speculate that the PUM RBD may activate decapping independently of deadenylation, in yeast, the *HO* mRNA is deadenylated extremely rapidly, and this is promoted by Puf5p. However, deadenylation is not required for repression by Puf5p. Eap1p is required however, and has no impact on the rate of deadenylation, but promotes removal of the 5' cap; demonstrating the ability of a PUF protein to independently

activate multiple steps of mRNA regulation that have varying degrees of impact on the overall protein output of the mRNA.

There are several open questions that will more clearly define the specific mechanism of repression by the PUM RBD. One important question is: does the PUM RBD directly contact the decapping enzyme, and/or Pabp? It seems likely that the PUM RBD may be a central physical link that allows for the formation of a large repressive complex on a targeted mRNA. To address this it will be important to delineate the direct physical connections that PUM forms with each of these co-factors. It is also crucial to determine what the mechanism is behind PUM targeting Pabp for translational repressive activities. Both the Musashi and Sex Lethal RBPs bind to PABP and block binding to eIF-4G, effectively de-circularizing the mRNA. Is this the case with the PUM RBD?

In vitro competition binding experiments will be helpful to determine if the PUM RBD blocks eIF-4G binding to PABP. Finally, there is still significant decay elicited by the PUM RBD when deadenylation and decapping are impaired. Two likely possibilities can explain this: decapping is not blocked by Dcp1 knock-down, therefore PUM activated degradation of the mRNA may be caused by recruitment of the decapping machinery to a targeted mRNA, alternatively, the PUM RBD may recruit the 3' – 5' exonuclease machinery to destroy the mRNA after deadenylation. Therefore, knock-down of exosome subunits will be a useful tool to ask if 3' -5' decay is important for PUM repression. Also, the use of dominant negative decapping enzyme along with knockd-down of Dcp1 should more severely impair decapping,

and thus we would expect much less repression and degradation promoting activity via the PUM RBD.

4.4 Materials and Methods:

Northern Analysis: For detailed protocol refer to Blewett et. al., MCB 2012. Briefly 20µg RNA was separated in a 0.85% agarose MOPS/formaldehyde gel. RNAs were transferred to nytran membrane with TurboBlotter™ for 3 hours. Membranes were U.V. crosslinked and probed for the RNAs indicated.

Rnase H Cleavage: For detailed protocol refer to Blewett et. al., MCB 2012. Briefly, 15-20µg RNA was annealed to cleavage oligo NB119. 2U Rnase H was added to each reaction, oligo dT reaction received 5ug oligo dT. RNAs were cleaved 1 hour at 37 °C, then precipitated with 1/10 volume 3M Sodium Acetate, and 3 volumes 100% Ethanol for 1 hour at -20°C RNAs were pelleted, washed with 70% ethanol and resuspended in denaturing RNA loading buffer. RNAs were separated in 5% polyacrylamide, 7M urea, 0.5X TBE gels. Electrophoretic transfer was performed with BioRad TransBlot Cell for 1 hour at 60V. Membranes were then probed for the indicated RNAs.

Oligos:

Renilla-3X NRE T7 transcription primers:

Forward

NB113: 5’ GCCCGTGGCTAGATGCATCATCC 3’

T7 promoter Reverse:

NB114: 5’ GGATCCTAATACGACTCACTATAGGGCGGACAATCTGGACGACGTCGG3’

Rnase H cleavage oligo:

NB120: 5’ CCTTGAATGGCTCCAGGTA 3’

Renilla-3X NRE poly(A) tail T7 transcription primers

Forward:

NB119: 5’ GGGCGAGGTTAGACGGCCTACCCT 3’

T7 promoter Reverse:

NB118: 5’ GGATCCTAATACGACTCACTATAGGGGCGGCCAGCGGCCTTGG 3’

YL41 oligo probe:

NB129: 5’ TTTAGGGCCACCATTTTAGGGCTACCCAGTCGGCG 3’

7SL ncRNA oligo probe:

NB117: 5’ CACCCCTGGCCCGGTTCATCCCTCCTTAGCCAACCTGAATGCCACGG 3’

LacZ control, forward primer: 5’

dGGATCCTAATACGACTCACTATAGGGTGACGTCTCGTTGCTGCATAAAC3’

LacZ reverse primer: 5’

dGGATCCTAATACGACTCACTATAGGG**GGCGTTAAAGTTGTTCTGCTTCATC**;

***Pop2*, forward primer:**

5 –dGGATCCTAATACGACTCACTATAGGG**GGACACCGAGTTTCCAGGCG**

reverse primer:

5 –dGGATCCTAATACGACTCACTATAGGG**GAAGAAGGCCATGCCCGTCAGC**

***Ccr4*, forward primer:**

5 –dGGATCCTAATACGACTCACTATAGGG**GGAAGTACGTCGATGGCTGTGC**

reverse primer:

5 –dGGATCCTAATACGACTCACTATAGGG**CGAACGTATAGTTGGTGTGCGGCATT**

dsRNA templates: From each PCR template, double-stranded RNA (dsRNA) was transcribed *in vitro* with the T7 RiboMAX large-scale RNA production system (Promega), treated with Turbo DNase (Ambion) for 3 h, and purified using the SV total RNA isolation system (Promega). For knockdown of each gene's expression, 6 g of dsRNA per well of a 6-well plate was added to cells 10 min before transfection of reporters and expression vectors.

RNAi Experiments: Double-stranded RNAs (dsRNAs) were generated for RNAi of non-targeting control (NTC) LacZ, Pop2, and CCR4 as previously described **(Weidmann, Van Etten)**. New primers with T7 promoter sequence underlined and gene specific regions bolded include: AGO1 forward primer, 5'-dGGATCCTAATACGACTCACTATAGG**CCAATCACTTCCAGGTGACAATGC**, and reverse primer, 5'-dGGATCCTAATACGACTCACTATAGG**CCACTGCGAGGGCCTTACG**; AGO2 forward primer, 5'-dGGATCCTAATACGACTCACTATAGG**GGATGGAGCAACTCAGGTGGC**, and reverse primer, 5'-dGGATCCTAATACGACTCACTATAGG**GAGGAATAATCACAATTGCCAGATCG**; pAbp forward primer, 5'-dGGATCCTAATACGACTCACTATAGG**GCGTATGCAGCAGCTGGGACAG**, and reverse primer, 5'-dGGATCCTAATACGACTCACTATAGG**CCTTGCAATTGCTGTGGAATTGGC**.

Corresponding regions were amplified via PCR from D.mel-2 cells and dsRNA was transcribed *in vitro* and purified as previously described (Weidmann and Goldstrohm 2012). For knockdown, each 6-well of cells with total volume 2.2 mL was treated with 6µg dsRNA for 5 minutes before

transfection. For knockdown during transcription shutoff assays, 20mL total volume was treated with 60µg dsRNA 5 minutes before transfection.

Transcription Shutoff: Two days post-transfection in a T-150 flask transfection (14.6mL 1M/mL D.mel-2 cells, 5.4 mL sf900iii media, 3636ng pIZ vector, 91ng Renilla vector, 45.5ng Firefly vector, 818µl EC buffer, 29.1µl Enhancer, 36.36µl Effectene), 5µg/mL of Actinomycin D was added. RNA was harvested from 3.5mL of transfection once immediately before addition of Actinomycin D (0hr) and at distinct time points after addition. Cells were washed twice in PBS and RNA was prepared using the LEV simplyRNA Tissue Kit and the Maxwell 16 instrument (Promega)

Chapter Five

Concluding Thoughts and Future Directions:

Analysis of mRNA Decapping *in vivo:* Removal of the 5′ cap from an mRNA is tightly regulated, and commits the mRNA to destruction. The decapped mRNA is highly labile due to the activity of Xrn1p, the 5′ – 3′ exonuclease. Because the decapped mRNA species is so fleeting, it has been difficult to measure the process of decapping quantitatively. Several methods have been used to assess decapping, but these involve the use of: reporter mRNAs with extreme secondary structure to block 5′-3′ degradation (He and Parker 1999), or reconstituted *in vitro* systems (Zhang, Williams et al. 1999). All of these methods have been useful in identifying and characterizing the 5′ mRNA decay pathway however, quantitative *in vivo* analysis of endogenous mRNA decapping has been difficult to achieve. In Chapter 2, I presented a manuscript published in the journal RNA in 2011, a novel, quantitative-Splinted Ligation-Reverse Transcription Polymerase Chain Reaction (q-SL-RT-PCR) assay to measure decapping of endogenous mRNAs *in vivo*; this represents the first assay to quantitatively assess the rate of decapping for an endogenous mRNA (Blewett, Coller et al. 2011). I have shown that decapped mRNA can be detected across several orders of magnitude, with precise reproducibility.

Mechanistic analysis of decapping in mammalian cells has been recalcitrant to investigation, primarily because the use of strong secondary structure in a reporter mRNA does not block degradation of the mRNA as it does in yeast. The q-SL-RT-PCR assay is well-suited to directly analyze mRNA decapping in mammalian cell culture models. Efficient knock-down

of Xrn1 is crucial to quantitative analysis of decapping. It may be worthwhile to establish Xrn1 siRNA expressing, stable clonal lines for optimal knock-down. Alternatively, RNAi in *D. melanogaster* S2 cells is particularly effective, and mechanistic analysis of decapping for PUM targets would be another valuable experimental path which would likely yield valuable insight into post-transcriptional control of eukaryotic gene expression.

Given the role I have demonstrated for *PUF5* in yeast in promotion of decapping and mRNA degradation (Blewett and Goldstrohm 2012), the role demonstrated for human PUM in activation of deadenylation and mRNA decay (Van Etten, Schagat et al. 2012), and the presence of PUM Recognition Elements in the 3′UTR of a tumor suppressor (Kedde, van Kouwenhove et al. 2010), it is likely that PUM controls the stability of mRNAs are involved in cell-cycle regulation and cancer formation. It will be informative to analyze the decapping rate of mRNAs which contain PUF sites, and have been associated with cancer formation. The qSL-RT-PCR assay could be used to compare the rate of decapping for PUM target mRNAs in healthy prostate cells, as well as prostate cancer cell lines. The 5′ transcriptional start site (TSS) of the tumor suppressor p27 would be mapped via 5′ Rapid Amplification of cDNA Ends (5' RACE). Based on the 5′ RACE identification of the p27 TSS a DNA splint would be designed which hybridizes to the 5′ end of the p27 mRNA, and to a synthetic RNA anchor. Then, Xrn1 will be knocked down along with either non-targeting siRNAs, or siRNAs targeting both PUM1 and PUM2. Initially it will be beneficial to determine if there is a decrease in the amount of decapped p27 when PUMs are knocked-down. Subsequent experiments utilizing Actinomycin D will then be employed to determine the decapping rate on p27 with or without PUM knock-down. As a

complement to this approach it will also be useful to determine the p27 mRNA half-life in these experiments, which can then be correlated with effects on decapping.

PUF5 and EAP1: Control of mRNA Stability and Interplay with the Translational Machinery: In Chapter 3, I presented a manuscript published in the journal Molecular Cellular Biology, in 2012, which demonstrated a novel function for the eIF-4E binding protein *EAP1* in the activation of mRNA decapping. I showed that *EAP1* is required for *PUF5* mediated repression of its target, *HO* mRNA, and that unexpectedly *EAP1* did not inhibit the translation of *HO* mRNA, but accelerated its destruction. The activity of *EAP1* was not limited to *HO* mRNA; *EAP1* also strongly accelerates the decay of the non-PUF target *RNR1* mRNA without impacting the translation of this message either. It should be noted that the abundant and stable *RPL41* mRNA was not impacted by *EAP1* activity.

All mRNAs have a 5′ cap, and are bound by eIF-4E, but not all mRNAs are susceptible to 4EBP regulation equally (Dowling, Topisirovic et al. 2010; Blewett and Goldstrohm 2012). One way that RNA-binding proteins exert regulation on bound mRNAs is to recruit effector proteins through physical association, and increase the local concentration of repressive proteins. It is possible that Eap1p may be a component of the general decapping machinery, which is then recruited to certain mRNAs through a variety of RNA-binding proteins. In fact, Puf5p is not the only RNA-binding protein to utilize Eap1p to activate mRNA degradation. Another RBP known as Vts1p has recently been demonstrated to associate with Eap1p, which results in activation of decapping and degradation (Rendl, Bieman et al. 2012). It is likely that Puf5p and Vts1p are not

the only RNA-binding proteins to utilize Eap1p, and it is important to understand which, and how many mRNAs are affected by *EAP1* at the level of stability.

Global analysis of the effects of *EAP1* on ribosome occupancy has been performed (Cridge, Castelli et al. 2010): however effects on mRNA half-life by *EAP1* were not assessed. It is important to note that *eap1* deletion results in an increase in *HO* mRNA ribosome occupancy, however, this simply reflects an overall increase in total *HO* mRNA due to impaired decapping and degradation. Therefore global analysis of mRNA half-lives in wild-type and *eap1* yeast will yield valuable insight into the extent of Eap1p-mediated activation of mRNA decapping. This could be achieved through inhibition of transcription, RNA would then be extracted at prescribed time points after inhibition from wild-type and *eap1* mutant cultures with biological replicates. A high-throughput RNA-sequencing library would be produced and sequenced to generate global mRNA decay rates (Tani, Mizutani et al. 2012) between wild-type and *eap1* mutants. mRNAs that undergo *EAP1*-mediated degradation could then be searched for enrichment of known RNA-binding protein recognition sequences; it is likely that this method will uncover novel, functional RBP-4EBP mediated mRNA regulatory complexes.

Another interesting facet of Eap1p post-transcriptional regulation is that no effects are seen on ribosome occupancy for repressed mRNAs. In fact, polyribosome analysis of *HO* mRNA revealed somewhat surprisingly that in wild-type cells *HO* mRNA is 90% occupied by ribosomes; there is almost no free *HO* mRNA in the pre-80s fractions of the polysome sucrose density gradient. Because there is very little detectable *HO* mRNA that is not engaged with ribosomes, there must be a very rapid transition between the translation of *HO* mRNA by several

ribosomes, to an mRNA which is committed to destruction. Previous work has shown that decapped mRNAs can be engaged with multiple ribosomes, and suggests that Xrn1p destroys mRNAs in a 5′ -3′ manner immediately behind the last transiting ribosome (Hu, Sweet et al. 2009; Hu, Petzold et al. 2010).

Destroying an mRNA immediately behind the final ribosome represents an efficient method of insuring complete silencing of gene expression. In the case of *HO* endonuclease, there is a short window of expression to facilitate mating-type switching, but mis-expression of *HO* results in inappropriate *HO* endonuclease activity, and cell-cycle arrest, which highlights the need for efficient, rapid destruction of the message. My findings are consistent with a model in which *HO* mRNA is exported into the cytoplasm, and is immediately engaged by several ribosomes. Once Puf4p, and Puf5p bind to the 3′ UTR, the deadenylase machinery as well as Eap1p are recruited. Eap1p disrupts the interaction between eIF-4E and eIF-4G, causing decircularization of the mRNA and exposing the Poly(A) tail to recruited deadenylases. Disruption of the eIF-4F complex weakens the association of eIF-4E with the 5′ cap, allowing the decapping machinery to compete more effectively with eIF-4E for binding to the 5′ cap, the mRNA is then destroyed by the processive activity of Xrn1p immediately behind the last transiting ribosome.

Several questions remain unanswered regarding the specific physical interactions that link Puf5p and Eap1p. I have shown that Puf5p, Dhh1p, and Eap1p associate *in vivo*, but it remains unclear if Eap1p directly contacts Puf5p or Dhh1p, or rather, if the observed association is bridged by another protein. Efforts to produce recombinant, purified, full-length Eap1p and

Puf5p were not successful. The majority of products produced in *E. coli* were truncated, to remedy this, efforts were made to supply rare tRNAs. Also, several different translation induction protocols utilizing different temperatures, and times were attempted, none of which were successful. *EAP1* production was also attempted in wheat germ extract, as well as rabbit reticulocyte lysate, which both yielded poor results. As a result of the limited amount of purified protein available, *in vitro* pull-down assays were inconclusive. Previous work has demonstrated that Puf5p directly binds Pop2p, and also associates with the decapping enzyme co-factor, Dcp1p (Goldstrohm, Hook et al. 2006). It would be very intriguing to understand mechanistically, and sequentially how Puf5p co-ordinates the recruitment of deadenylases, Eap1p and the decapping machinery.

One way to define the specific protein contacts that form the complex, Puf5p, Eap1p, Dhh1p, and Dcp1p, is through a co-immunoprecipitation strategy where components of the proposed PUF-decapping complex are deleted. Eap1p would be immunoprecipitated with Puf5p in the context of *dhh1*, *pat1*, *pop2* or *dcp1* mutant backgrounds to determine if the association between Eap1p and Puf5p relies on any of these proteins. A similar strategy could be carried out to determine if Eap1p association with Dhh1p relies of Puf5p. Because there are likely other proteins that associate with Puf5p and Eap1p and participate in the activation of decapping, this method will not prove that Eap1p and Puf5p physically associate, but it will serve to better resolve how Puf5p orchestrates multiple repressive activities.

The function of the extended C-terminus of Eap1p remains unknown; there are no clear regions of sequence conservation in *EAP1* outside of the eIF-4E binding motif. In order to gain a clearer understanding of how Eap1p activates mRNA decapping and degradation it will be useful to identify *EAP1* mutants which are unable to rescue the decay phenotype of the *eap1* deletion mutant. I have shown that the eIF-4E binding activity is not absolutely necessary for activation of mRNA decay; therefore *EAP1* could be divided into N and C-terminal fragments to ask which region promotes mRNA decay. Further sub-division should yield a minimal *EAP1* fragment which is still capable of accelerating mRNA decay. After identification of regions important for activity, co-immunoprecipitation experiments could be performed to ask if Puf5p, and Dhh1p still associate with the inactive mutant. Another benefit of this strategy is that smaller regions of *EAP1*, which are still active for decay promotion, may prove easier to translate either in *E. coli.*, or with *in vitro* systems. If sufficient amounts of Eap1p could be produced, *in vitro* pull-down experiments would then be a feasible option to determine if Eap1p contacts Puf5p, or Dhh1p directly. The pull-down data could then be correlated to the functional rescue experiment outlined above to more precisely define how Puf5p recruits Eap1p, Dhh1p, and Dcp1p to *HO* mRNA. Identification of the specific physical interactions that form the Puf5p recruited repressive complex will be crucial in determining specifically how Eap1p promotes decapping. This is a relevant question, as Eap1p can promote mRNA degradation in the absence of deadenylation.

The general mRNA decay pathway is thought to proceed via a step-wise process that initiates with deadenylation, and loss of Pab1p from the poly(A) tail, and eIF-4E from the 5′ cap. The Lsm complex along with Pat1p and Dhh1p then associate with the short oligo(A) tailed

mRNA and recruit the decapping machinery to the exposed 5′ cap resulting in decapping and 5′ – 3′ degradation of the mRNA. Dhh1p stimulates the *in vitro* activity of the purified decapping enzyme (Fischer and Weis 2002), yet, Dhh1p is also able to destabilize the 48s pre-initiation complex, and inhibit both cap-dependent and cap-independent translation *in vitro* with no impact on mRNA stability (Coller and Parker 2005). Another component of the general decapping machinery is Pat1p which was originally identified as an activator of decapping (Tharun, He et al. 2000). Further work demonstrated that Pat1 inhibits the formation of, or destabilizes the 48s pre-initiation ternary complex in an *in vitro* translation extract, also, *in vitro* pull-down assays indicated that Pat1p directly interacts with Dhh1p as well as Dcp1p (Nissan, Rajyaguru et al. 2010). Pat1p and Dhh1p play multiple roles, both in direct activation of the decapping enzyme, and in destabilizing the 48s pre-initiatiation complex: it is not currently known if decapping activation and inhibition of early initiation steps by Pat1p or Dhh1p are separable activities. Aside from the multiple functional roles Pat1p plays in mRNA regulation, it also serves as a scaffold to physically link the components of the deadenylation, and decapping machinery, forming a complex on deadenylated mRNAs that simultaneously silences translation and activates mRNA decay.

Interestingly, repression by Puf5p does not require deadenylation, but does require Eap1p, which activates decapping, apparently circumventing the need for an initiating deadenylation event. Puf5p may be able to activate deadenylation-independent decapping through direct recruitment of Pat1p, Dhh1p, and Eap1p. The role of Dhh1p and Pat1p appear to be destabilization of the 48s pre-initiation complex, whereas Eap1p binding to eIF-4E results in dissociation of eIF-4G, causing linearization of the mRNA. Puf5p also appears able to target

Pab1p for repression *in vitro* (Chritton and Wickens 2011). Aside from recruitment of Eap1p to *HO* mRNA, Puf5p may also promote disruption of the circularized mRNA through association with Pab1p.

While difficult to undertake, a reconstituted system which re-capitulates the circularized protected mRNA would prove extremely useful to test the above model. Cap-bound eIF-4E competes effectively with the decapping machinery, and inhibits decapping (Schwartz and Parker 2000). Also, the eIF-4F complex consisting of cap-bound eIF-4E, eIF4G, and Pab1p bound to the poly(A) tail is known to strengthen the association of eIF-4E with the 5′ cap. Our model suggests that Eap1p weakens the association of eIF-4E with the 5′ cap, in the context of competition with the decapping machinery, and it seems likely that Dhh1p may also be involved in evicting the translation initiation machinery, possibly through its ATPase/helicase activity. One way to test this model will be to mutate the ATPase domain of *dhh1*, and ask if the Dhh1p mutant is able to complement the defect in mRNA decay for *HO* mRNA seen in the *dhh1* deletion mutant.

To ask if Eap1p or Dhh1p facilitate access of the decapping machinery to a circularized mRNA, the first step is to recapitulate mRNA circularization *in vitro*, with purified eIF-4E, eIF-4G, and poly(A) binding protein (Wells, Hillner et al. 1998; Deshmukh, Jones et al. 2008). Components of the eIF-4F complex, as well as the decapping complex Dcp1p/Dcp2p can be expressed and purified from bacteria with affinity tags (Steiger, Carr-Schmid et al. 2003). For the purposes of this experiment it will be important to use an RNA substrate which is long enough to accommodate circularization, and also approximate an average mRNA. A PCR

product would be generated to construct a T7 RNA polymerase template of roughly 1kb in length. The synthetic RNA would be purified, and capped using commercially available vaccinia virus capping enzyme, the RNA will then be poly-adenylated using commercially available poly(A) polymerase.

The most important piece of the assay is Eap1p, as stated above; Eap1p is extremely difficult to produce *in vitro* or with bacteria translation systems. There are two potential paths to overcome this limitation; the first involves successful identification of a smaller fragment of Eap1p that still retains the ability to activate decapping. It is not guaranteed that a smaller fragment of Eap1p will be translated more efficiently, but it would be worth the effort, and be useful for a variety of experimental purposes. As complement to the first approach, it could be informative to immunopurify Eap1p from yeast, in the context of various deletion strains such as: *dhh1*, *puf5*, *dcp1*, etc. This approach would be geared towards understanding the nature of the complex that Eap1p is associated with, and its' functional impact on decapping.

Given a supply of Eap1p, whether as a minimal fragment, or as a purified complex, the assay would be performed as follows: The capped, poly-adenylated RNA will be pre-incubated with the eIF-4F components. In one reaction Dcp1p/Dcp2p would be added. In another reaction, the decapping machinery and Eap1p are added together. Negative controls would include a reaction consisting of just eIF-4F complex alone. Another reaction will include naked RNA, or naked RNA and Eap1p by itself. Several factors could be monitored from this reaction. First, because mRNA decay is not active, decapped RNA molecules will remain stable. Thus, the accumulation of decapped RNA could be monitored over time with the qSL-RT-PCR assay

to afford quantitative assessment of decapping rates. Alternatively, decapping could be monitored with the use of Thin Layer Chromatography to resolve the cleaved, radioactively-labeled cap structure.

Our model predicts that, under competition with the decapping complex, Eap1p will promote the dissociation of eIF-4E from the cap. To test this prediction eIF-4E could be immunoprecipitated from each of the above conditions using a radio-labeled synthetic capped RNA. RNA would be extracted from eIF-4E pull-down in the context of the eIF-4F complex alone, or with the addition of Eap1p, Dhh1p, or both together. The amount of RNA engaged with eIF-4E could then be quantitated by Northern blot and phosphorimage analysis. If correct, our model would predict that addition of Eap1p would reduce the association of eIF-4E with the RNA.

A complementary, however technically challenging, approach would be to use Fluorescence Resonance Energy Transfer (FRET) to ask if addition of Eap1p results in decircularization of the RNA. I would take a similar approach to that used by (Abelson, Blanco et al. 2010); in this case I would label the extreme 5′ end of the RNA with a donor Cy3 and the 3′ UTR immediately adjacent to the synthetic poly(A) tail would be modified with acceptor Cy5 flourophore. The experimental conditions outlined above would be used, along with naked RNA to control for the natural conformational dynamics the RNA will undergo. It will be very interesting just to monitor the difference in FRET values between the naked RNA and that bound by eIF-4E; this should increase the FRET value if *bona fide* circularization is occurring.

Subsequent addition of the decapping machinery and Eap1p respectively will allow us to test this model of Puf5p and Eap1p activated decapping.

There are certain to be technical challenges associated with the application of FRET to this assay. The foremost challenge will be generation of robust, specific, reproducible FRET signal. The orientation angle between the FRET donor and acceptor will dictate the efficiency of resonant energy transfer, and it must be empirically determined whether the fluorophores placed at the 5′ and 3′ end of the RNA are capable of FRET. If this proves to be unfeasible, an alternative and potentially informative approach could be taken wherein either eIF-4E, and Pab1p, or eIF-4G and Pab1p would be labeled with donor and acceptor fluors through Chemoselective Ligation (CLick) chemistry. Briefly, CLick chemistry has been applied in a variety of ways to specifically label a modified, unnatural amino acid, in this case L-azidohomoalanine, which can be incorporated during translation. After affinity purification, the protein will be modified with a Cy3 or Cy5 alkyne fluorescent molecule using commercially available sources. Through this battery of conditions utilizing FRET moieties on a combination of both proteins and RNA we can begin to develop a more sophisticated view of the dynamics of mRNA regulation.

I have demonstrated a novel activity for an eIF-4E binding protein in the activation of mRNA decapping. The results presented in Chapter Three (Blewett and Goldstrohm 2012) indicate that some 4EBPs are able to carry-out repressive mechanisms that diverge from the initial model of inhibition of translation initiation. As indicated above, little is known about the function of the C-terminus of Eap1p due to lack of sequence conservation or functional analysis.

A *Drosophila* 4EBP, Cup, inhibits translation by activation of deadenylation and, surprisingly, stabilizes the silenced mRNA. Yet when Cup was dissected into three functional domains, a mid and q-rich domain both activate deadenylation and decapping in S2 cells (Igreja and Izaurralde 2011). It appears that full-length Cup contains a domain that impairs the activation of decapping via the mid, and Q-rich domain. Perhaps there are stimulus-dependent, or cell-type specific conditions where Cup does promote decapping and decay, very little is known about potential regulatory mechanisms that modulate Cup repression and/or activity.

Another example of a 4EBP activating mRNA decay comes from the human eIF-4E Transporter (4E-T). Knock-down of 4E-T results in stabilization of an AU-Rich Element (ARE) mRNA (Ferraiuolo, Basak et al. 2005), suggesting that an ARE-binding protein may recruit 4E-T to activate mRNA decay on targeted messages. It is not clear what role nucleo-cytoplasmic shuttling of eIF-4E by 4E-T (Dostie, Ferraiuolo et al. 2000) plays in activation of mRNA decay, but 4E-T and eIF-4E co-localize in P-bodies (Ferraiuolo, Basak et al. 2005), which are known to be sites of mRNA decay and translational repression. The examples above demonstrate that post-transcriptional regulation by 4EBPs is exerted through a variety of mechanisms that are likely dictated by regions outside of the eIF-4E binding motif, probably through specific protein associations.

It is not clear at present how responsive Eap1p and Cup are to inhibition of the Target of Rapamycin (TOR) Pathway. 4E-BP1 and 4E-BP2 both inhibit the translation of specific mRNAs upon TOR inhibition in mammalian cells (Dowling, Topisirovic et al. 2010). Another *Drosophila* 4EBP, *Thor*, plays an integral role in the metabolism and mainentance of adipose

tissue. *Thor* mutant flies expend their fat stores more quickly than wild-type flies under starvation conditions, and the *Thor* mutants also die more quickly when starved (Teleman, Chen et al. 2005). It will be beneficial to our understanding of 4EBP regulation to carry-out mechanistic analysis of 4EBP function in yeast and *Drosophila* S2 cells with and without TOR inhibition. Another relevant question is: what effect does recruitment by an RNA-binding protein have on 4EBP activity? We know that 4EBPs are capable of carrying-out repression independently, however specific association with RNA-binding proteins may add to 4EBP regulation in a combinatorial fashion. Puf5p activates deadenylation in addition to recruiting Eap1p to *HO* mRNA. Therefore, RNA-binding proteins have the potential to impact the activity of 4EBPs through nucleation of a complex that contains multiple repressive activities.

Mechanisms of mRNA Regulation via the Conserved PUM RNA Binding Domain (RBD) in *D. melanogaster*. In Chapter Three I investigated what factors contribute to repression by the PUM RBD, and what functional effects are exerted on the mRNA itself. These experiments were designed to test a very recent model for PUM RBD repression; this model proposed that the RBD associates with Elongation Factor 1A (eEF1A) and (Argonaute) Ago to repress translation elongation for PUM targets. The Goldstrohm lab has developed a functional assay for PUM regulation in *Drosophila* S2 cells, in which multiple components can be perturbed to ask mechanistic questions about the nature of PUM RBD-mediated mRNA regulation *in vivo*, which enabled the relevance of the PUM-Ago model to be functionally tested. Collectively our data strongly suggest that the PUM RBD does not require interaction with Ago or eEF1A to inhibit expression of a targeted reporter mRNA. We found that the PUM RBD activates mRNA degradation on the reporter mRNA through conserved mechanisms involving

acceleration of deadenylation, and promotion of mRNA decay through decapping. Dcp1 is not absolutely required for decapping, but does activate catalysis by Dcp2, and couples decapping to 5′ -3′ decay by Xrn1/Pacman (Braun, Truffault et al. 2012). Because *Dcp1* knock-down is not 100% effective, and the decapping enzyme was not targeted, it is unclear what the absolute contribution of decapping is to repression via the RBD.

One approach to complement our data that *dcp1* knock-down impairs PUF RBD repression is to express a catalytically inactive decapping enzyme in addition to *Dcp2* knock-down. Previous work has shown that expression of the inactive mutant Dcp2 strongly impairs decapping (Igreja and Izaurralde 2011). To ask if the RBD is utilizing decapping for repression, the PUM RBD or R7mut would be transfected along with the reporter and dominant negative Dcp2 expression construct. Repression of reporter protein output would be monitored relative to R7mut expression to first ask if dominant negative Dcp2 expression results in reduced repression via the RBD. Reporter mRNA levels would be quantitated to ask if the RBD is still able to reduce mRNA abundance. If decapping plays a significant role in RBD repression, expression of the dominant negative Dcp2 should result in impaired repression, at both the mRNA and protein levels. In a related approach to ask if cap removal is important for PUM repression and degradation promotion, a synthetic PBE mRNA encoding Renilla Luciferase will be capped with either m^7G or a non-hydrolyzable cap analog (Rydzik, Lukaszewicz et al. 2009). Each RNA would be transfected along with a control Firefly Luciferase, and either wild-type RBD, or mutant RBD which cannot bind the PBE. If decapping is targeted by the PUM RBD we would expect repression to be dramatically decreased for the non-hydrolyzable capped RNA. However,

if the PUM RBD is targeting translation initiation, the non-hydrolyzable capped RNA should be repressed as well as the m^7G capped RNA.

Thus far, we have taken a candidate approach to identifying the pathway(s) required for RBD-activated mRNA decay. To identify and characterize factors that co-operate with the PUM RBD to activate mRNA decay, I propose the following RNA pull-down, mass spectrometry experiment. The intent of this experiment is to isolate a functionally repressed reporter mRNA that is bound by the PUM RBD as well as yet to be identified repressive co-factors. The difference between this experiment and traditional co-immunoprecipitation, mass-spectrometry is that the protein complexes will be isolated from a functionally repressed mRNA; this may lead to identification of associations that have direct functional relevance to PUM mRNA regulation.

To accomplish this goal, MS2 binding-site, stem loop sequences were cloned into the 3'UTR of Renilla Luciferase 3X-PBE reporter construct used in Chapter Three. Because the MS2 stem loops were inserted in relatively close proximity to the 3X-PBE, I asked if PUM is still able to repress the modified reporter mRNA. Full-length, or R7mut PUM were transfected along with the RnLuc-3XPBE-MS2 reporter and the un-regulated Firefly control reporter. The Dual-Glo™ assay was performed on four replicates, Renilla-MS2-PBE luminescence was normalized to Firefly, and then repression was quantified relative to R7mut repression. Full-length Pumilio repressed the modified MS2 reporter by 40% relative to the R7mut. Therefore, Pumilio is able to repress the modified PBE-MS2 reporter, albeit with reduced efficiency. The MS2 coat protein was then fused to the HaloTag™ (Promega) affinity handle (MS2-HT), and this construct was expressed and translated in *E. coli* cells using a rhamnose T7 induction

system. MS2-HT was purified and covalently immobilized on HaloLink™ (Promega) resin to produce an affinity support for isolation of the RnLuc-3X-PBE-MS2 reporter mRNA.

To confirm that PUM is specifically associated with the reporter mRNA, V5-tagged wild-type RBD or R7mut, would be expressed, and the reporter purified via MS2 RNA pull-down. Western analysis of eluates will be performed to determine if wild-type, but not R7mut come down with the reporter. Also, silver stain of the same pull-down will be performed to ask if the proteins which come down with wild-type PUM display differences from the R7mut. Another important optimization will be to confirm that the reporter mRNA is being effectively isolated via the MS2 purification. RNA will be extracted from the pull-down with the HT-MS2 beads and the 3XPBE reporter with, or without MS2 stem loops; this experiment will demonstrate specificity for MS2 pull-down in order to move forward with confidence. Once the pull-down has been optimized and specificity shown, R7mut and wild-type PUM will be transfected along with the PBE-MS2 reporter, the MS2 affinity pull-down will be performed under stringent conditions empirically determined through the above experiments, the resulting isolated peptides will be identified via liquid chromatography tandem mass-spectrometry.

PUM reduces reporter mRNA levels significantly, therefore, it may be useful to knock-down *ccr4/pop2* to increase the overall mRNA levels and obtain more robust pull-down. Aside from the issue of mRNA abundance, PUM causes a reduction in mRNA levels that does not rely on deadenylation. Therefore, to increase the odds of identifying a novel repressive co-factor, and improve mRNA pull-down, it may in fact be beneficial to impair deadenylation.

Because a functionally repressed mRNA is the bait for pull-down, this should increase the likelihood that proteins found associated with PUM on the targeted mRNA will be of importance to PUMs repressive activity. The use of the mutant PBE reporter and subsequent identification of the resident proteins in a well-translated mRNA will then be cross-referenced against the proteins identified on the PUM-targeted mRNA. This approach has the potential to provide more nuanced protein association data than a traditional co-immunoprecipitation mass-spectrometry experiment, as the proteins found through the traditional method are not necessarily involved in the particular activity being studied, in this case repression of a targeted mRNA.

The PUM RBD is clearly activating degradation of the targeted reporter mRNA, however, this activity does account for the full-repressive activity of the RBD. The RBD has a versatile toolkit to repress mRNA expression, aside from activation of mRNA decay, the RBD targets Pabp to cause translational inhibition. Because *PUF5* in yeast is known to utilize *PAB1* for optimal repression (Chritton and Wickens 2011), we asked if this might be the case for the *Drosophila* PUM RBD. We found that *Pabp* knock-down resulted in an inability of the RBD to accelerate deadenylation relative to the R7 mutant, and importantly, impaired repression by 50%. This data suggests a model in which the PUM RBD targets Pabp to inhibit translation, which then acts as a signal to promote deadenylation at a step immediately after inhibition of translation. Therefore, while we can impair deadenylation by knocking-down the enzymes, the PUM RBD still utilizes Pabp to repress the mRNA through a translational mechanism.

Drosphila PUM is not the only post-transcriptional repressor to target Pabp for translational repression. One of the earliest descriptions of translation inhibition through a Pabp-

mediated mechanism comes from Paip2. Poly(A) Interacting Proteins play positive and negative roles with regard to translation, where Paip1 binds Pabp and activates translation (Craig, Haghighat et al. 1998). In contrast, Paip2 binds Pabp and inhibits translation. Paip2 represses cap-dependent translation, which requires eIF-4G, but not cap-independent translation. Also, Paip2 binding to Papb results in a decrease in the affinity of Pabp for the poly(A) tail (Khaleghpour, Svitkin et al. 2001). In addition to decreasing affinity for the poly(A) tail, Paip2 competes with eIF-4G for Pabp-binding, via what is called a PAM2 motif (Roy, De Crescenzo et al. 2002; Karim, Svitkin et al. 2006). However, competition with eIF-4G through a PAM2 motif is not the only mechanism a repressor uses to target Pabp. Another case involving translational repression exerted through an RNA-binding protein is the female-specific Sex Lethal (Sxl) protein. Sxl binds to the 3′ and 5′ UTR of Male-Specific Lethal 2 (Msl-2), and recuits the UNR co-repressor which inhibits translation of the mRNA: repression is important for sex-specific dosage compensation (Bashaw and Baker 1997; Duncan, Grskovic et al. 2006). Interestingly, repression by Sxl represses both cap-dependent and independent translation, suggesting a mechanism other than blocking eIF-4G binding to Pabp (Gebauer, Grskovic et al. 2003). In fact, Sxl bound to the 3'UTR of Msl-2, recruits the UNR co-repressor which binds to Pabp, then blocks 40s ribosomal subunit recruitment, but leaves the eIF-4G-Pabp interaction unperturbed.

Yet another example of Pabp-mediated repression comes from the post-transcriptional repressor, GW182. GW182 associates with the miRNA RISC complex, and is thought to recruit deadenylase and decapping enzymes, and also inhibit translation translation (Chen, Zheng et al. 2009; Fabian, Mathonnet et al. 2009). It is thought that GW182 is able to repress translation through a mechanism that results in dissociation of Pabp from the poly(A) tail, and this involves

interactions between GW182 and the deadenylase complex. Surprisingly, deadenylation is not required for GW182-mediated Pabp dissociation (Zekri, Kuzuoglu-Ozturk et al. 2013). Additionally, GW182 contains PAM2 motifs similar to Paip2, which enable GW182 to bind Pabp, therefore GW182 may act similarly to Paip2 in decreasing the affinity of Pabp for the poly(A) tail (Huntzinger, Braun et al. 2010).

Our unpublished results indicate that the PUM RBD binds to Pabp in RNase-treated extracts, yet, the RBD contains no apparent PAM2 motifs. Also, PUM activated deadenylation requires Pabp, but deadenylation is not required for repression, however, a poly(A) tail is required. Therefore, if a poly(A) tail is required, and deadenylation occurs after the Pabp-promoted step, it seems unlikely that PUM is causing Papb to dissociate from the tail as GW182 and Paip2 do. It is possible that PUM association with Pabp forms a complex on the targeted mRNA that blocks ribosome recruitment. However, it will be important to functionally test if Pabp dissociates from the poly(A) tail in a PUM-dependent manner. It is remarkable that many RNA binding proteins that post-transcriptionally regulate target mRNAs do so in a manner that targets either eIF-4E or Pabp function. And while the same translational components are targeted, the mechanisms used and the outcomes of repression differ significantly. We have shown that the PUM RBD accelerates deadenylation, activates mRNA decay possibly through activation of decapping, and also exerts translational repression through a Pabp-mediated mechanism. However, it must be stressed that repression elicited by the RBD is relatively minor in comparison to full-length PUM. Within the N-terminus, three domains have been functionally identified that are capable of carrying out repression individually (Weidmann and Goldstrohm 2012). Also, while our data concerning the RBD suggest that a translational mechanism is

exerted through targeting of Pabp, the N-terminus reduces mRNA levels much more effectively than the RBD is capable of; this suggests that individual domains within PUM are capable of directing more robust mRNA decay activities. There is little known about the function of the N-terminus of both fly and human PUFs. Future PUF research will benefit from focused efforts to dissect the multiple activities, as well as potential regulation mediated via the N-terminus of PUF proteins.

Bibliography

Abelson, J., M. Blanco, et al. (2010). "Conformational dynamics of single pre-mRNA molecules during in vitro splicing." Nat Struct Mol Biol **17**(4): 504-512.

Altmann, M., I. Edery, et al. (1985). "Purification and characterization of protein synthesis initiation factor eIF-4E from the yeast Saccharomyces cerevisiae." Biochemistry **24**(22): 6085-6089.

Altmann, M., M. Krieger, et al. (1989). "Nucleotide sequence of the gene encoding a 20 kDa protein associated with the cap binding protein eIF-4E from Saccharomyces cerevisiae." Nucleic Acids Res **17**(18): 7520.

Altmann, M., P. P. Muller, et al. (1989). "A mammalian translation initiation factor can substitute for its yeast homologue in vivo." J Biol Chem **264**(21): 12145-12147.

Altmann, M., N. Schmitz, et al. (1997). "A novel inhibitor of cap-dependent translation initiation in yeast: p20 competes with eIF4G for binding to eIF4E." Embo J **16**(5): 1114-1121.

Anderson, J. S. and R. P. Parker (1998). "The 3' to 5' degradation of yeast mRNAs is a general mechanism for mRNA turnover that requires the SKI2 DEVH box protein and 3' to 5' exonucleases of the exosome complex." Embo J **17**(5): 1497-1506.

Anderson, W. F. and D. A. Shafritz (1971). "Methionine transfer RNAF: the initiator transfer RNA for hemoglobin biosynthesis." Cancer Res **31**(5): 701-703.

Araki, Y., S. Takahashi, et al. (2001). "Ski7p G protein interacts with the exosome and the Ski complex for 3'-to-5' mRNA decay in yeast." Embo J **20**(17): 4684-4693.

Arava, Y., Y. Wang, et al. (2003). "Genome-wide analysis of mRNA translation profiles in Saccharomyces cerevisiae." Proc Natl Acad Sci U S A **100**(7): 3889-3894.

Asaoka-Taguchi, M., M. Yamada, et al. (1999). "Maternal Pumilio acts together with Nanos in germline development in Drosophila embryos." Nat Cell Biol **1**(7): 431-437.

Barker, D. D., C. Wang, et al. (1992). "Pumilio is essential for function but not for distribution of the Drosophila abdominal determinant Nanos." Genes Dev **6**(12A): 2312-2326.

Barreau, C., L. Paillard, et al. (2005). "AU-rich elements and associated factors: are there unifying principles?" Nucleic Acids Res **33**(22): 7138-7150.

Bashaw, G. J. and B. S. Baker (1997). "The regulation of the Drosophila msl-2 gene reveals a function for Sex-lethal in translational control." Cell **89**(5): 789-798.

Beelman, C. A., A. Stevens, et al. (1996). "An essential component of the decapping enzyme required for normal rates of mRNA turnover." Nature **382**(6592): 642-646.

Behm-Ansmant, I., J. Rehwinkel, et al. (2006). "mRNA degradation by miRNAs and GW182 requires both CCR4:NOT deadenylase and DCP1:DCP2 decapping complexes." Genes Dev **20**(14): 1885-1898.

Bender, M., S. Horikami, et al. (1988). "Identification and expression of the gap segmentation gene hunchback in Drosophila melanogaster." Dev Genet **9**(6): 715-732.

Bergmann, J. E. and H. F. Lodish (1979). "A kinetic model of protein synthesis. Application to hemoglobin synthesis and translational control." J Biol Chem **254**(23): 11927-11937.

Blewett, N., J. Coller, et al. (2011). "A quantitative assay for measuring mRNA decapping by splinted ligation reverse transcription polymerase chain reaction: qSL-RT-PCR." Rna **17**(3): 535-543.

Blewett, N. H. and A. C. Goldstrohm (2012). "An eIF4E-binding protein promotes mRNA decapping and is required for PUF repression." Mol Cell Biol.

Both, G. W., Y. Furuichi, et al. (1975). "Ribosome binding to reovirus mRNA in protein synthesis requires 5' terminal 7-methylguanosine." Cell **6**(2): 185-195.

Braun, J. E., V. Truffault, et al. (2012). "A direct interaction between DCP1 and XRN1 couples mRNA decapping to 5' exonucleolytic degradation." Nat Struct Mol Biol **19**(12): 1324-1331.

Brewer, G. and J. Ross (1988). "Poly(A) shortening and degradation of the 3' A+U-rich sequences of human c-myc mRNA in a cell-free system." Mol Cell Biol **8**(4): 1697-1708.

Brown, J. T., X. Bai, et al. (2000). "The yeast antiviral proteins Ski2p, Ski3p, and Ski8p exist as a complex in vivo." Rna **6**(3): 449-457.

Cao, D. and R. Parker (2001). "Computational modeling of eukaryotic mRNA turnover." Rna **7**(9): 1192-1212.

Capasso, O., G. C. Bleecker, et al. (1987). "Sequences controlling histone H4 mRNA abundance." EMBO J **6**(6): 1825-1831.

Celesnik, H., A. Deana, et al. (2007). "Initiation of RNA decay in Escherichia coli by 5' pyrophosphate removal." Mol Cell **27**(1): 79-90.

Celesnik, H., A. Deana, et al. (2008). "PABLO analysis of RNA 5'-phosphorylation state and 5'-end mapping." Methods Enzymol **447**: 83-98.

Chagnovich, D. and R. Lehmann (2001). "Poly(A)-independent regulation of maternal hunchback translation in the Drosophila embryo." Proc Natl Acad Sci U S A **98**(20): 11359-11364.

Chen, C. Y., R. Gherzi, et al. (2001). "AU binding proteins recruit the exosome to degrade ARE-containing mRNAs." Cell **107**(4): 451-464.

Chen, C. Y., D. Zheng, et al. (2009). "Ago-TNRC6 triggers microRNA-mediated decay by promoting two deadenylation steps." Nat Struct Mol Biol **16**(11): 1160-1166.

Chen, D., W. Zheng, et al. (2012). "Pumilio 1 Suppresses Multiple Activators of p53 to Safeguard Spermatogenesis." Curr Biol **22**(5): 420-425.

Chial, H. J., A. J. Stemm-Wolf, et al. (2000). "Yeast Eap1p, an eIF4E-associated protein, has a separate function involving genetic stability." Curr Biol **10**(23): 1519-1522.

Cho, P. F., C. Gamberi, et al. (2006). "Cap-dependent translational inhibition establishes two opposing morphogen gradients in Drosophila embryos." Curr Biol **16**(20): 2035-2041.

Chowdhury, A., J. Mukhopadhyay, et al. (2007). "The decapping activator Lsm1p-7p-Pat1p complex has the intrinsic ability to distinguish between oligoadenylated and polyadenylated RNAs." Rna **13**(7): 998-1016.

Chowdhury, A. and S. Tharun (2009). "Activation of decapping involves binding of the mRNA and facilitation of the post-binding steps by the Lsm1-7-Pat1 complex." Rna **15**(10): 1837-1848.

Chritton, J. J. and M. Wickens (2010). "Translational repression by PUF proteins in vitro." Rna **16**(6): 1217-1225.

Chritton, J. J. and M. Wickens (2011). "A role for the poly(A)-binding protein Pab1p in PUF protein-mediated repression." J Biol Chem **286**(38): 33268-33278.

Clark, B. F., S. K. Dube, et al. (1968). "Specific codon-anticodon interaction of an initiator-tRNA fragment." Nature **219**(5153): 484-485.

Coller, J. and R. Parker (2004). "Eukaryotic mRNA decapping." Annu Rev Biochem **73**: 861-890.

Coller, J. and R. Parker (2005). "General translational repression by activators of mRNA decapping." Cell **122**(6): 875-886.

Coller, J. M., M. Tucker, et al. (2001). "The DEAD box helicase, Dhh1p, functions in mRNA decapping and interacts with both the decapping and deadenylase complexes." Rna **7**(12): 1717-1727.

Coppola, J. A., A. S. Field, et al. (1983). "Promoter-proximal pausing by RNA polymerase II in vitro: transcripts shorter than 20 nucleotides are not capped." Proc Natl Acad Sci U S A **80**(5): 1251-1255.

Cosentino, G. P., T. Schmelzle, et al. (2000). "Eap1p, a novel eukaryotic translation initiation factor 4E-associated protein in Saccharomyces cerevisiae." Mol Cell Biol **20**(13): 4604-4613.

Couttet, P., M. Fromont-Racine, et al. (1997). "Messenger RNA deadenylylation precedes decapping in mammalian cells." Proc Natl Acad Sci U S A **94**(11): 5628-5633.

Couttet, P. and T. Grange (2004). "Premature termination codons enhance mRNA decapping in human cells." Nucleic Acids Res **32**(2): 488-494.

Craig, A. W., A. Haghighat, et al. (1998). "Interaction of polyadenylate-binding protein with the eIF4G homologue PAIP enhances translation." Nature **392**(6675): 520-523.

Cridge, A. G., L. M. Castelli, et al. (2010). "Identifying eIF4E-binding protein translationally-controlled transcripts reveals links to mRNAs bound by specific PUF proteins." Nucleic Acids Res **38**(22): 8039-8050.

Crittenden, S. L., D. S. Bernstein, et al. (2002). "A conserved RNA-binding protein controls germline stem cells in Caenorhabditis elegans." Nature **417**(6889): 660-663.

De Benedetti, A. and J. R. Graff (2004). "eIF-4E expression and its role in malignancies and metastases." Oncogene **23**(18): 3189-3199.

Decker, C. J. and R. Parker (1993). "A turnover pathway for both stable and unstable mRNAs in yeast: evidence for a requirement for deadenylation." Genes Dev **7**(8): 1632-1643.

Deshmukh, M. V., B. N. Jones, et al. (2008). "mRNA decapping is promoted by an RNA-binding channel in Dcp2." Mol Cell **29**(3): 324-336.

Doma, M. K. and R. Parker (2006). "Endonucleolytic cleavage of eukaryotic mRNAs with stalls in translation elongation." Nature **440**(7083): 561-564.

Dostie, J., M. Ferraiuolo, et al. (2000). "A novel shuttling protein, 4E-T, mediates the nuclear import of the mRNA 5' cap-binding protein, eIF4E." Embo J **19**(12): 3142-3156.

Dowling, R. J., I. Topisirovic, et al. (2010). "mTORC1-mediated cell proliferation, but not cell growth, controlled by the 4E-BPs." Science **328**(5982): 1172-1176.

Dubnau, J., A. S. Chiang, et al. (2003). "The staufen/pumilio pathway is involved in Drosophila long-term memory." Curr Biol **13**(4): 286-296.

Duncan, K., M. Grskovic, et al. (2006). "Sex-lethal imparts a sex-specific function to UNR by recruiting it to the msl-2 mRNA 3' UTR: translational repression for dosage compensation." Genes Dev **20**(3): 368-379.

Duncan, K. E., C. Strein, et al. (2009). "The SXL-UNR corepressor complex uses a PABP-mediated mechanism to inhibit ribosome recruitment to msl-2 mRNA." Mol Cell **36**(4): 571-582.

Dunckley, T. and R. Parker (1999). "The DCP2 protein is required for mRNA decapping in Saccharomyces cerevisiae and contains a functional MutT motif." EMBO J **18**(19): 5411-5422.

Eberle, A. B., S. Lykke-Andersen, et al. (2009). "SMG6 promotes endonucleolytic cleavage of nonsense mRNA in human cells." Nat Struct Mol Biol **16**(1): 49-55.

Eckner, R., W. Ellmeier, et al. (1991). "Mature mRNA 3' end formation stimulates RNA export from the nucleus." EMBO J **10**(11): 3513-3522.

Edery, I., M. Humbelin, et al. (1983). "Involvement of eukaryotic initiation factor 4A in the cap recognition process." J Biol Chem **258**(18): 11398-11403.

Engler, M. J. a. R., C.C. (1982). DNA Ligases. The Enzymes. P. D. Boyer. New York, New York, Academic Press. **15:** 3-29.

Eystathioy, T., E. K. Chan, et al. (2002). "A phosphorylated cytoplasmic autoantigen, GW182, associates with a unique population of human mRNAs within novel cytoplasmic speckles." Mol Biol Cell **13**(4): 1338-1351.

Fabian, M. R., G. Mathonnet, et al. (2009). "Mammalian miRNA RISC recruits CAF1 and PABP to affect PABP-dependent deadenylation." Mol Cell **35**(6): 868-880.

Fenger-Gron, M., C. Fillman, et al. (2005). "Multiple processing body factors and the ARE binding protein TTP activate mRNA decapping." Mol Cell **20**(6): 905-915.

Ferraiuolo, M. A., S. Basak, et al. (2005). "A role for the eIF4E-binding protein 4E-T in P-body formation and mRNA decay." J Cell Biol **170**(6): 913-924.

Fischer, N. and K. Weis (2002). "The DEAD box protein Dhh1 stimulates the decapping enzyme Dcp1." Embo J **21**(11): 2788-2797.

Forbes, A. and R. Lehmann (1998). "Nanos and Pumilio have critical roles in the development and function of Drosophila germline stem cells." Development **125**(4): 679-690.

Franks, T. M. and J. Lykke-Andersen (2008). "The control of mRNA decapping and P-body formation." Mol Cell **32**(5): 605-615.

Friend, K., Z. T. Campbell, et al. (2012). "A conserved PUF-Ago-eEF1A complex attenuates translation elongation." Nat Struct Mol Biol **19**(2): 176-183.

Fromont-Racine, M., E. Bertrand, et al. (1993). "A highly sensitive method for mapping the 5' termini of mRNAs." Nucleic Acids Res **21**(7): 1683-1684.

Furuichi, Y., A. LaFiandra, et al. (1977). "5'-Terminal structure and mRNA stability." Nature **266**(5599): 235-239.

Gamberi, C., D. S. Peterson, et al. (2002). "An anterior function for the Drosophila posterior determinant Pumilio." Development **129**(11): 2699-2710.

Garneau, N. L., J. Wilusz, et al. (2007). "The highways and byways of mRNA decay." Nat Rev Mol Cell Biol **8**(2): 113-126.

Gatfield, D. and E. Izaurralde (2004). "Nonsense-mediated messenger RNA decay is initiated by endonucleolytic cleavage in Drosophila." Nature **429**(6991): 575-578.

Gavis, E. R. (2001). "Over the rainbow to translational control." Nat Struct Biol **8**(5): 387-389.

Gebauer, F., M. Grskovic, et al. (2003). "Drosophila sex-lethal inhibits the stable association of the 40S ribosomal subunit with msl-2 mRNA." Mol Cell **11**(5): 1397-1404.

Gerber, A. P., D. Herschlag, et al. (2004). "Extensive association of functionally and cytotopically related mRNAs with Puf family RNA-binding proteins in yeast." PLoS Biol **2**(3): E79.

Gerber, A. P., S. Luschnig, et al. (2006). "Genome-wide identification of mRNAs associated with the translational regulator PUMILIO in Drosophila melanogaster." Proc Natl Acad Sci U S A **103**(12): 4487-4492.

Gkogkas, C., N. Sonenberg, et al. (2010). "Translational control mechanisms in long-lasting synaptic plasticity and memory." J Biol Chem **285**(42): 31913-31917.

Goldstrohm, A. C., B. A. Hook, et al. (2006). "PUF proteins bind Pop2p to regulate messenger RNAs." Nat Struct Mol Biol **13**(6): 533-539.

Goldstrohm, A. C., D. J. Seay, et al. (2007). "PUF protein-mediated deadenylation is catalyzed by Ccr4p." J Biol Chem **282**(1): 109-114.

Goldstrohm, A. C. and M. Wickens (2008). "Multifunctional deadenylase complexes diversify mRNA control." Nat Rev Mol Cell Biol **9**(4): 337-344.

Goodman, H. M. and A. Rich (1963). "Mechanism of Polyribosome Action during Protein Synthesis." Nature **199**: 318-322.

Green, M. R., T. Maniatis, et al. (1983). "Human beta-globin pre-mRNA synthesized in vitro is accurately spliced in Xenopus oocyte nuclei." Cell **32**(3): 681-694.

Grifo, J. A., S. M. Tahara, et al. (1983). "New initiation factor activity required for globin mRNA translation." J Biol Chem **258**(9): 5804-5810.

Gross, J. D., N. J. Moerke, et al. (2003). "Ribosome loading onto the mRNA cap is driven by conformational coupling between eIF4G and eIF4E." Cell **115**(6): 739-750.

Gu, W., Y. Deng, et al. (2004). "A new yeast PUF family protein, Puf6p, represses ASH1 mRNA translation and is required for its localization." Genes Dev **18**(12): 1452-1465.

Gualerzi, C., G. Risuleo, et al. (1977). "Initial rate kinetic analysis of the mechanism of initiation complex formation and the role of initiation factor IF-3." Biochemistry **16**(8): 1684-1689.

Haghighat, A., S. Mader, et al. (1995). "Repression of cap-dependent translation by 4E-binding protein 1: competition with p220 for binding to eukaryotic initiation factor-4E." Embo J **14**(22): 5701-5709.

Haghighat, A. and N. Sonenberg (1997). "eIF4G dramatically enhances the binding of eIF4E to the mRNA 5'-cap structure." J Biol Chem **272**(35): 21677-21680.

Harland, R. and L. Misher (1988). "Stability of RNA in developing Xenopus embryos and identification of a destabilizing sequence in TFIIIA messenger RNA." Development **102**(4): 837-852.

He, F. and A. Jacobson (2001). "Upf1p, Nmd2p, and Upf3p regulate the decapping and exonucleolytic degradation of both nonsense-containing mRNAs and wild-type mRNAs." Mol Cell Biol **21**(5): 1515-1530.

He, W. and R. Parker (1999). "Analysis of mRNA decay pathways in Saccharomyces cerevisiae." Methods **17**(1): 3-10.

Herrick, D., R. Parker, et al. (1990). "Identification and comparison of stable and unstable mRNAs in Saccharomyces cerevisiae." Mol Cell Biol **10**(5): 2269-2284.

Hoerz, W. and K. S. McCarty (1969). "Evidence for a proposed initiation complex for protein synthesis in reticulocyte polyribosome profiles." Proc Natl Acad Sci U S A **63**(4): 1206-1213.

Hook, B. A., A. C. Goldstrohm, et al. (2007). "Two yeast PUF proteins negatively regulate a single mRNA." J Biol Chem **282**(21): 15430-15438.

Houshmandi, S. S. and W. M. Olivas (2005). "Yeast Puf3 mutants reveal the complexity of Puf-RNA binding and identify a loop required for regulation of mRNA decay." Rna **11**(11): 1655-1666.

Hsu, C. L. and A. Stevens (1993). "Yeast cells lacking 5'-->3' exoribonuclease 1 contain mRNA species that are poly(A) deficient and partially lack the 5' cap structure." Mol Cell Biol **13**(8): 4826-4835.

Hu, W., C. Petzold, et al. (2010). "Nonsense-mediated mRNA decapping occurs on polyribosomes in Saccharomyces cerevisiae." Nat Struct Mol Biol **17**(2): 244-247.

Hu, W., T. J. Sweet, et al. (2009). "Co-translational mRNA decay in Saccharomyces cerevisiae." Nature **461**(7261): 225-229.

Hulskamp, M., C. Schroder, et al. (1989). "Posterior segmentation of the Drosophila embryo in the absence of a maternal posterior organizer gene." Nature **338**(6217): 629-632.

Huntzinger, E., J. E. Braun, et al. (2010). "Two PABPC1-binding sites in GW182 proteins promote miRNA-mediated gene silencing." EMBO J **29**(24): 4146-4160.

Huntzinger, E., D. Kuzuoglu-Ozturk, et al. (2013). "The interactions of GW182 proteins with PABP and deadenylases are required for both translational repression and degradation of miRNA targets." Nucleic Acids Res **41**(2): 978-994.

Ibrahimo, S., L. E. Holmes, et al. (2006). "Regulation of translation initiation by the yeast eIF4E binding proteins is required for the pseudohyphal response." Yeast **23**(14-15): 1075-1088.

Igreja, C. and E. Izaurralde (2011). "CUP promotes deadenylation and inhibits decapping of mRNA targets." Genes Dev **25**(18): 1955-1967.

Jackson, J. S., Jr., S. S. Houshmandi, et al. (2004). "Recruitment of the Puf3 protein to its mRNA target for regulation of mRNA decay in yeast." Rna **10**(10): 1625-1636.

Jimenez, A., D. J. Tipper, et al. (1973). "Mode of action of thiolutin, an inhibitor of macromolecular synthesis in Saccharomyces cerevisiae." Antimicrob Agents Chemother **3**(6): 729-738.

Jinek, M., S. M. Coyle, et al. (2011). "Coupled 5' nucleotide recognition and processivity in Xrn1-mediated mRNA decay." Mol Cell **41**(5): 600-608.

Jivotovskaya, A. V., L. Valasek, et al. (2006). "Eukaryotic translation initiation factor 3 (eIF3) and eIF2 can promote mRNA binding to 40S subunits independently of eIF4G in yeast." Mol Cell Biol **26**(4): 1355-1372.

Jones, B. N., D. U. Quang-Dang, et al. (2008). "A kinetic assay to monitor RNA decapping under single- turnover conditions." Methods Enzymol **448**: 23-40.

Jones, T. R. and M. D. Cole (1987). "Rapid cytoplasmic turnover of c-myc mRNA: requirement of the 3' untranslated sequences." Mol Cell Biol **7**(12): 4513-4521.

Jung, M. Y., L. Lorenz, et al. (2006). "Translational control by neuroguidin, a eukaryotic initiation factor 4E and CPEB binding protein." Mol Cell Biol **26**(11): 4277-4287.

Kahvejian, A., Y. V. Svitkin, et al. (2005). "Mammalian poly(A)-binding protein is a eukaryotic translation initiation factor, which acts via multiple mechanisms." Genes Dev **19**(1): 104-113.

Kappen, L. S., H. Suzuki, et al. (1973). "Inhibition of reticulocyte peptide-chain initiation by pactamycin: accumulation of inactive ribosomal initiation complexes." Proc Natl Acad Sci U S A **70**(1): 22-26.

Karim, M. M., Y. V. Svitkin, et al. (2006). "A mechanism of translational repression by competition of Paip2 with eIF4G for poly(A) binding protein (PABP) binding." Proc Natl Acad Sci U S A **103**(25): 9494-9499.

Kawahara, H., T. Imai, et al. (2008). "Neural RNA-binding protein Musashi1 inhibits translation initiation by competing with eIF4G for PABP." J Cell Biol **181**(4): 639-653.

Kedde, M., M. van Kouwenhove, et al. (2010). "A Pumilio-induced RNA structure switch in p27-3' UTR controls miR-221 and miR-222 accessibility." Nat Cell Biol **12**(10): 1014-1020.

Kessler, S. H. and A. B. Sachs (1998). "RNA recognition motif 2 of yeast Pab1p is required for its functional interaction with eukaryotic translation initiation factor 4G." Mol Cell Biol **18**(1): 51-57.

Khaleghpour, K., Y. V. Svitkin, et al. (2001). "Translational repression by a novel partner of human poly(A) binding protein, Paip2." Mol Cell **7**(1): 205-216.

Kozak, M. (1980). "Binding of wheat germ ribosomes to bisulfite-modified reovirus messenger RNA: evidence for a scanning mechanism." J Mol Biol **144**(3): 291-304.

Kozak, M. (1980). "Role of ATP in binding and migration of 40S ribosomal subunits." Cell **22**(2 Pt 2): 459-467.

Kozak, M. and A. J. Shatkin (1978). "Migration of 40 S ribosomal subunits on messenger RNA in the presence of edeine." J Biol Chem **253**(18): 6568-6577.

Kurschat, W. C., J. Muller, et al. (2005). "Optimizing splinted ligation of highly structured small RNAs." Rna **11**(12): 1909-1914.

Lackner, D. H., T. H. Beilharz, et al. (2007). "A network of multiple regulatory layers shapes gene expression in fission yeast." Mol Cell **26**(1): 145-155.

Ladhoff, A. M., I. Uerlings, et al. (1981). "Electron microscopic evidence of circular molecules in 9-S globin mRNA from rabbit reticulocytes." Mol Biol Rep **7**(1-3): 101-106.

LaGrandeur, T. E. and R. Parker (1998). "Isolation and characterization of Dcp1p, the yeast mRNA decapping enzyme." EMBO J **17**(5): 1487-1496.

Lai, E. C. (2002). "Micro RNAs are complementary to 3' UTR sequence motifs that mediate negative post-transcriptional regulation." Nat Genet **30**(4): 363-364.

Lake, J. A. (1977). "Aminoacyl-tRNA binding at the recognition site is the first step of the elongation cycle of protein synthesis." Proc Natl Acad Sci U S A **74**(5): 1903-1907.

Larimer, F. W., C. L. Hsu, et al. (1992). "Characterization of the XRN1 gene encoding a 5'-->3' exoribonuclease: sequence data and analysis of disparate protein and mRNA levels of gene-disrupted yeast cells." Gene **120**(1): 51-57.

Lau, N. C., L. P. Lim, et al. (2001). "An abundant class of tiny RNAs with probable regulatory roles in Caenorhabditis elegans." Science **294**(5543): 858-862.

Lee, B., T. Udagawa, et al. (2007). "Yeast phenotypic assays on translational control." Methods Enzymol **429**: 105-137.

Lee, R. C. and V. Ambros (2001). "An extensive class of small RNAs in Caenorhabditis elegans." Science **294**(5543): 862-864.

Lehmann, R. and C. Nusslein-Volhard (1987). "Involvement of the pumilio gene in the transport of an abdominal signal in the Drosophila embyro." Nature **329**: 167-170.

Lehmann, R. and C. Nusslein-Volhard (1991). "The maternal gene nanos has a central role in posterior pattern formation of the Drosophila embryo." Development **112**(3): 679-691.

Levin, D. H., D. Kyner, et al. (1973). "Protein initiation in eukaryotes: formation and function of a ternary complex composed of a partially purified ribosomal factor, methionyl transfer RNA, and guanosine triphosphate." Proc Natl Acad Sci U S A **70**(1): 41-45.

Levy, N. S., S. Chung, et al. (1998). "Hypoxic stabilization of vascular endothelial growth factor mRNA by the RNA-binding protein HuR." J Biol Chem **273**(11): 6417-6423.

Lin, H. and A. C. Spradling (1997). "A novel group of pumilio mutations affects the asymmetric division of germline stem cells in the Drosophila ovary." Development **124**(12): 2463-2476.

Liu, H., N. D. Rodgers, et al. (2002). "The scavenger mRNA decapping enzyme DcpS is a member of the HIT family of pyrophosphatases." EMBO J **21**(17): 4699-4708.

Liu, S. W., X. Jiao, et al. (2004). "Functional analysis of mRNA scavenger decapping enzymes." RNA **10**(9): 1412-1422.

Livak, K. J. and T. D. Schmittgen (2001). "Analysis of relative gene expression data using real-time quantitative PCR and the 2(-Delta Delta C(T)) Method." Methods **25**(4): 402-408.

Lockwood, A. H., P. Sarkar, et al. (1972). "Release of polypeptide chain initiation factor IF-2 during initiation complex formation." Proc Natl Acad Sci U S A **69**(12): 3602-3605.

Lu, G., S. J. Dolgner, et al. (2009). "Understanding and engineering RNA sequence specificity of PUF proteins." Curr Opin Struct Biol **19**(1): 110-115.

Lykke-Andersen, J. and E. Wagner (2005). "Recruitment and activation of mRNA decay enzymes by two ARE-mediated decay activation domains in the proteins TTP and BRF-1." Genes Dev **19**(3): 351-361.

Lykke-Andersen, S., D. E. Brodersen, et al. (2009). "Origins and activities of the eukaryotic exosome." J Cell Sci **122**(Pt 10): 1487-1494.

Lykke-Andersen, S., R. Tomecki, et al. (2011). "The eukaryotic RNA exosome: same scaffold but variable catalytic subunits." RNA Biol **8**(1): 61-66.

Mader, S., H. Lee, et al. (1995). "The translation initiation factor eIF-4E binds to a common motif shared by the translation factor eIF-4 gamma and the translational repressors 4E-binding proteins." Mol Cell Biol **15**(9): 4990-4997.

Mangus, D. A., M. C. Evans, et al. (2003). "Poly(A)-binding proteins: multifunctional scaffolds for the post-transcriptional control of gene expression." Genome Biol **4**(7): 223.

Marcus, A., D. P. Weeks, et al. (1970). "Protein chain initiation by methionyl-tRNA in wheat embryo." Proc Natl Acad Sci U S A **67**(4): 1681-1687.

Maroney, P. A., S. Chamnongpol, et al. (2007). "A rapid, quantitative assay for direct detection of microRNAs and other small RNAs using splinted ligation." Rna **13**(6): 930-936.

Maroney, P. A., S. Chamnongpol, et al. (2008). "Direct detection of small RNAs using splinted ligation." Nat Protoc **3**(2): 279-287.

Matsuo, Y., A. Muramatsu, et al. (2004). "Stacking of molecules possessing a fullerene apex and a cup-shaped cavity connected by a silicon connection." J Am Chem Soc **126**(2): 432-433.

Meier, K. D., O. Deloche, et al. (2006). "Sphingoid base is required for translation initiation during heat stress in Saccharomyces cerevisiae." Mol Biol Cell **17**(3): 1164-1175.

Mendelsohn, B. A., A. M. Li, et al. (2003). "Genetic and biochemical interactions between SCP160 and EAP1 in yeast." Nucleic Acids Res **31**(20): 5838-5847.

Menon, K. P., S. Sanyal, et al. (2004). "The translational repressor Pumilio regulates presynaptic morphology and controls postsynaptic accumulation of translation factor eIF-4E." Neuron **44**(4): 663-676.

Merrick, W. C. (1979). "Evidence that a single GTP is used in the formation of 80 S initiation complexes." J Biol Chem **254**(10): 3708-3711.

Miller, M. A. and W. M. Olivas (2011). "Roles of Puf proteins in mRNA degradation and translation." Wiley Interdiscip Rev RNA **2**(4): 471-492.

Moore, M. J. and C. C. Query (2000). "Joining of RNAs by splinted ligation." Methods Enzymol **317**: 109-123.

Mourelatos, Z., J. Dostie, et al. (2002). "miRNPs: a novel class of ribonucleoproteins containing numerous microRNAs." Genes Dev **16**(6): 720-728.

Muhlrad, D., C. J. Decker, et al. (1994). "Deadenylation of the unstable mRNA encoded by the yeast MFA2 gene leads to decapping followed by 5'-->3' digestion of the transcript." Genes Dev **8**(7): 855-866.

Muhlrad, D., C. J. Decker, et al. (1995). "Turnover mechanisms of the stable yeast PGK1 mRNA." Mol Cell Biol **15**(4): 2145-2156.

Muhlrad, D. and R. Parker (1992). "Mutations affecting stability and deadenylation of the yeast MFA2 transcript." Genes Dev **6**(11): 2100-2111.

Mukherjee, D., M. Gao, et al. (2002). "The mammalian exosome mediates the efficient degradation of mRNAs that contain AU-rich elements." Embo J **21**(1-2): 165-174.

Mukherjee, N., D. L. Corcoran, et al. (2011). "Integrative regulatory mapping indicates that the RNA-binding protein HuR couples pre-mRNA processing and mRNA stability." Mol Cell **43**(3): 327-339.

Murata, Y. and R. P. Wharton (1995). "Binding of pumilio to maternal hunchback mRNA is required for posterior patterning in Drosophila embryos." Cell **80**(5): 747-756.

Muthukrishnan, S., G. W. Both, et al. (1975). "5'-Terminal 7-methylguanosine in eukaryotic mRNA is required for translation." Nature **255**(5503): 33-37.

Nakamura, A., K. Sato, et al. (2004). "Drosophila cup is an eIF4E binding protein that associates with Bruno and regulates oskar mRNA translation in oogenesis." Dev Cell **6**(1): 69-78.

Nasrin, N., M. F. Ahmad, et al. (1986). "Protein synthesis in yeast Saccharomyces cerevisiae. Purification of Co-eIF-2A and 'mRNA-binding factor(s)' and studies of their roles in Met-tRNAf.40S.mRNA complex formation." Eur J Biochem **161**(1): 1-6.

Nelson, M. R., A. M. Leidal, et al. (2004). "Drosophila Cup is an eIF4E-binding protein that functions in Smaug-mediated translational repression." Embo J **23**(1): 150-159.

Nissan, T., P. Rajyaguru, et al. (2010). "Decapping activators in Saccharomyces cerevisiae act by multiple mechanisms." Mol Cell **39**(5): 773-783.

Ogilvie, R. L., M. Abelson, et al. (2005). "Tristetraprolin down-regulates IL-2 gene expression through AU-rich element-mediated mRNA decay." J Immunol **174**(2): 953-961.

Olivas, W. and R. Parker (2000). "The Puf3 protein is a transcript-specific regulator of mRNA degradation in yeast." Embo J **19**(23): 6602-6611.

Oliveira, C. C. and J. E. McCarthy (1995). "The relationship between eukaryotic translation and mRNA stability. A short upstream open reading frame strongly inhibits translational initiation and greatly accelerates mRNA degradation in the yeast Saccharomyces cerevisiae." J Biol Chem **270**(15): 8936-8943.

Palayoor, T., D. E. Schumm, et al. (1981). "Transport of functional messenger RNA from liver nuclei in a reconstituted cell-free system." Biochim Biophys Acta **654**(2): 201-210.

Parisi, M. and H. Lin (1999). "The Drosophila pumilio gene encodes two functional protein isoforms that play multiple roles in germline development, gonadogenesis, oogenesis and embryogenesis." Genetics **153**(1): 235-250.

Parisi, M. and H. Lin (2000). "Translational repression: a duet of Nanos and Pumilio." Curr Biol **10**(2): R81-83.

Parker, R. and H. Song (2004). "The enzymes and control of eukaryotic mRNA turnover." Nat Struct Mol Biol **11**(2): 121-127.

Passos, D. O. and R. Parker (2008). "Analysis of cytoplasmic mRNA decay in Saccharomyces cerevisiae." Methods Enzymol **448**: 409-427.

Pause, A., G. J. Belsham, et al. (1994). "Insulin-dependent stimulation of protein synthesis by phosphorylation of a regulator of 5'-cap function." Nature **371**(6500): 762-767.

Peng, S. S., C. Y. Chen, et al. (1998). "RNA stabilization by the AU-rich element binding protein, HuR, an ELAV protein." EMBO J **17**(12): 3461-3470.

Penman, S., K. Scherrer, et al. (1963). "Polyribosomes in Normal and Poliovirus-Infected Hela Cells and Their Relationship to Messenger-Rna." Proc Natl Acad Sci U S A **49**(5): 654-662.

Pestova, T. V., I. N. Shatsky, et al. (1996). "Functional dissection of eukaryotic initiation factor 4F: the 4A subunit and the central domain of the 4G subunit are sufficient to mediate internal entry of 43S preinitiation complexes." Mol Cell Biol **16**(12): 6870-6878.

Peterson, D. T., W. C. Merrick, et al. (1979). "Binding and release of radiolabeled eukaryotic initiation factors 2 and 3 during 80 S initiation complex formation." J Biol Chem **254**(7): 2509-2516.

Peterson, D. T., B. Safer, et al. (1979). "Role of eukaryotic initiation factor 5 in the formation of 80 S initiation complexes." J Biol Chem **254**(16): 7730-7735.

Pfaffl, M. W. (2001). "A new mathematical model for relative quantification in real-time RT-PCR." Nucleic Acids Res **29**(9): e45.

Poole, T. L. and A. Stevens (1997). "Structural modifications of RNA influence the 5' exoribonucleolytic hydrolysis by XRN1 and HKE1 of Saccharomyces cerevisiae." Biochem Biophys Res Commun **235**(3): 799-805.

Poulin, F., A. C. Gingras, et al. (1998). "4E-BP3, a new member of the eukaryotic initiation factor 4E-binding protein family." J Biol Chem **273**(22): 14002-14007.

Preiss, T. and M. W. Hentze (1998). "Dual function of the messenger RNA cap structure in poly(A)-tail-promoted translation in yeast." Nature **392**(6675): 516-520.

Ptacek, J., G. Devgan, et al. (2005). "Global analysis of protein phosphorylation in yeast." Nature **438**(7068): 679-684.

Ptushkina, M., T. von der Haar, et al. (1998). "Cooperative modulation by eIF4G of eIF4E-binding to the mRNA 5' cap in yeast involves a site partially shared by p20." Embo J **17**(16): 4798-4808.

Rabbitts, P. H., A. Forster, et al. (1985). "Truncation of exon 1 from the c-myc gene results in prolonged c-myc mRNa stability." EMBO J **4**(13B): 3727-3733.

Raghavan, A., R. L. Ogilvie, et al. (2002). "Genome-wide analysis of mRNA decay in resting and activated primary human T lymphocytes." Nucleic Acids Res **30**(24): 5529-5538.

Rehwinkel, J., I. Behm-Ansmant, et al. (2005). "A crucial role for GW182 and the DCP1:DCP2 decapping complex in miRNA-mediated gene silencing." Rna **11**(11): 1640-1647.

Rendl, L. M., M. A. Bieman, et al. (2012). "The eIF4E-binding protein Eap1p functions in Vts1p-mediated transcript decay." PLoS One **7**(10): e47121.

Rousseau, D., A. C. Gingras, et al. (1996). "The eIF4E-binding proteins 1 and 2 are negative regulators of cell growth." Oncogene **13**(11): 2415-2420.

Roy, G., G. De Crescenzo, et al. (2002). "Paip1 interacts with poly(A) binding protein through two independent binding motifs." Mol Cell Biol **22**(11): 3769-3782.

Rydzik, A. M., M. Lukaszewicz, et al. (2009). "Synthetic dinucleotide mRNA cap analogs with tetraphosphate 5',5' bridge containing methylenebis(phosphonate) modification." Org Biomol Chem **7**(22): 4763-4776.

Saguez, C., J. R. Olesen, et al. (2005). "Formation of export-competent mRNP: escaping nuclear destruction." Curr Opin Cell Biol **17**(3): 287-293.

Schmittgen, T. D. and K. J. Livak (2008). "Analyzing real-time PCR data by the comparative C(T) method." Nat Protoc **3**(6): 1101-1108.

Schroder, H. C., M. Bachmann, et al. (1987). "Transport of mRNA from nucleus to cytoplasm." Prog Nucleic Acid Res Mol Biol **34**: 89-142.

Schwartz, D. C. and R. Parker (1999). "Mutations in translation initiation factors lead to increased rates of deadenylation and decapping of mRNAs in Saccharomyces cerevisiae." Mol Cell Biol **19**(8): 5247-5256.

Schwartz, D. C. and R. Parker (2000). "mRNA decapping in yeast requires dissociation of the cap binding protein, eukaryotic translation initiation factor 4E." Mol Cell Biol **20**(21): 7933-7942.

Schweers, B. A., K. J. Walters, et al. (2002). "The Drosophila melanogaster translational repressor pumilio regulates neuronal excitability." Genetics **161**(3): 1177-1185.

Schwer, B., X. Mao, et al. (1998). "Accelerated mRNA decay in conditional mutants of yeast mRNA capping enzyme." Nucleic Acids Res **26**(9): 2050-2057.

Seay, D., B. Hook, et al. (2006). "A three-hybrid screen identifies mRNAs controlled by a regulatory protein." Rna **12**(8): 1594-1600.

Sezen, B., M. Seedorf, et al. (2009). "The SESA network links duplication of the yeast centrosome with the protein translation machinery." Genes Dev **23**(13): 1559-1570.

Sharova, L. V., A. A. Sharov, et al. (2009). "Database for mRNA half-life of 19 977 genes obtained by DNA microarray analysis of pluripotent and differentiating mouse embryonic stem cells." DNA Res **16**(1): 45-58.

Shatkin, A. J. and J. L. Manley (2000). "The ends of the affair: capping and polyadenylation." Nat Struct Biol **7**(10): 838-842.

Shaw, G. and R. Kamen (1986). "A conserved AU sequence from the 3' untranslated region of GM-CSF mRNA mediates selective mRNA degradation." Cell **46**(5): 659-667.

She, M., C. J. Decker, et al. (2008). "Structural basis of dcp2 recognition and activation by dcp1." Mol Cell **29**(3): 337-349.

Shima, D. T., U. Deutsch, et al. (1995). "Hypoxic induction of vascular endothelial growth factor (VEGF) in human epithelial cells is mediated by increases in mRNA stability." FEBS Lett **370**(3): 203-208.

Shimizu-Yoshida, Y., M. Sasamoto, et al. (1999). "Mouse CAF1, a mouse homologue of the yeast POP2 gene, complements the yeast pop2 null mutation." Yeast **15**(13): 1357-1364.

Shyu, A. B., J. G. Belasco, et al. (1991). "Two distinct destabilizing elements in the c-fos message trigger deadenylation as a first step in rapid mRNA decay." Genes Dev **5**(2): 221-231.

Siekierka, J., V. Manne, et al. (1983). "Polypeptide chain initiation in eukaryotes: reversibility of the ternary complex-forming reaction." Proc Natl Acad Sci U S A **80**(5): 1232-1235.

Sonenberg, N. and A. G. Hinnebusch (2009). "Regulation of translation initiation in eukaryotes: mechanisms and biological targets." Cell **136**(4): 731-745.

Sonenberg, N., M. A. Morgan, et al. (1978). "A polypeptide in eukaryotic initiation factors that crosslinks specifically to the 5'-terminal cap in mRNA." Proc Natl Acad Sci U S A **75**(10): 4843-4847.

Sonenberg, N., K. M. Rupprecht, et al. (1979). "Eukaryotic mRNA cap binding protein: purification by affinity chromatography on sepharose-coupled m7GDP." Proc Natl Acad Sci U S A **76**(9): 4345-4349.

Sonoda, J. and R. P. Wharton (2001). "Drosophila Brain Tumor is a translational repressor." Genes Dev **15**(6): 762-773.

Sprinzl, M., T. Wagner, et al. (1976). "Regions of tRNA important for binding to the ribosomal A and P sites." Biochemistry **15**(14): 3031-3039.

Stebbins-Boaz, B., Q. Cao, et al. (1999). "Maskin is a CPEB-associated factor that transiently interacts with elF-4E." Mol Cell **4**(6): 1017-1027.

Steiger, M., A. Carr-Schmid, et al. (2003). "Analysis of recombinant yeast decapping enzyme." RNA **9**(2): 231-238.

Stevens, A., C. L. Hsu, et al. (1991). "Fragments of the internal transcribed spacer 1 of pre-rRNA accumulate in Saccharomyces cerevisiae lacking 5'----3' exoribonuclease 1." J Bacteriol **173**(21): 7024-7028.

Suh, N., S. L. Crittenden, et al. (2009). "FBF and its dual control of gld-1 expression in the Caenorhabditis elegans germline." Genetics **181**(4): 1249-1260.

Tadauchi, T., K. Matsumoto, et al. (2001). "Post-transcriptional regulation through the HO 3'-UTR by Mpt5, a yeast homolog of Pumilio and FBF." Embo J **20**(3): 552-561.

Tani, H., R. Mizutani, et al. (2012). "Genome-wide determination of RNA stability reveals hundreds of short-lived noncoding transcripts in mammals." Genome Res **22**(5): 947-956.

Tarun, S. Z., Jr. and A. B. Sachs (1996). "Association of the yeast poly(A) tail binding protein with translation initiation factor eIF-4G." EMBO J **15**(24): 7168-7177.

Tarun, S. Z., Jr., S. E. Wells, et al. (1997). "Translation initiation factor eIF4G mediates in vitro poly(A) tail-dependent translation." Proc Natl Acad Sci U S A **94**(17): 9046-9051.

Teleman, A. A., Y. W. Chen, et al. (2005). "4E-BP functions as a metabolic brake used under stress conditions but not during normal growth." Genes Dev **19**(16): 1844-1848.

Tharun, S., W. He, et al. (2000). "Yeast Sm-like proteins function in mRNA decapping and decay." Nature **404**(6777): 515-518.

Tharun, S. and R. Parker (2001). "Targeting an mRNA for decapping: displacement of translation factors and association of the Lsm1p-7p complex on deadenylated yeast mRNAs." Mol Cell **8**(5): 1075-1083.

Thoreen, C. C., L. Chantranupong, et al. (2012). "A unifying model for mTORC1-mediated regulation of mRNA translation." Nature **485**(7396): 109-113.

Tomecki, R. and A. Dziembowski (2010). "Novel endoribonucleases as central players in various pathways of eukaryotic RNA metabolism." Rna **16**(9): 1692-1724.

Tucker, M., R. R. Staples, et al. (2002). "Ccr4p is the catalytic subunit of a Ccr4p/Pop2p/Notp mRNA deadenylase complex in Saccharomyces cerevisiae." Embo J **21**(6): 1427-1436.

Tucker, M., M. A. Valencia-Sanchez, et al. (2001). "The transcription factor associated Ccr4 and Caf1 proteins are components of the major cytoplasmic mRNA deadenylase in Saccharomyces cerevisiae." Cell **104**(3): 377-386.

Uchida, N., S. Hoshino, et al. (2004). "Identification of a human cytoplasmic poly(A) nuclease complex stimulated by poly(A)-binding protein." J Biol Chem **279**(2): 1383-1391.

Ulbricht, R. J. and W. M. Olivas (2008). "Puf1p acts in combination with other yeast Puf proteins to control mRNA stability." Rna **14**(2): 246-262.

Van Etten, J., T. L. Schagat, et al. (2012). "Human Pumilio proteins recruit multiple deadenylases to efficiently repress messenger RNAs." J Biol Chem **287**(43): 36370-36383.

Wakiyama, M., K. Takimoto, et al. (2007). "Let-7 microRNA-mediated mRNA deadenylation and translational repression in a mammalian cell-free system." Genes Dev **21**(15): 1857-1862.

Wang, X., J. McLachlan, et al. (2002). "Modular recognition of RNA by a human pumilio-homology domain." Cell **110**(4): 501-512.

Wang, Z., X. Jiao, et al. (2002). "The hDcp2 protein is a mammalian mRNA decapping enzyme." Proc Natl Acad Sci U S A **99**(20): 12663-12668.

Wang, Z. and M. Kiledjian (2001). "Functional link between the mammalian exosome and mRNA decapping." Cell **107**(6): 751-762.

Weidmann, C. A. and A. C. Goldstrohm (2012). "Drosophila Pumilio protein contains multiple autonomous repression domains that regulate mRNAs independently of Nanos and brain tumor." Mol Cell Biol **32**(2): 527-540.

Wells, S. E., P. E. Hillner, et al. (1998). "Circularization of mRNA by eukaryotic translation initiation factors." Mol Cell **2**(1): 135-140.

Wharton, R. P., J. Sonoda, et al. (1998). "The Pumilio RNA-binding domain is also a translational regulator." Mol Cell **1**(6): 863-872.

Wharton, R. P. and G. Struhl (1991). "RNA regulatory elements mediate control of Drosophila body pattern by the posterior morphogen nanos." Cell **67**(5): 955-967.

White, F. C., S. M. Carroll, et al. (1995). "VEGF mRNA is reversibly stabilized by hypoxia and persistently stabilized in VEGF-overexpressing human tumor cell lines." Growth Factors **12**(4): 289-301.

Wickens, M., D. S. Bernstein, et al. (2002). "A PUF family portrait: 3'UTR regulation as a way of life." Trends Genet **18**(3): 150-157.

Wiederhold, K. and L. A. Passmore (2010). "Cytoplasmic deadenylation: regulation of mRNA fate." Biochem Soc Trans **38**(6): 1531-1536.

Wilhelm, J. E., M. Hilton, et al. (2003). "Cup is an eIF4E binding protein required for both the translational repression of oskar and the recruitment of Barentsz." J Cell Biol **163**(6): 1197-1204.

Wreden, C., A. C. Verrotti, et al. (1997). "Nanos and pumilio establish embryonic polarity in Drosophila by promoting posterior deadenylation of hunchback mRNA." Development **124**(15): 3015-3023.

Wright, R. M., B. Rosenzweig, et al. (1989). "Organization and expression of the COX6 genetic locus in Saccharomyces cerevisiae: multiple mRNAs with different 3' termini are transcribed from COX6 and regulated differentially." Nucleic Acids Res **17**(3): 1103-1120.

Wu, D. Y. and R. B. Wallace (1989). "Specificity of the nick-closing activity of bacteriophage T4 DNA ligase." Gene **76**(2): 245-254.

Wu, L., J. Fan, et al. (2006). "MicroRNAs direct rapid deadenylation of mRNA." Proc Natl Acad Sci U S A **103**(11): 4034-4039.

Wurmbach, P. and K. H. Nierhaus (1979). "Codon-anticodon interaction at the ribosomal P (peptidyl-tRNA)site." Proc Natl Acad Sci U S A **76**(5): 2143-2147.

Yu, X. and J. R. Warner (2001). "Expression of a micro-protein." J Biol Chem **276**(36): 33821-33825.

Zamore, P. D., D. P. Bartel, et al. (1999). "The PUMILIO-RNA interaction: a single RNA-binding domain monomer recognizes a bipartite target sequence." Biochemistry **38**(2): 596-604.

Zamore, P. D., J. R. Williamson, et al. (1997). "The Pumilio protein binds RNA through a conserved domain that defines a new class of RNA-binding proteins." Rna **3**(12): 1421-1433.

Zdanowicz, A., R. Thermann, et al. (2009). "Drosophila miR2 primarily targets the m7GpppN cap structure for translational repression." Mol Cell **35**(6): 881-888.

Zekri, L., D. Kuzuoglu-Ozturk, et al. (2013). "GW182 proteins cause PABP dissociation from silenced miRNA targets in the absence of deadenylation." EMBO J.

Zhang, B., M. Gallegos, et al. (1997). "A conserved RNA-binding protein that regulates sexual fates in the C. elegans hermaphrodite germ line." Nature **390**(6659): 477-484.

Zhang, S., C. J. Williams, et al. (1999). "Monitoring mRNA decapping activity." Methods **17**(1): 46-51.